# DNA based networks, nanostructures, and meta-stable states

By

CHIH-TA LIN

BSc (Honours) University of Cape Town



THESIS

Submitted as in fulfillment of the requirements
for the degree of Doctor of Philosophy in Molecular and Cell Biology
in
University of Cape Town, 2006
Cape Town, Western Cape Province
Republic of South Africa

## Acknowledgement

I would like to thank Prof. H.H. Klump for his advices and guidance through this entire work. With his astonishing knowledge, I have gained lots of skills and knowledge from him.

I also would like to thank following colleagues: Madhu Chauhan and Dr. Martin Mills for sharing laboratory work experiences and advices; Pei-yin Ma for DNA synthesis; Mohammed Jaffar for transmission electron microscope work; and John Moore for greatful advices and experiences.

I want to thank my family (my parents and sister) for encouraging me all the way through this study, this work can not be completed without their support.

Last but not least, I would like to thank all my friends who are supporting and encouraging me whenever I encounter any difficulties.

This work is funded by National Foundation Research.

# Abstract


## Abstract

Nanotechnology is defined as the technology that allows to fabricate nanoscale materials and manipulate them at the molecular or atomic level. Nano-biotechnology is one of the sub-disciplines of nanotechnology. Materials used for nano-biotechnology are macromolecular materials found in nature with specific mechanical and biological functions. One of the most important materials is deoxyribonucleic acid (DNA). DNA has several unique properties that make it a good candidate for nanotechnology research.

The primary aim of this research is to use DNA three-way junctions as building blocks and to assemble them into a huge DNA networks through self assembly followed by DNA ligation. The second step aims at assembling six DNA three-way junctions with different sticky end sequences to form an opto-mechanical hexagonal DNA nano-switch. The switching mechanism in the ring is based on the conformational change of B- to Z- DNA. This change is influenced by the environmental cation concentrations. The third approach presented here aims to create meta-stable DNA nanostructures based on a DNA hairpin loop that can mimic the enzyme-substrate binding mechanism. This mechanism is demonstrated using a

"strand displacement strategy" (SDS). Lastly, we employed a novel way of organizing hairpin loop DNA structures based on the orientation of consecutive hairpin loop DNA structures "on top" of one another.

The DNA three-way junctions and the nanostructures created by them can be used for drug delivery systems such as transcription factor carriers, for separation of specific proteins, for creating molecular memory, protein conveyance carrier or DNA nano-wires. Through DNA sequence design, a whole variety of potential and useful nanostructures can be produced.

## Abbreviations

| | |
|---|---|
| 3WJ | Three-way junction |
| BAC | Benzyldimethylalkylammonium Chloride |
| CD | Circular Dichroism |
| DNA | Deoxyribonucleic Acid |
| dsDNA | Double-stranded DNA |
| EDTA | Ethylenediaminetetraacetic acid |
| EtBr | Ethidium bromide |
| nm | Nanometer |
| PAGE | Polyacrylamide gel electrophoresis |
| RNA | Ribonucleic Acid |
| sds | Strand Displacement Strategy |
| SE(s) | Sticky end(s) |
| ssDNA | Single-stranded DNA |
| TEM | Transmission Electron Microscope |
| Tm | Melting temperature |
| UV | Ultra-violet |
| $\Delta\Delta G$ | Free energy changes |

# Table of Contents

# Chapter 1 Introduction

## 1.1 Introduction to nanotechnology

Nanotechnology is defined as the ability to fabricate nanoscale materials and manipulate them at the molecular or atomic level. The size of nanomaterials can range from 1 to 100 nanometers (nm)[1]. The concept of nanotechnology was firstly popularized by physicist Richard Feynman in 1959, with the talk entitled "There is a plenty room at the bottom." which described a number of possible ways to manipulate atoms so as to perform particular tasks[2]. The era of nanotechnology was thus started. With the invention and development of the scanning tunnelling microscope[3] and the atomic force microscope[4], manipulation of substances at the atomic level was no longer a dream. The principle of nanotechnology repudiates the conventional methods in the materials sciences, which favour the "*Top-down*" approach. This "*Top-down*" approach involves manufacturing products on a very small scale by modifying and reducing the size of large pieces of raw materials. The opposite method, mimicking what nature does, is known as the "*Bottom-up*" approach. The principle of this method is to build up materials from the smallest units such as atoms or molecules into defined macromolecular structures. The advantage of using "*Bottom-up*" methods as an approach to build higher order material structures is that there is greater control over the product's size. As it turns out the conventional "*Top-down*" method

encounters a major problem of size limitation which is known as the bottle-neck of this technique. The "*Bottom-up*" method is based on the process known as the "Self-assembly"[5, 6, 7]. All materials consist of atoms, and atoms in the condensed phase are connected through chemical bonds. Through defined chemical bonds between atoms, various molecules are created with the same number and type of atoms but with different physical and chemical properties. These properties enable the molecules of certain kind to recognize related or identical molecules, which is known as self-recognition. Once these molecules recognize each other, they undergo the process called self-assembly. This arrangement process of the same species results in a regular pattern that combines the most stable structure and the least spatial occupancy. The self-assembly process is driven by the second law of thermodynamics and it is spontaneous. Therefore the products can be produced in a very short time, and the process can be controlled by changing the surrounding conditions such as temperature, buffers or pH. Self-assembled structures or devices such as electronic devices[8], monolayer films[9], and nanostructures from biomaterials[10, 11] are designed on the basis of this concept.

Self-assembly can be divided into either static or dynamic approaches. The differences between approaches rests on the flow of energy in the process. The

dynamic approach is based on the dissipation of energy while static self-assembly does not require energy dissipation[12]. The aim of self-assembly process is to reach an equilibrium which results in the most stable structure[5].

## 1.2 Nanomaterials

When the particle sizes approach the nanometer scale, the conventional laws of physics are no longer applicable to assemblies of particles. As Schrödinger described: "It is in that way that the events acquire truly orderly features. All the physical and chemical laws that are known to play an important part in the life of organisms are of this statistical kind; any other kind of lawfulness and orderliness that one might think of is being perpetually disturbed and made in operatively by the unceasing heat motion of the atoms", thereby stating that physical laws are only just approximations[1]. These nanoscale materials appear to have new physical properties that can be described by quantum theory. This new behaviour of these materials has to be taken into account in the design of nanomaterials. Quantum behaviour becomes important in the design of these materials. Before we can safely manufacture and release these nanomaterials, special considerations have to go into safety aspects. The new dimension of environmental hazards resulting from artificially made nanomaterials is a concern in nanotechnology research. With the development of various new

nanomaterials, the exposure to these materials could possibly cause unknown risks related to the enhanced surface area of these nanomaterials, and therefore the investigation of possible risks should be made compulsory[13]. For examples, the experiments of C60 and single walled carbon nanotubes have been studied on the toxicity effects in rats[14,15].

### 1.3 Nanobiotechnology

Nanobiotechnology is the one of the subdisciplines of nanotechnology research. Materials used for nanobiotechnology are macromolecular materials found in nature with specific mechanical and biological functions. A cell is an excellent natural environment for the nanobiotechnology research, as it contains a range of different nanobiomaterials. Each of these biomaterials is produced using bottom-up method based on self-assembly[16,17]. Biomaterials such as proteins, phospholipids, nucleic acids and polymeric carbohydrates are all macromolecules present in biological systems. All of these macromolecular structures can be used individually or in combination as building blocks in nanobiotechnology.

Proteins are assembled from amino acids to form primary and secondary structures. There are 20 canonical amino acids in living creatures that can be grouped into three

different categories: polar non-charged, neutral, and polar charged. They are linked together via peptide bonds. The native proteins have been the subject of natural selection with respect to folding and function. Any attempt to design new proteins has to take these two aspects into account, in order to preserve the active sites and folding. For example, a biomolecular motor made from $F_1$-adenosine triphosphate synthase ($F_1$-ATPase) as the movable part, and using Nickel whiskers as the propeller. This synthase has a diameter of 150 nm while the propeller has a length of approximately 750 to 1400 nm. By adding ATP as the power source, the maximum propeller speed can reach 8 revolutions per second[18].

Phospholipids are important components of membranes in that they act as the boundary between neighbouring cells and separate cellular organelles as well as maintaining the balance between the inside and the outside of cells. All phospholipids consist of a hydrophilic head group that is linked to the hydrophobic tail via the phosphate groups. In an aqueous environment, the phospholipids form bilayers with the hydrophobic residues at the inside facing each other and hydrophilic head groups facing the water. The closed phospholipids bilayer creates a spherical volume that contains small amounts of active ingredients. On fusing the bilayer membrane with cellular membrane, the content can be transferred into the cell. Such a transfer system

can be used in designing delivery vehicles for gene therapy in the form of liposomes[19].

Nucleic acids are known to be the materials that are responsible in providing information for protein synthesis. According to the dogma of molecular biology, DNA makes RNA, and RNA makes protein[20]. A unit of the nucleic acids (nucleotide) consists of a nitrogen base (A, T, C, G), a pentose sugar (ribose or deoxyribose) and a phosphate group. There are two types of nucleic acids: ribonucleic acid (RNA) and deoxyribonucleic acid (DNA). The difference between RNA and DNA is that there is a 2'–OH group in $C_2$ position of pentose sugar ring in RNA which is absent in DNA. This difference makes RNA more prone to hydrolysis, and therefore RNA is less stable than DNA. The other difference is that the uracil nucleobase in RNA is replaced by the thymine in DNA. The applications of nucleic acids such as DNA in nanobiotechnology have been pioneered by N. Seeman[21-23]. The complementarity of the two strands and stability of the base pairs are unique properties that are suitable to make complex two- and three-dimensional structures.

## 1.4 DNA as native material

### *1.4.1 General introduction*

Deoxyribonucleic acid (DNA) was firstly discovered and described by Friedrich Miescher in 1869. He isolated the materials from the nucleus of living cells. The structure of DNA was discovered by Francis Crick and James Watson in 1953 explaining that DNA was a double helix (double strand DNA, dsDNA). They proposed that two polynucleotide chains (single strand DNA, ssDNA) run in opposite directions and are held together by hydrogen bonds between base pairs[24]. The backbone consists of alternating phosphate groups and deoxyribose sugars link by phosphodiester bonds. The nitrogen base is linked with the pentose sugar through a glycosidic bond. Each base pair consist of a pyrimidine linked to a complementary purine. Pyrimidine is a single six-membered heterocyclic ring containing two nitrogen atoms; while purine can be described as a pyrimidine fused with an imidazole ring. There are two purines (adenine and guanine) and two pyrimidines (cytosine and thymine) found in DNA. Adenine is paired with thymine via two hydrogen bonds; while guanine is paired with cytosine via three hydrogen bonds. Through the complementarity, one strand of DNA is the backup for the other strand. This is basis of the storage of the information for cellular components and genetic inheritance, and the information is extracted by transcription and translation processes.

### *1.4.2 DNA properties*

DNA can be described as a natural nano-material, as it has several unique properties that make DNA a good candidate in nanotechnology research. These properties include:

1. Size on the nanoscale;
2. Ultraviolet (UV) absorbance maximum at 260 nm;
3. Tunable stickiness through base sequences;
4. Selective sticky ends (unpaired ssDNA ends);
5. Localized chemical modification of bases;
6. Alternative stable conformers of DNA (A-, B- and Z-form DNA);
7. Uncommon forms of DNA (branched DNA junctions);



On average, each DNA base spans approximately 1 nm, and so a base pair measures 2 nm from backbone to backbone. The thickness of a base measured along the helical axis is approximately 0.34 nm (Figure 1.4.1). Accordingly, one helical turn corresponds to 3.4 nm. Given these dimensions, it is straightforward that DNA structures with precise sizes can be designed. Furthermore their stabilities can be carefully controlled.

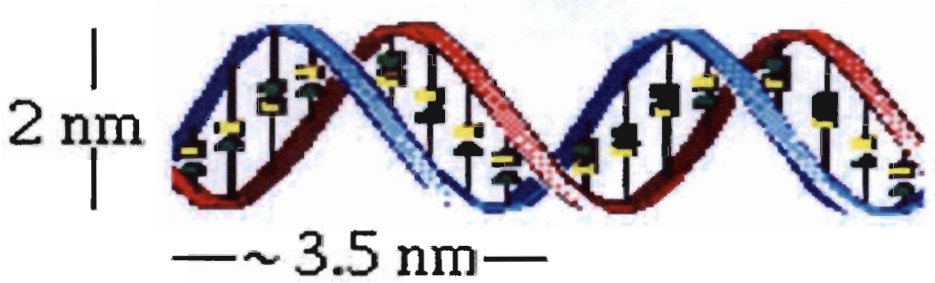


**A:T base pair**

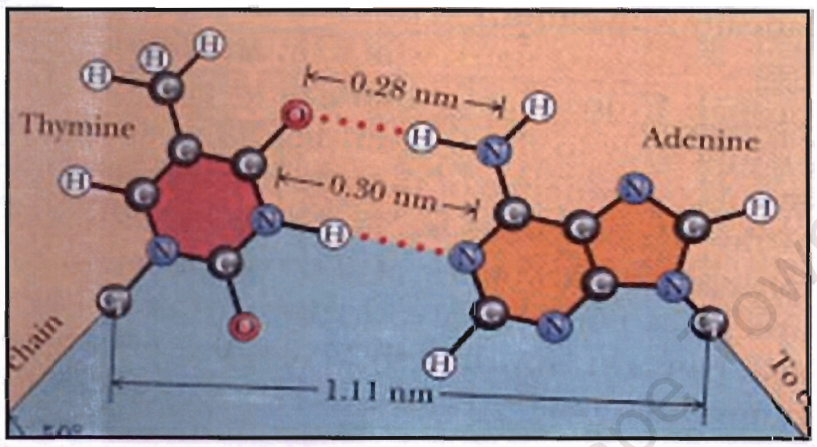


**G:C base pair**

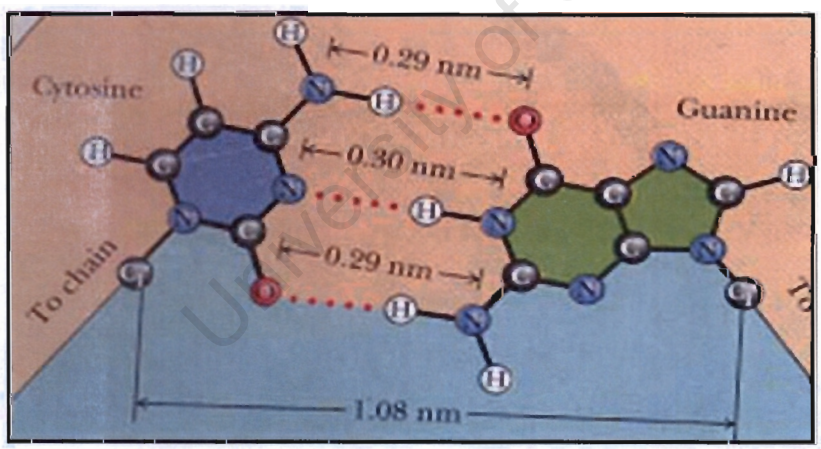


Figure 1.4.1 The size of a dsDNA and size between two types of base pairs.

DNA has a unique UV absorbance spectrum centred on a wavelength of approximately 260 nm. This absorbance is due to the transition moment of the π electrons in the heterocyclic bases[25]. Different bases have different maxima UV

absorbance wavelength (A: 261 nm; G: 276 nm; C: 267 nm; T: 266 nm). This unique UV absorbance changes with temperature because dsDNA is melted (strand dissociation) into ssDNA. ssDNA absorbs more UV light then dsDNA. This property of ssDNA allows DNA stability to be assayed using UV spectroscopy. The stability of dsDNA is goverened by the melting temperature (Tm) of the dsDNA solution[26]. Tm is defined as the temperature at which 50% of measured absorbance change or a hyperchromic change has been observed[27]. The hyperchromic shift is due to the breaking of hydrogen bonds between base pairs, and the consequential de-stacking of the bases. Melting curves can be used to calculate thermodynamic parameters[28].

The third property of DNA is its tunable stickiness which is governed by the DNA nucleotide sequence. A single base pair difference between two double helical DNA sequences of the same length will result in different genetic information being carried (e.g. mutation). This property enables DNA's helical stability to be tunable (modification). For example, the annealing of a single strand 5'-GTTACT binds more favourably to the single strand 5'-AGTAAC region than to the single strand 5'-ACTAAG region because the 5'-AGTAAC sequence is the perfect complementary strand whereas binding 5'-ACTAAG will result in four matches and two mismatches. It will not anneal with a single strand 5'-TGCTTA at all because this is not the

matching sequence.

DNA is able to form sticky end regions which have considerable utility in DNA biotechnology. Sticky ends are the single strand extensions of the 5'/3'- ends of a DNA double helix. Complementary 5'/3'- extensions will anneal to double helices. DNA sticky ends were firstly observed when restriction enzymes cleaved a dsDNA sequence and generated complementary single strand extensions. This discovery was the basis for the development of recombinant DNA technology. The restriction class II restriction enzyme is able to create identical sticky end regions in any dsDNA no matter what the source of the DNA. Because of this property, the sticky end region created with this enzyme can be re-annealed with any matching sticky end. Following this example, one can design and assemble networks of DNA sequences by using the stickiness of single strand extensions. In DNA nanotechnology, the sequences of sticky ends can be created without using restriction enzymes. These links can be made permanent by sealing the gap in the backbone using the enzyme T4 DNA ligase. This process was copied from nature where the integration of T4 phage into the genome of *E. coli* follows an identical process. During *in vitro* ligation, the 5'-position of sticky end sequences have to be phosphorylated prior to the ligation. The phosphorylation can be done with the enzyme, DNA kinase.

The kinase and ligase reaction are illustrated in Figure 1.4.2. These processes require ATP as an energy source and can be carried out at room temperature[29,30].

**DNA kinase reaction**

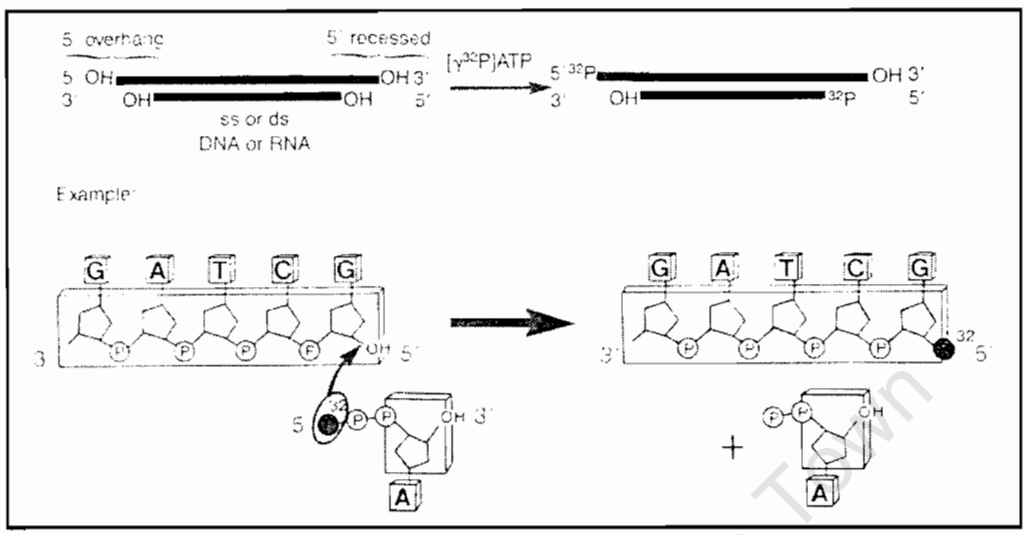


**DNA ligation reaction**

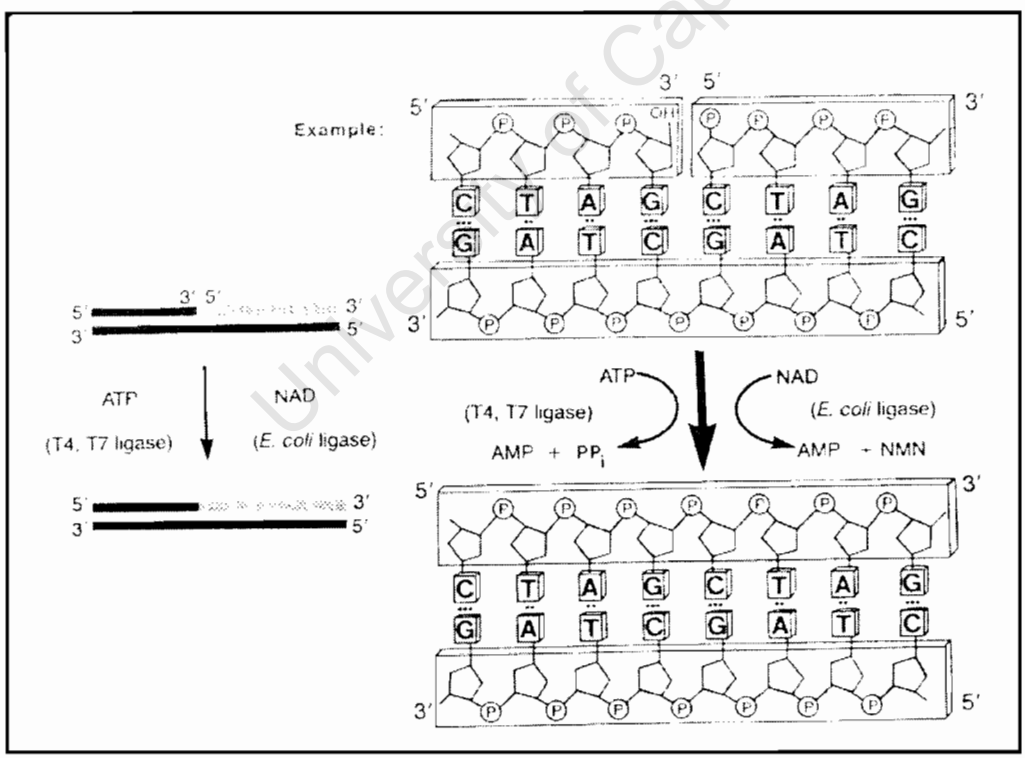


Figure 1.4.2 The kinase reaction scheme using DNA kinase (top); the ligation reaction scheme using DNA ligase (bottom).

A further property of DNA is the potential for chemical modification of the nucleobases outside the Watson-Crick face. This modification helps to make unusual connections between the nucleotide bases and the target nanosurfaces. (examples using nanoparticles[31]) In nature, the most prominent example is the methylation of cytosine [32]. Addition of a base specific fluorescent tag to DNA is very useful to detect whether a particular base is involved in through space interactions[33]. Biotinylation is also frequently used in DNA backbone/base modification in order to facilitate DNA attachment to surfaces or spherical particles like magnetic beads [34].

DNA polymorphism is another useful property of DNA which can be used for nanotechnology research. Depending on the environmental conditions, particularly the state of hydration of the DNA double helix, can result in the DNA switching between a number of conformations: A-, B- and Z-form (Figure 1.4.3).

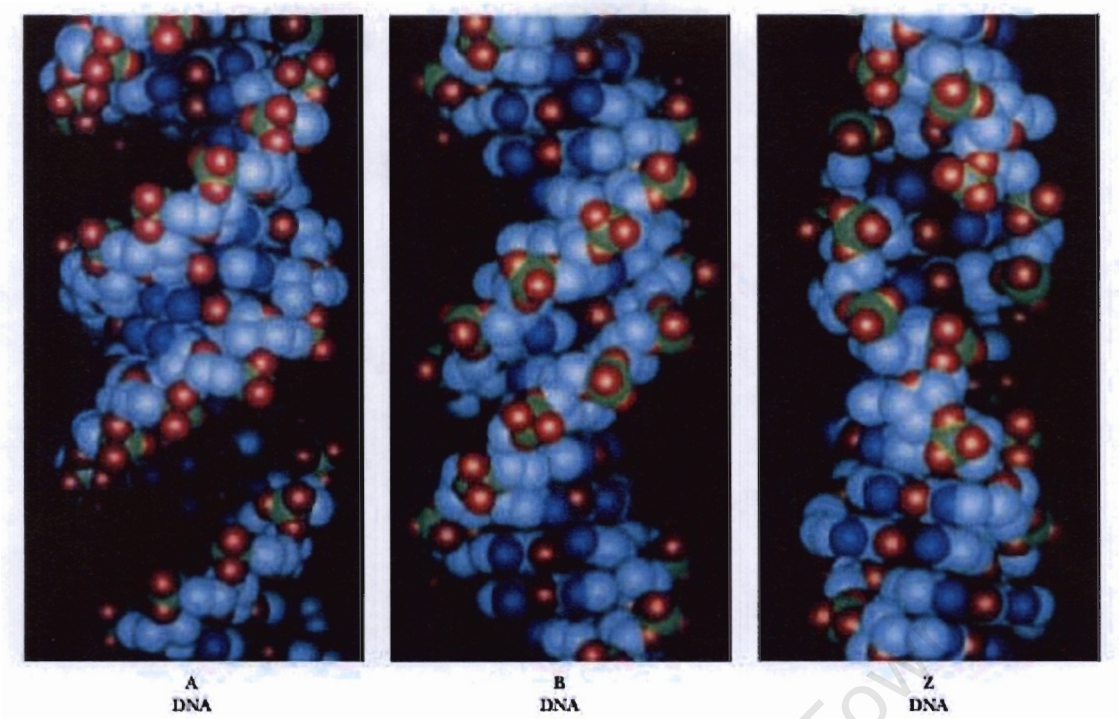


Figure 1.4.2.3 Structures of the A, B-, and Z-forms of the DNA double helix.



The most abundant DNA conformation in the cellular environment is the B-form DNA. In some cases of double-stranded DNA helices, the bases are slightly tilted, and 11 base pairs form the helical repeat unit. This conformation is called the A-form DNA. Both A- and B-form DNA are right-handed helix structures, while the Z-form DNA is a left-handed structure. The structural characteristics of Z-form DNA include: the helix diameter is about 1.8 nm, making it a slightly narrower helix with 12 base pairs per helical turn. The biological role of the Z-form DNA is still under investigation. Alternating purine and pyrimidine sequences particularly CG repeat sequences[35] have been observed to occurr naturally in the Z conformation. One of the driving forces to convert the B-form of DNA to the Z-form of DNA is the

supercoiling of plasmid DNA. But *in vitro*, chemical modification of cytosine such as methylation favours the Z-conformation over the normal B-form of DNA. One of the characteristics of the Z-form of DNA is that the purine residues in alternating sequences are in the unusual *syn* conformation, while the pyrimidine residues stay in the canonical *anti* conformational state (Figure 1.4.4).

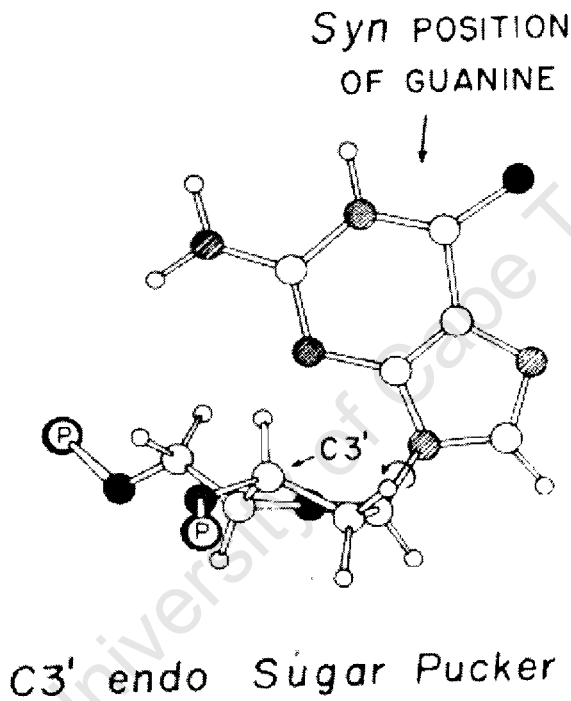




Figure 1.4.4 The *syn* conformation of Z-form DNA.

This regular shift from the *syn* to the *anti* conformation along the backbone results in the Z-form structure forming (Z refers to zigzag formation).

Recently a biological function of Z-form DNA has been observed in transcriptional

control[36], in gene recombination[37] and in gene modification by methylation[38]. This Z-DNA conformation in these biological systems is stabilized by negative supercoils[39]. It was found that the addition of 4M sodium chloride to the poly d(CG) DNA sequence resulted in the formation of the Z-form of DNA. The presence of Z-DNA was determined using CD spectroscopy. The CD spectrum of Z-DNA is the inverted trace of that obtained using B-DNA[40]. The CD spectrum of the Z-form DNA has a characteristic negative band at 290 nm and a positive peak at 265 nm, which is almost the mirror image of the CD spectrum of the A- and B-form DNA[41].

The left-handness of the Z-form DNA structure was further confirmed by x-ray crystallographic studies[42]. Wang and Rich crystallized $(CG)_4$ sequences and discovered that the helix formed by two complementary single strands was left-handed. It was further found that a B- to Z-DNA conformational change could be induced by the methylation of cytosine residues of one strand of DNA double helix. Studies also showed that DNA possessing stretches of d(CA/TG)n sequences and immersed in a high salt buffer induced Z- DNA formation in the mixed alternating purine and pyrimidine sequence regions[43-46]. Poly d(AT) sequences can form Z-DNA structures but under more specific conditions than that used for other DNA sequences. Z-DNA formation in poly d(AT) sequences can be achieved by adding a small amount

of transition metal ions, such as nickel or copper, to the sodium chloride solution. The thermodynamic parameters of the B- to Z- DNA conversion have been determined experimentally for different transition metal ions [47-51].

DNA is also able to branch and in so doing form unusual structures [52-53]. In nature branched DNA has been observed in DNA replication as a short-lived unstable intermediate (DNA fork) and in DNA recombination as a temporary four-way junction (Holliday junction). The branch points in these intermediates are movable. The formation of branched DNA is based on the partial complementarity of opposite strands. Stable branched DNA can be created artificially by design. Single stranded DNA sequences are chemically synthesized to be partially complementary to each other (Figure1.4.5).

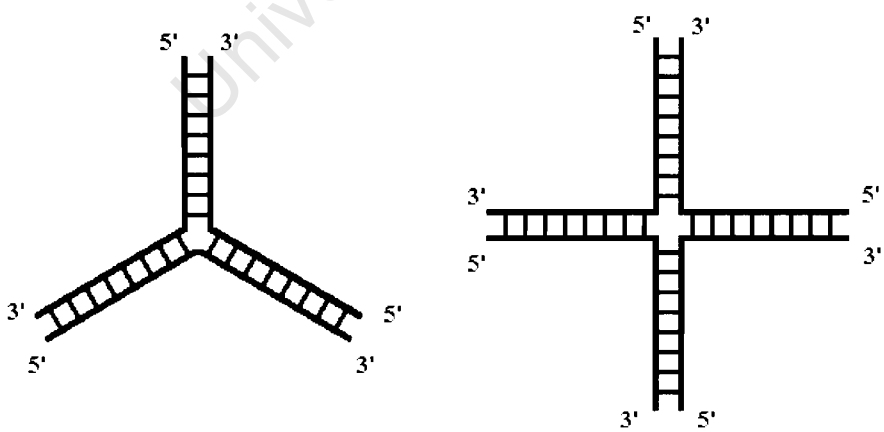


Figure 1.4.5 The schematic diagram of branched DNA. Left: three-way junction DNA; Right: Four-way junction DNA.

When these strands anneal through secondary bonds, an immobilized branch point is created. The number of arms in a branched DNA structure is dependent on the number of partially complementary DNA strands involved in the annealing process. The simplest form of branched DNA is the three-way junction. Nature has also provided nanotechnologists with a whole family of four-way junctions which we know as t-RNAs. The only free ends available in t-RNA is the acceptor stem, which is incapable of annealing with other acceptor stems. Therefore in order to create extended networks based on branched DNA three-way junctions, one has to design three sequences which are partially complementary to each other, and engineer sticky ends into these sequences which will anneal to one another (details will be discussed in the next chapter). Apart from these common structures, there are other natural structures such as hairpin loop structures. A single stranded DNA sequence with complementary bases at the 5'- and 3'- ends can self-anneal so as to form a hairpin loop structure. Hairpin loop structures can be amplified by either attaching further DNA sequences to the stem (provided the stem has a single strand extension) or to the loop (this will be discussed in later chapters). Recent research has focused on multi-stranded DNA structures such as G-quartet structures or i-motifs. Samples of these structures are shown in Figure1.4.6.

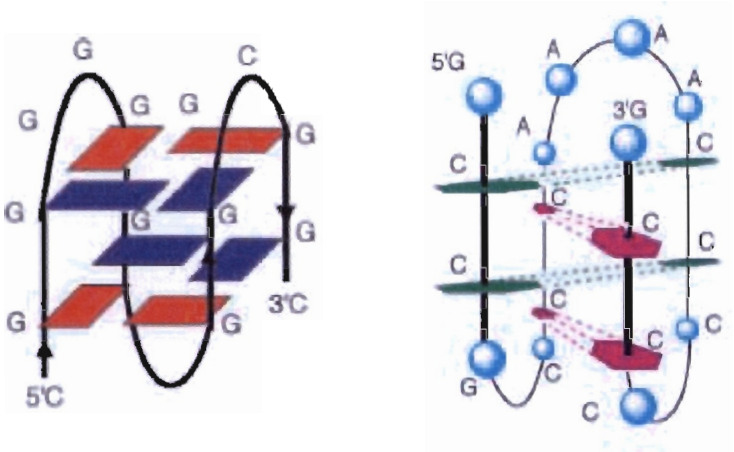


**G-quartet** **i-Motif**

Figure 1.4.6 The schematic diagram of G-quartet (left) and i-Motif (right).

To date, multi-stranded helices have not been utilized in building DNA based nanostructures.

### *1.4.3 The use of DNA in nanotechnology*

The use of DNA in nanotechnology, in creating unique structures and devices, has been developed and facilitated by the unique properties of DNA summarised previously. Research in DNA nanotechnology is currently divided into either building a large DNA framework or developing nano-structures to perform specific tasks.

In order for large frameworks to be built from DNA, double helical DNA has to be branched to form two- or three-dimensional DNA structures. To achieve this aim, three- or four-way junction DNA are designed as the building materials. A three-way junction DNA is created from three ssDNA with sequences that are partially

complementary to each other. The complementary sections of each strand will spontaneously hybridize, resulting in a branched DNA structure with three arms (Figure 1.4.7).


Figure 1.4.7 A schematic diagram of a three-way junction DNA formed by sequence design.

If all the complementary sections are of equal length, all three arms will be of equal length but with blunt ends. To initiate the spontaneous assembly of three-way junction DNA into a large network, identical complementary sticky ends have to be included in each arm region. The 3WJ DNA branch point needs to be immobile so as to stabilize the structure. The structure of 3WJ DNA has been thoroughly investigated in the past[54-58]. To reduce strain at the branch point, the addition of an extra unpaired base at the junction point has proven beneficial[59-61]. For example, a DNA ribbon was created from three-way junction DNA composed of two identical arms and the complementary sticky end regions were used to link strand backbones together permanently using DNA ligase[62]. In a similar approach, the three-way junction zones

were combined in a sequential process carefully matching sticky ends to build up dendrimer structures which were stabilized by ligating the backbones on each side of the sticky ends[63].

The formation of a four-way junction follows the same design principles as the formation of the three-way junction. In principle, one can build up zeolite-like three-dimensional structures using four-way junctions with four identical sticky ends. By connecting consecutive tetrahedral four-way junctions, a three-dimensional network can be created that resembles the crystal structures of $SiO_2$. But this design hypothesis has not yet been tested experimentally.

To improve the stability of regular DNA based nanostructures, four-way junctions based on a cross-over DNA with sticky ends were used as the main building material. The construction process resulted in the formation of a two-dimensional rectangular DNA framework[64,65]. This building material was further modified into a double cross-over DNA structure. The formation of a double cross-over DNA structure required five ssDNAs (two short ssDNAs, two medium length ssDNAs and a large ssDNA). The sequences of two short ssDNAs were designed so as to be partly complementary to one end of the two medium length ssDNAs, and the sequence of

the large ssDNA was designed to be partially complementary to the middle section of the two medium length ssDNA (Figure 1.4.8).

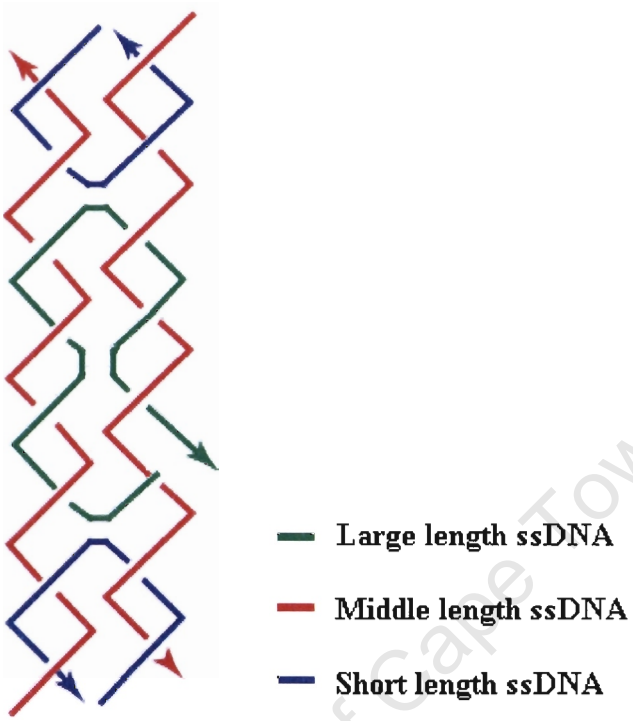


Figure 1.4.8 The schematic diagram of a double-cross over DNA made by hybridizing 5 different lengths ssDNA[64].



When hybridizing these five ssDNAs, a rectangular tile of DNA with two cross-overs was formed. By adding the extra sticky ends on both ends, this double cross-over DNA could be used as the building material[66]. In this case, the DNA tile pattern created by this material was more rigid than the pattern created by using single cross-over DNA[67]. Further research using this aspect of the tile pattern formation resulted in the development of the barcode DNA array, where different cross-over DNAs were linked to represent different codes[68,69].

Using DNA nanostructures to perform a specific task has become popular in recent time. These investigations aim at providing potential practical applications for DNA nanostructures. One of the approaches described in the literature[70-72] is the use of DNA as a sensor. To detect certain environmental conditions, DNA conformational change can be utilized as a sensor of local conditions. This is achived by favouring a conformation where two single strand ends, tagged with acceptor and emitter flourescent molecules, approach each other, and so allow for fluorescence energy transfer. The most prominent example for this technology is a strcuture called a molecular beacon. A molecular beacon is a DNA hairpin loop with one end of the hairpin attached to a fluorescein molecule, and the other end attached to quencher molecule. When the stem structure of the hairpin loop is formed, the fluorescein residue and the quencher are located next to each other, and the quenching effect takes place, results in no light being emitted by the fluorescein residue. Once the stem helix is disrupted, the fluorescein is no longer located next to the quencher, and consequentially light will be emitted. Accordingly, the detection of light emission acts as an indicator implying a conformational change in the DNA molecule has taken place. Light emission or quenching are the result of facilitated or repressed fluorescence energy transfer[73]. When the fluorophore is excited, the resonance energy

is dissipated as light emission. If there is a quencher near by, then the energy will be absorbed by the quencher and no light will be emitted. This process is strongly distance dependent and as a result it is inversely proportional to the quenching efficiency.

As an example, PCR amplification can be monitored by molecular beacon technology. A molecular beacon was designed to contain the sequences that were complemetary to the PCR amplified products. When a correct product was amplified after the extension step, the molecular beacon hybridizes with the product to form a double helix, and the stem structure is then disrupted and so results in light emission which can then be detected in real time[74]. A different approach uses a primer next to a molecular beacon. After the extension step, the molecular beacon once again changes conformation to hybridize with the extended sequences, and the light emission can be detected[75]. Molecular beacons can also be applied to monitor DNA ligation. The sequences in the unpaired loop section of molecular beacons were designed to hybridize with two ssDNAs. DNA ligase was added to ligate these two ssDNAs after alignment. As the result of the formation of the longer complementary double helix within the loop sequence, the molecular beacon structure unfolds due to the tension on the loop section. The emission of light from the fluorescein residue indicates that the ligation was successful[76]. These examples are demonstrated in Figure 1.4.9.

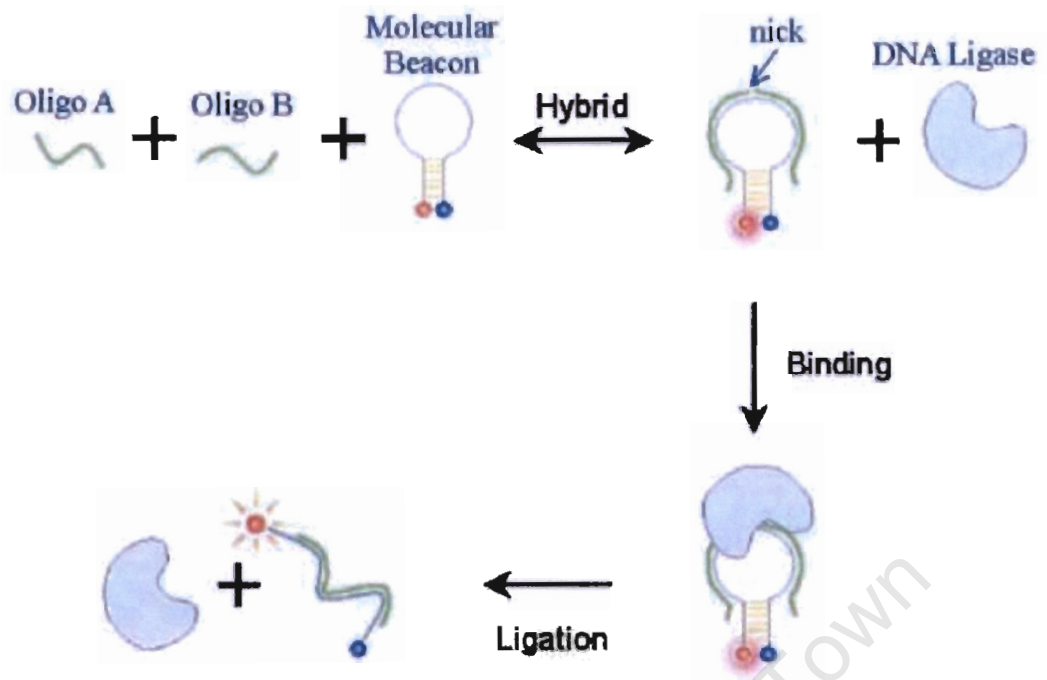


Figure 1.4.9 The schematic diagram of DNA ligation monitored in real time using molecular beacon[76].

A promising application of DNA nanotechnology is the use of DNA as a nano-wire capable of conducting electricity. This would open up a potentially new field of nanoelectronics. Unmodified DNA is very poor conductor. It requires either covalent modification of the bases, or the attachment of conducting ion to the backbone. Recently, silver was introduced as coating of the DNA double helix to enhance the conductivity. The nanoparticle responsible for conducting electricity is the linear array of silver particles (Ag). The Ag nanoparticles were mixed with DNA, and the positively charged Ag nanoparticles were attracted by negatively charged DNA phosphates. The deposition of Ag nanoparticles was carried out by using a

hydroquinone containing solution[77] similar to that used in the development of photographs. Similarly, Ag nanoparticles deposited on DNA fibres using the same deposition method, have resulted in the DNA fibres becoming a conductive platform [78]. An alternative method uses gold (Au) nanoparticles that are first deposited on the DNA backbone, and then Ag is applied so as to enhance the conductivity of the structure[79].

Other methods involve attaching gold nanoparticles to ssDNA containing thiol groups by heating[80,81]. The combined gold nanoparticle ssDNA structure can be used to bind specific DNA sequences through hybridization. The resulting hybrized complex produces a colour which is dependent on the size of Au nanoparticles present. With the longer hybridization periods, more Au nanoparticles will accumulate at the hybridization sites, resulting in sequential colour changes[82-85]. (Figure 1.4.10)

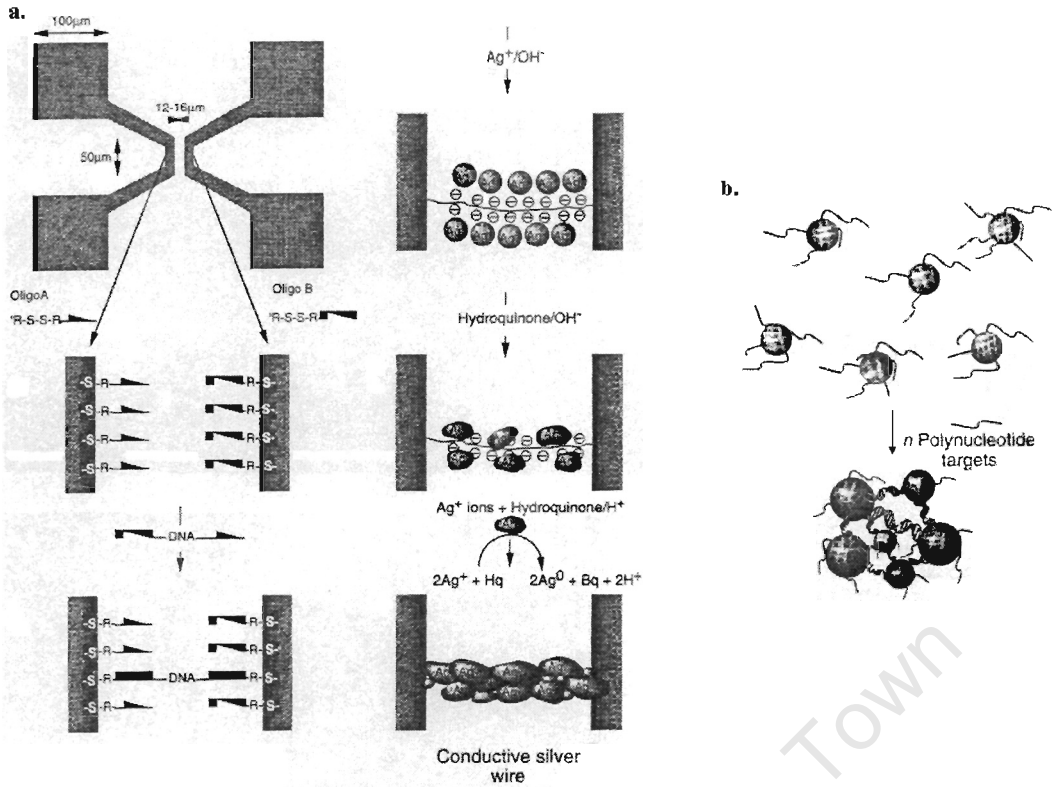


Figure 1.4.10 The schematic diagram of use of nanoparticles with DNA. a) DNA nano-wire using gold and sliver nanoparticle deposition[79]; b) Hybridization of DNA containing gold nanoparticles[82].

DNA can be used to perform specific tasks based on the interaction between meta-stable states of DNA structures. This approach requires a defined meta-stable DNA structure as the reference state. Additional DNA sequences are added to this initial state so as to compete for binding sites on the structure. This results in another meta-stable state that is closer to the equilibrium state but doesn't reach it fully. In the next stage, a complementary single strand DNA is added to compete for the binding of the first additional strand. Since by design, the additional strands are complementary to each other, they will form a perfect double helix which is the

lowest energy state. The meta-stable structure will then return to its initial state.

The first application that demonstrated this concept of metastable state intermediates was the development of DNA forceps[86]. The design of DNA forceps requires a DNA structure with two arms that can move so as to mimic the forceps' action. A piece of dsDNA with two sticky ends was selected as the starting DNA structure (Figure 1.4.11).

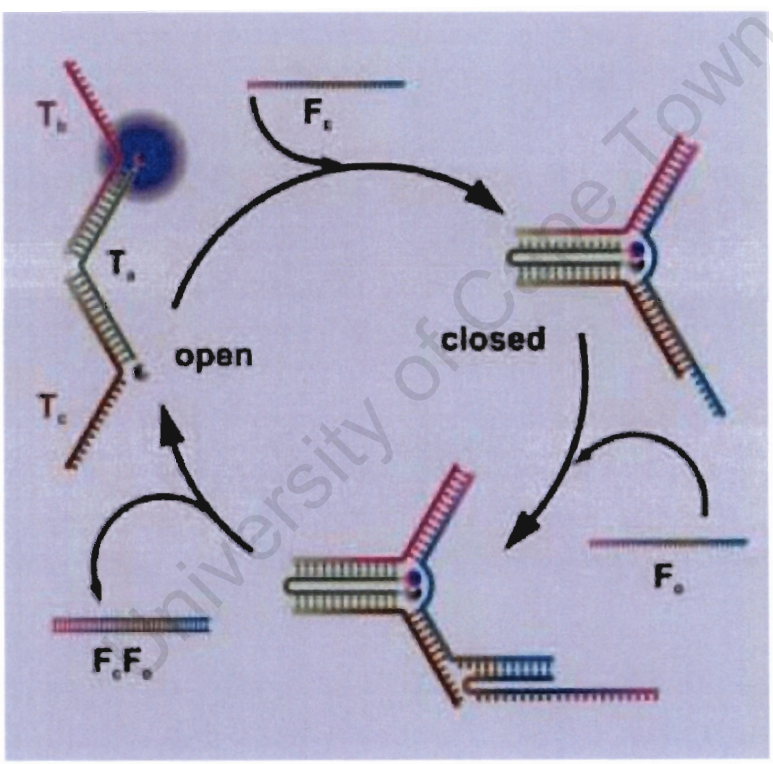


Figure 1.4.11 The mechanism of a molecular forceps made by DNA[86]. ("T" defines as the "tweezer" strand, and "F" is the fuel strand)

This dsDNA structure contains a fluorescein group attached to one of the sticky ends, and a quencher attached to the other. In order to initiate the forcep's movements, a

ssDNA was added to bind to both sticky ends forming short double helices. And this shortening of the single strand forces this structure to bend. In the bended structure, the fluorescein group and the quencher are located next to each other, and light emission was quenched. To return to the open state of the forceps, another ssDNA was added to the system which is complementary to the previous ssDNA forcing this sequence into a double helix. This results in the forceps returning to the initial state. This return to the initial state is indicated by the re-occurrence of the fluorescence.

Another example of this concept involves a piece of dsDNA with two sticky ends which is designed to be sequentially dislocated from short partially complementary single strand DNA. This results in a walking type movement of the DNA structure across the supporting platform[87]. The walking mechanism is driven by the sequential DNA hybridization of sticky ends. In this experiment, the sticky ends of this elaborate dsDNA were firstly hybridized to two neighbouring attachment sites on the platform. In a consecutive step, one of the "legs" is detached and can move to the nearest unoccupied position where it binds to the platform. Now the second "leg" is detached and free to move to the next unoccupied site, so that the walking device is re-attached to a new position on the platform (Figure 1.4.12).

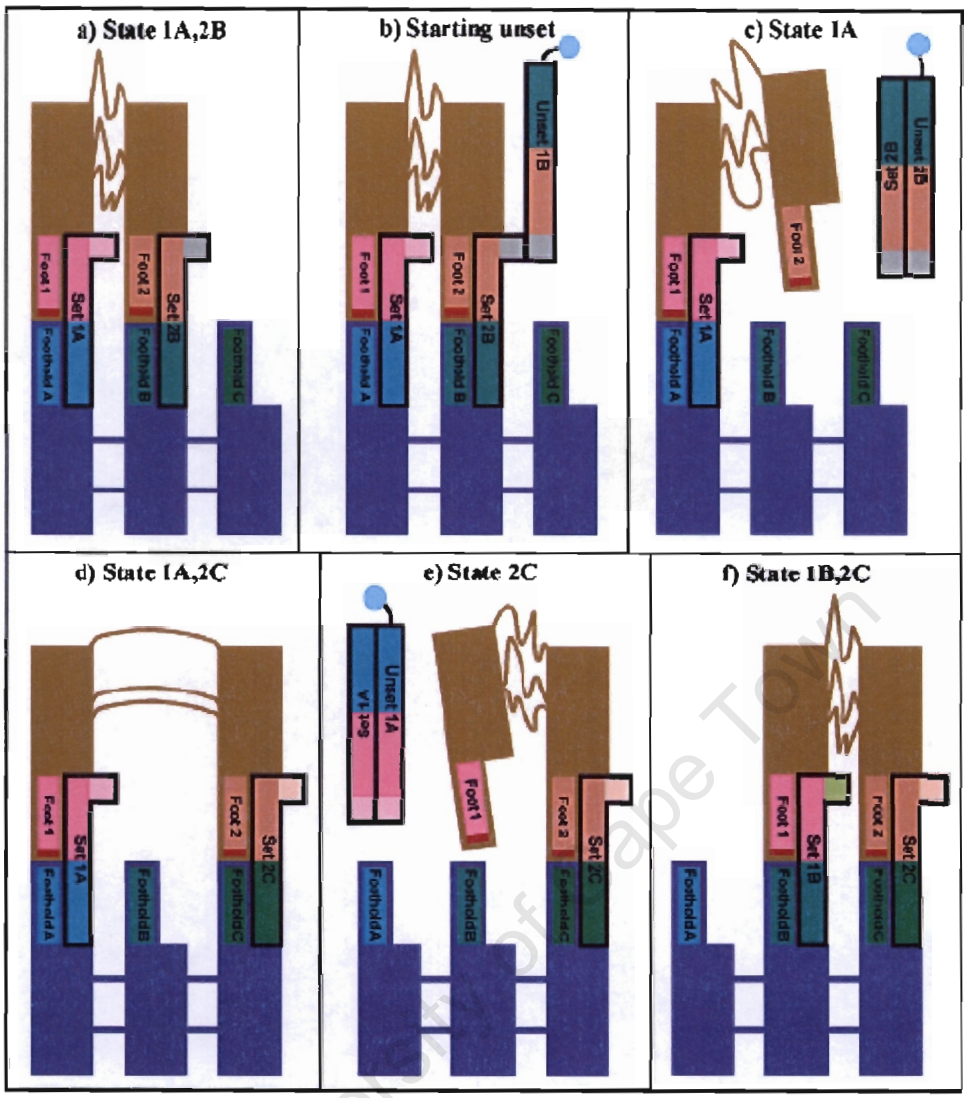


Figure 1.4.12 A biped walking DNA across the supporting platform[87].

Complementary strand displacement around two ssDNA circles has been called a molecular gear system[88]. (Figure 1.4.13)

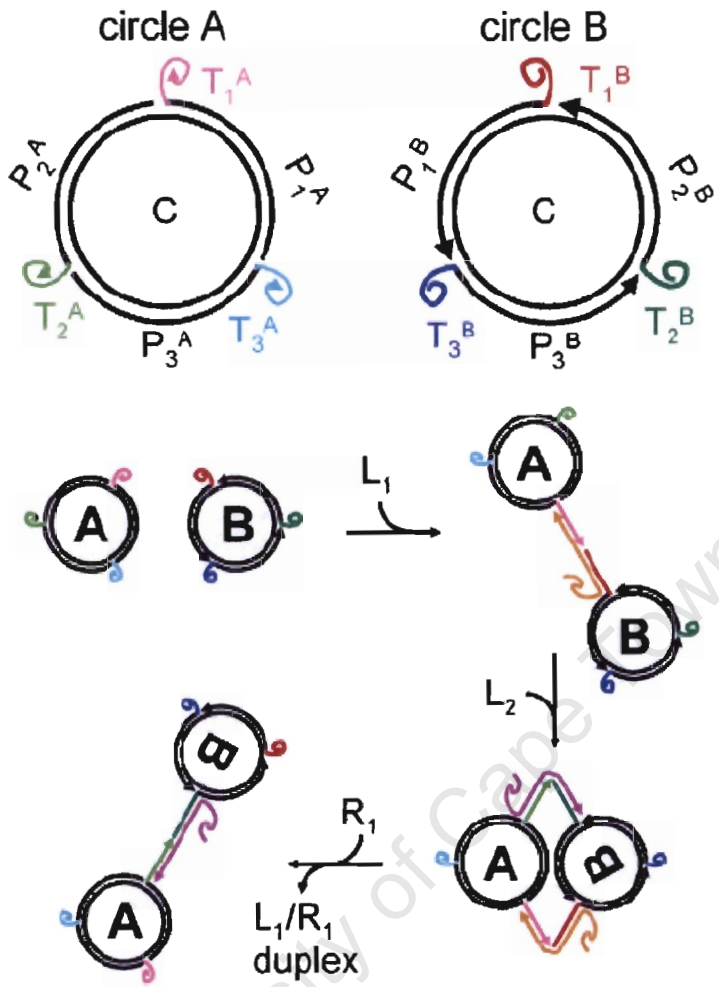


Figure 1.4.13 A molecular gear system made by two circular ssDNA and their interactions[88].



Through sequential addition of ssDNA and followed by a displacement reaction, the two ssDNA circles are rotated towards each other. This is not a continuous rotating system but takes place in stages. The added "fuel strand" are selected to be complementary to one third of the circular DNA sequence at a time. In each intermediate state, a double stranded bridging DNA helix connects to the two rings. Before one of the fuel strands can be removed, a second bridge has to be built so that

after removal of the first fuel strand, a new connection is formed between two rings. This system can be repeated through the addition of the next fuel strand.

A further example of a static DNA nanostructure is the DNA octahedron[89] which self assembles from DNA building units into a geometrical object made of 1.7 kbases. This work reported "the design and synthesis of a 1,669-nucleotide, single-stranded DNA molecule that is readily amplified by polymerases and that, in the presence of five 40-mer synthetic oligodeoxynucleotides, folds into an octahedron structure by a simple denaturation-renaturation procedure." and "DNA strands fold successfully, with 12 struts or edges joined at six four-way junctions to form hollow octahedra approximately 22 nanometres in diameter."

The formation of the aptamers can be used to create nanosystems that consist of single stranded folded DNA sequences and small molecules. These aptamer based nanosystems are designed to carry a specific protein based on the interaction between a protein and G-quartet structure[90]. The DNA was designed to contain sequences capable of forming a G-quartet structure, and the specific protein (thrombin) was found to bind to G-quartet structures specifically. In an aqueous buffer solution, thrombin forms a stable complex with the aptamer. In order to release the protein, a

complementary ssDNA was designed to hybridize the G-rich sequences to form a piece of dsDNA. This results in the G-quartet structure being unable to form and so the protein is then released from the complex. This is the first description of usage of DNA as protein transporter *in vitro*. (Figure 1.4.14)

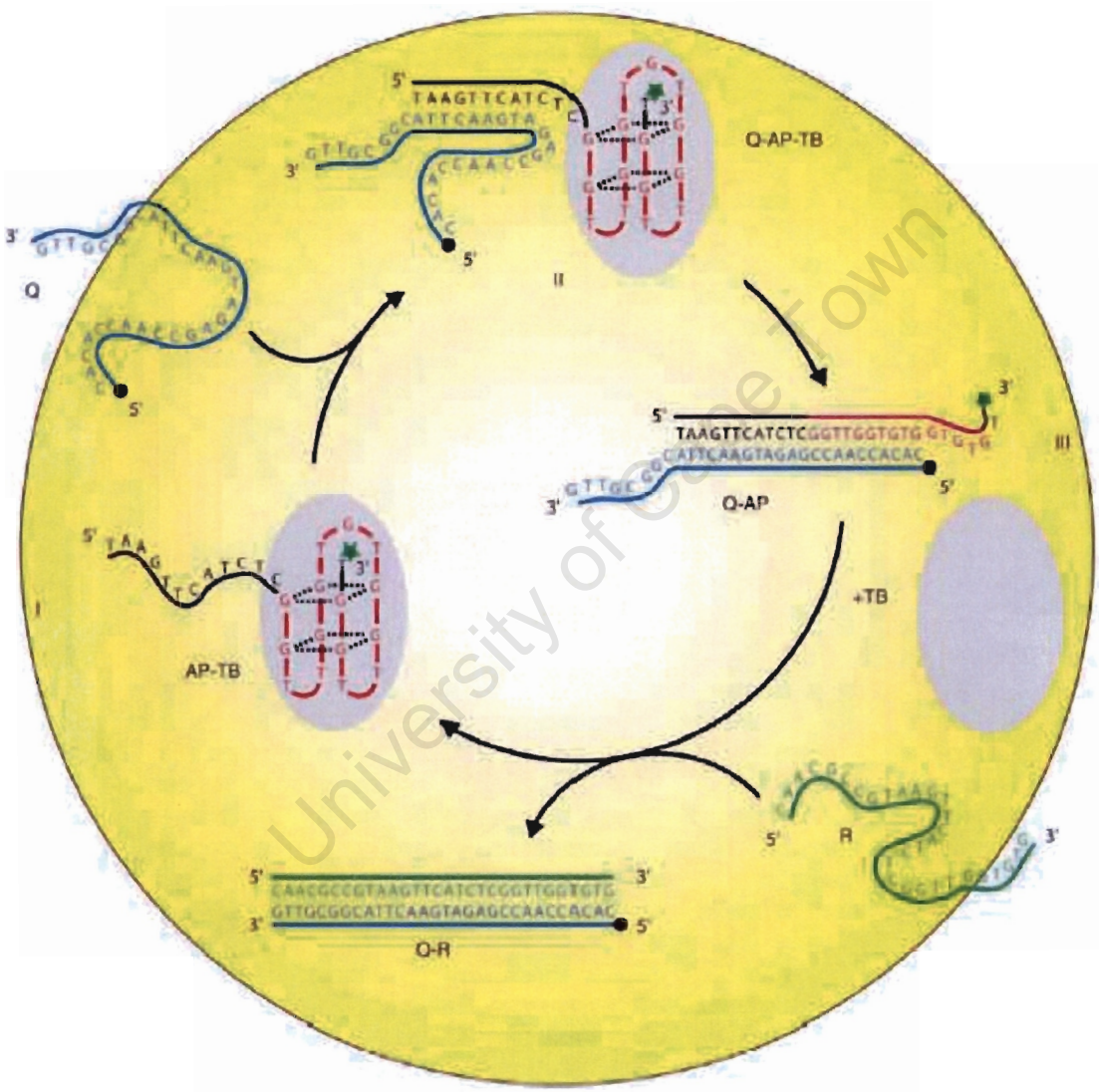


Figure 1.4.14 Thrombin conveyance system using G-quartet structure[90].

Over time, the concept of using the special properties of DNA to form complementary stable helical complexes, and at the same time allowing local binding to single

complementary ssDNA was designed to hybridize the G-rich sequences to form a piece of dsDNA. This results in the G-quartet structure being unable to form and so the protein is then released from the complex. This is the first description of usage of DNA as protein transporter *in vitro*. (Figure 1.4.14)

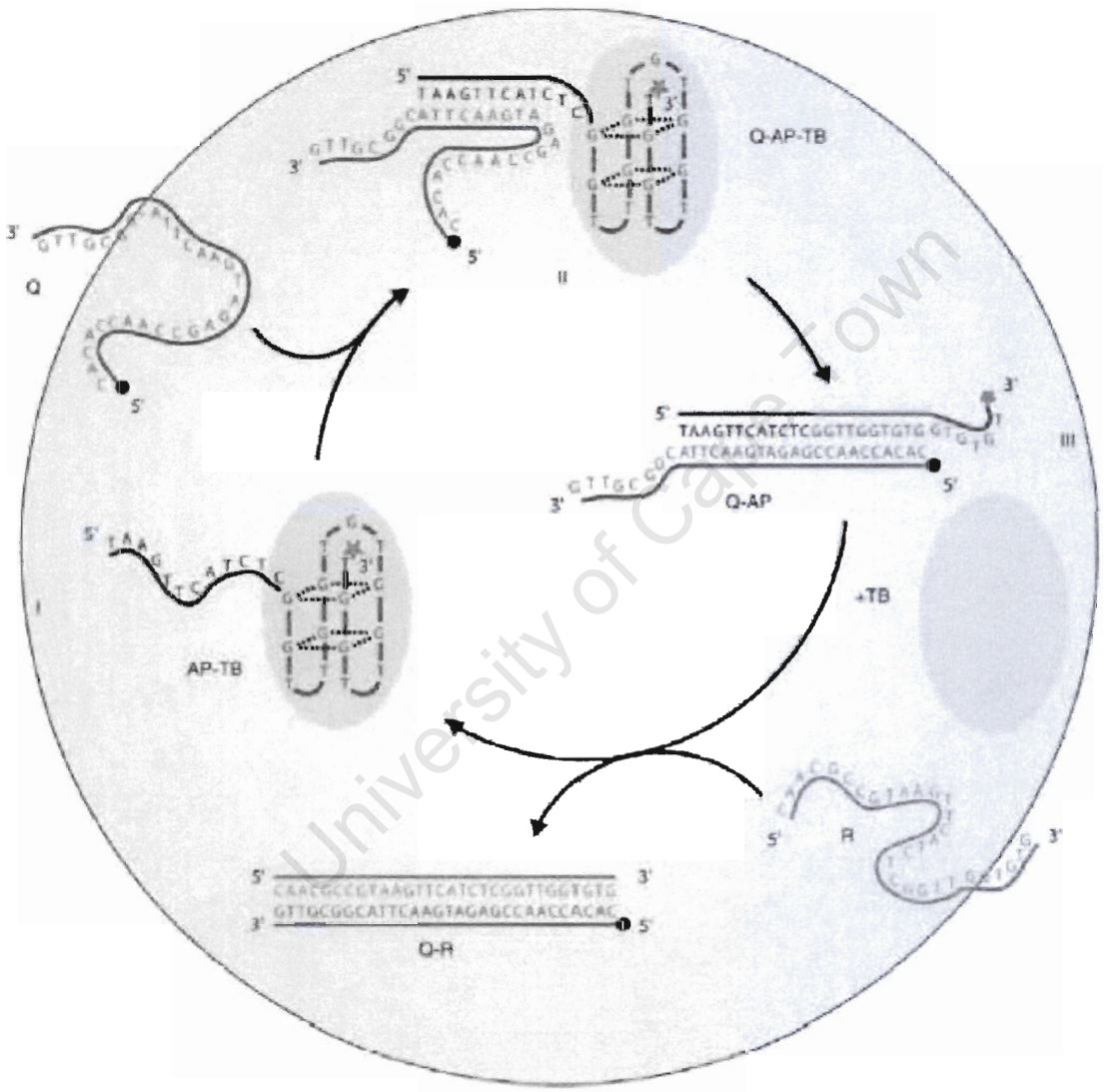


Figure 1.4.14 Thrombin conveyance system using G-quartet structure[90].

Over time, the concept of using the special properties of DNA to form complementary stable helical complexes, and at the same time allowing local binding to single

stranded sequences has evolved. And examples of this work will be described in the next section.

### 1.5 Research objectives

The aim of this research is to construct a hexagonal nano-switch using three-way junction DNA with a fluorescein group as an indicator for the switch state and the B- to Z-form transition as the mechanical base for the movement of the section of the molecule in space. Also developed was a system of nanostructures based on hairpin loop DNA to illustrate the sequential stabilization or destabilization of meta-stable states fuelled by binding various DNA sequences. Finally, a new way of linking hairpin loop structures by interactions of single strand extensions of the stem with matching sequences in the loop sequences is presented. This particular linking gives rise to a large family of two- or three- dimensional DNA structures that self assemble. This research is divided in to the following sequential phases:

1. Design and characterization of three-way junction DNA;
2. Construction of DNA networks from three-way junction DNA
3. Visualization of DNA networks by electron microscopy;
4. Design, construction and characterization of a opto-mechanical switch based on a open hexagonal DNA structure;

5. Investigation on B- to Z- DNA transition;

6. Development of meta-stable nanostructures using hairpin loop DNA;

7. Linking of hairpin loop DNA with single strand extensions;

8. Potential applications using DNA networks and these nanostructures.

The experimental work began with the use of three-way junction DNA to construct DNA networks (phase 1-3; see chapter 2). The design and the construction of the opto-mechanical switch based on similar three-way junctions is described in chapter 3 (phase 4 and 5). The meta-stable states system using DNA hairpin loops and the linkage of the DNA hairpin loop with single strand extensions are described in chapter 4 (phase 6 and 7); The discussion of applications of these DNA nanomaterials is described in chapter 5 (phase 8).

# Chapter 2 DNA network assembly using DNA three-way junction

## 2.1 Introduction

*The DNA three-way junction design*

The DNA three-way junction (3WJ DNA) consists of three ssDNAs with sequences that are partially complementary to each other. In this case of the 3WJ DNA design, each ssDNA is 16 bases long, with the first 8 bases complementary to a ssDNA and the last 8 bases are complementary to another ssDNA. This creates a 3WJ DNA with three arms consisting of 8 bp (Figure 2.1.1 left). The branch point of a 3WJ DNA has to be immobile otherwise the structure will be unstable after hybridization. The sequences of each ssDNA have to be unique and self-base pairing is not allowed. In order to link two or more 3WJ DNA, the sequences have to be designed as to contain sticky ends (SEs). The number of bases of the SE sequences in this experiment is set to 4 (Figure 2.1.1 right).

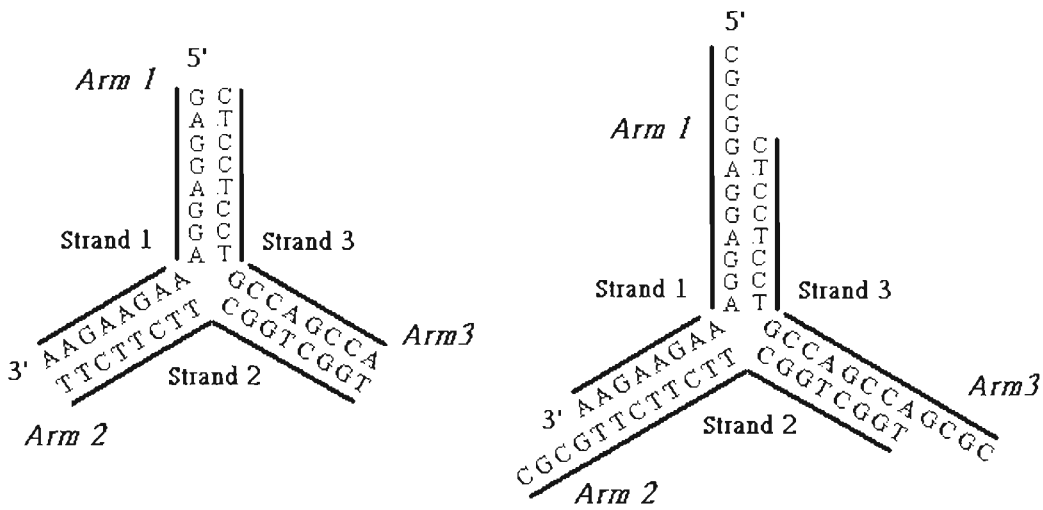


Figure 2.1.1 The schematic diagram of the three-way junction without sticky-ends (left) and with sticky-ends (right).

This result in each dsDNA becomes 20 bp long, and the distance between two branched points after annealing of SEs is two helical turns (20 bp apart). The sequences of SEs are designed to be identical to allow unlimited hybridization, and later the sequences can be re-designed to fit the experimental requirements. The number of hybridization in a 3WJ DNA system is changeable by mixing with the 3WJ DNA without SE sequences (Figure 2.1.2).

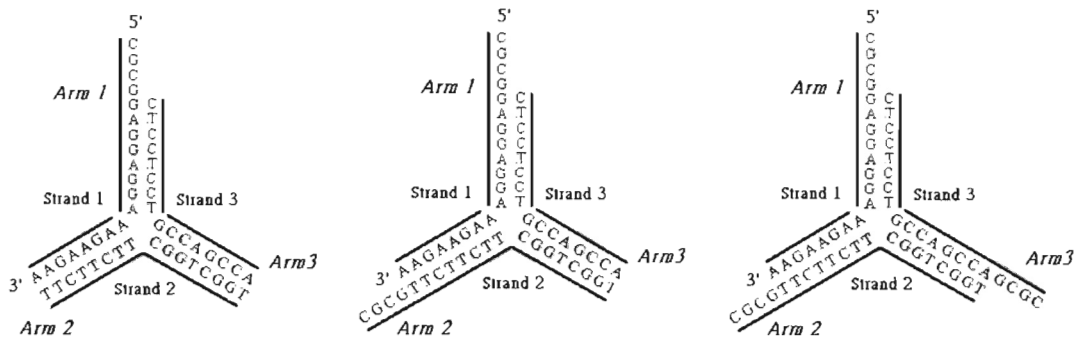


Figure 2.1.2 The schematic diagram of three-way junction DNA with different number of sticky ends: 1 sticky end (left); 2 sticky ends (middle); 3 sticky ends (right).

A 3WJ DNA can also have different SE in different arm. In later experiments, a 3WJ DNA with different SE sequences on each arm is created by hybridizing three ssDNA with different SE sequences. To link 3WJ DNA enzymatically, each ssDNA is phosphorylated prior to the ligation. The phosphorylation is carried out using T4 polynucleotide DNA kinase, and ligation is carried out using T4 DNA ligase. The ligation at a specific arm can be controlled using unphosphorylated SE, and will be described in the next chapter. The efficiency of the ligation is analyzed using polyacrylamide gel electrophoresis (PAGE) to separate the possible products.



*Thermodynamic characterization of three-way junction DNA*

In order to investigate the stability and thermal denaturation of a 3WJ, the thermodynamic analysis is performed by using Ultra-violet (UV) spectroscopy as function of the temperature. The thermodynamic profile is presented as a melting

curve. The analysis is performed on both unligated and ligated 3WJ DNA to observe the difference. The further characterization is carried out using circular dichroism (CD) spectroscopy to investigate the physical characteristics (helicity).

*Transmission electron microscopy*

The limit of resolution of a light microscope is approximately 0.2 μm, due to the interference and diffraction produced when light is passing aperture. This limit impedes the visualization of the delicate molecules created in biological systems. The size of a cell is approximately 3 or 4 μm in diameter, and the largest organelle is about a couple of hundred nm. The details of the organelles and the macromolecules that are smaller than 0.2 μm therefore can not be observed by using a light microscope. The invention of the electron microscope has solved this limitation problem. The electron microscope uses electrons as the illuminating source, with electromagnetic lenses instead of ordinary glass lenses to refract electrons. There are other features as well in the electron microscopes than features found in light microscopes. One of the features is that the system must be operated in high vacuum. In order to focus electrons to make them run smooth and un-interrupted, the electrons need to travel in vacuum to avoid the collision with air particles. The vacuum normally used in electron microscope is set between $10^{-4}$ to $10^{-6}$ torr. In principle, electrons required as electron

source in the electron microscope are generated by putting a large steady voltage on a wire. To produce such an enormous electron flow, the electron microscope contains a tungsten filament within an electron gun that is operated at a voltage of 100 KV. The electron gun is located at the top of the electron microscope. The electrons produced by the filament are focused into an electron beam through the condenser lens. There are different sizes of apertures located below the condenser lens to optimize the condensed electron beam and to reduce the possible damage to the samples. The adjusted electron beam after passing the sample goes through a series of electromagnetic lenses (objective lens, intermediate lens and projector lens) to magnify the image. The magnified image is revealed by sending the invisible electron beam onto a fluorescent plate to produce visible light. A camera is located under the fluorescent plate to take photographs of the image. The modern electron microscope can directly import images into software for further analysis.



Each 3WJ DNA used in this investigation has a dimension of approximately 5 x 5 nm, and the ligated 3WJ DNA forms larger product but is still too small to be analyzed using a conventional light microscope. Hence the structures made by 3WJ DNA are analyzed by using a transmission electron microscope (TEM). The conventional way of visualizing nucleic acid is to stain the nucleic acid with cytochrome C. But this

technique has better efficiency in visualizing large nucleic acid structure[91]. In this investigation, structures made by 3WJ DNA assembly are prepared using a surfactant chemical Benzyldimethylalkylammonium Chloride[92]. This chemical reduces the surface tension of the aqueous solution when mixing with the sample and brings DNA to the surface in order to be loaded to the electron microscope gird. DNA is then stained with uranyl acetate for visualization which provides the best visualization effect for nucleic acid[93].

*Investigation of the DNA structures produced by using different sticky ends*

In theory, a mixture of 3WJ DNA with the identical SEs should hybridize all the available SEs in a way that it grows in two dimensions. Similarly in the ligation reaction, all hybridized SEs should be ligated during a single ligation reaction. In this case, the average size of the structure made from ligating 3WJ DNAs is directly proportional to the amount of the 3WJ DNA in the reaction mixture.The structure made via 3WJ DNAs ligation is similar to a 2D crystallization. Each 3WJ start a new structure that grows exponentially. The size of the ligated structure is also directly proportional to the length of ligation time. In order to investigate the effects from these factors on the structure produced, several approaches are made to establish in the correlations between the size of the product and time or concentration. The first

approach is to investigate the effect of the ligation time; the second approach is to explore the effect of the number of SEs available in a 3WJ DNA; the third approach is to mix 3WJ DNAs containing different number of SEs in various mixing ratios; the last approach is to investigate the influence of different SEs' sequences in 3WJ DNAs.

## 2.2 Materials and methods

*Oligonucleotides sysnthesis*

The oligonucleotides listed in Table 2.2.1 were synthesized from oligonucleotide synthesis laboratory in University of Cape Town by phosphoramidate chemistry[94] using a Beckman 1000M DNA synthesizer. These oligonucleotides were design for the characterization of DNA networks.

The oligonucleotides were purified by DMT-on and DMT-off reverse-phase HPLC using an acetonitrile gradient and by cartridge methods respectively, and the amount of each oligonucleotide was determined by measuring the UV absorbance at 260nm. The corresponding OD reading of each strand was given. The extinction coefficient of each oligonucleotide was calculated spectrophotometrically at 260nm by using the following extinction coefficients: Adenine: 15400 $M^{-1}$ $cm^{-1}$; Guanine: 11500 $M^{-1}$ $cm^{-1}$; Cytosine: 7400 $M^{-1}$ $cm^{-1}$; and Thymine: 8700 $M^{-1}$ $cm^{-1}$ [95]. All oligonucleotides were checked using denaturing gel electrophoresis for the remaining level of failure sequences in relation to the full-length sequences. They were found to be of high purity. The oligonucleotide concentrations were calculated using Beer-Lamberts Law and the stock solutions were made to a final concentration of 100 μM in sterile Milli-Q water and stored in -20℃ for experimental use.

| Name | Sequence (5' to 3') | $\varepsilon$ ($M^{-1}$ $cm^{-1}$) |
|---|---|---|
| 01B1 | GAGGAGGAAAGAAGAA | 219100 |
| 02B1 | TTCTTCTTCGGTCGGT | 145200 |
| 03B1 | ACCGACCGTCCTCCTC | 146500 |
| 01S1 | CGCG GAGGAGGAAAGAAGAA | 256900 |
| 02S1 | CGCG TTCTTCTTCGGTCGGT | 183000 |
| 03S1 | CGCG ACCGACCGTCCTCCTC | 184300 |
| 01S2 | GCGC GAGGAGGAAAGAAGAA | 256900 |
| 02S2 | GCGC TTCTTCTTCGGTCGGT | 183000 |
| 03S2 | GCGC ACCGACCGTCCTCCTC | 184300 |
| 01S3 | GCAT GAGGAGGAAAGAAGAA | 262100 |
| 02S3 | GCAT TTCTTCTTCGGTCGGT | 188200 |
| 03S3 | GCAT ACCGACCGTCCTCCTC | 189500 |



Table 2.2.1: Details of the oligonucleotides synthesized by the DNA synthesis laboratory, University of Cape Town.

*Three-way junction DNA sample preparation*

The 3WJ DNA samples were prepared by mixing three oligonucleotides with sequences that are partially complementary to each other in a 1:1:1 ratio. The

oligonucleotides were mixed with appropriate buffer solutions as indicated in the experiments to fulfill the criteria. The corresponding 3WJ DNA sample was pre-heated to 80℃ for 5 minutes, and cooled down to room temperature for 10 minutes prior to any experiments or stored at 4℃.

*Ultraviolet melting analysis with temperature gradient*

Ultraviolet melting analyses were performed by using a Pye-Unicam SP1700 spectrophotometer with a custom made heating device. The UV absorbance (at 260nm) was recorded in 0.2℃ increments at a rate of 1℃/min. Oligonucleotides were mixed according to the specific experiment criteria and the concentration of each oligo mixed in different samples was adjusted to 1.5 μM with the buffer containing 1 M NaCl, 10 mM Tris and 5 mM phosphate at pH 7.0. The temperature range of each scan is basically from 20 to 100℃ unless specified. Each analytic scan was repeated twice and the melting temperature was obtained by the curve-fitting program[96]. Thermodynamic calculations of each sample were carried out using Microsoft Excel program.

*Circular Dichroism Spectroscopy*

CD analyses were performed by using a Jasco J-810 spectrophotometer with a

HAAKE temperature regulated water bath. Each analysis was carried in a wavelength range from 200 to 320 nm at a scanning speed of 100 nm per minute, and an accumulation of 10 scans. The scanning temperature was set at the room temperature or as otherwise noted according to the experimental criteria. The sample profile was plotted from imported data by using Microsoft Excel program.

*Polyacrylamide Gel Electrophoresis (PAGE)*

Native gel electrophoresis:

The native polyacrylamide gels were made up from the following stock solutions: 40% polyacrylamide solution (acrylamide/bis-acrylamide, 19:1), 10% ammonium persulphate (AMPs), 5x TBE (445 mM Tris, 445 mM boric acid and 1.25 mM EDTA) solution pH 7 and diluted with sterile water to an appropriate volume according to the number of samples loaded. The migration properties of a gel can be adjusted by changing the amount of the polyacrylamide solution in the mixed gel solution. The polymerization of the gel was obtained by addition of TEMED. The electrophoresis was performed either at room temperature or at 4℃ at the electrical field of approximately 10 V/cm for at least 3 hours depending on the length and the density of the gel. In a cationic PAGE, cation solution was replaced by specified amount and concentration of cationic solution to fulfill the experiment criteria. The native PAGE

samples were mixed with sample loading buffer containing bromophenol blue and ficoll at a ratio of 6:1 (v/v). The gel was stained using an ethidium bromide solution of a concentration of 5μg/ml for 10 minutes before digital recording. Digital recording was performed by visualizing stained DNA bands on a UV light box. The recorded images were scanned and saved as a Microsoft TIFF image.

Denaturing gel electrophoresis:

Denaturing polyacrylamide gel was made to a concentration of 20% with the same reagents as the native gel, but a fixed concentration of urea (final concentration of 7M) was added. The electrophoresis was performed at room temperature at high voltage (150~200V) for 2 hours. The denaturing PAGE samples were mixed with denaturing sample loading buffer containing either urea or formamide in the same ratio as in the native gel. The gel was stained in a "stains-all" solution containing water and formamide in the ratio of 1:1 for 45 minutes, and the de-stain procedure was done by placing the gel in water and exposing it to light for several hours. The digital recording was performed by visualizing stained DNA bands on a normal light box. The recorded images were scanned and saved as a Microsoft TIFF image.

*Agarose gel electrophresis*

50 ml of a 0.5% agarose gel was made by dissolving 0.25g of agarose in 50 ml 1x TBE buffer. The electrophoresis was performed at room temperature with a constant voltage of 60V for 1 hour. The loading sample was prepared in the same way as for the native gel electrophoresis experiment. The staining and the digital recording procedures are identical as to those described for the native gel electrophoresis experiment.

*Oligonucleotides phosphorylation*[29]

Oligonucleotides were phosphorylated by using T4 polynucleotide kinase purchased from Roche. Each oligonucleotide was mixed with 1X kinase buffer, 1 mM ATP, and appropriate unit of T4 polynucleotide kinase. Each mixed sample was incubated at 37℃ for 1~16 hours to ensure complete reaction. The phosphorylated samples can be transferred directly to the ligation process.

*Oligonucleotides ligation*[30]

The phosphorylated oligonucleotides were specificly mixed to generate 3WJ DNA (refer to sample preparation in 2.2.1). Each phosphorylated 3WJ DNA sample was mixed with appropriate 3WJ to anneal their particular sticky ends. The ligation

process was carried out on the latent network using T4 DNA ligase purchased from Roche. The amount of T4 DNA ligase used in each ligation experiment was according to the concentration determined in the test runs. The ligated samples were heated to 80℃ for 5 minutes to stop the enzymatic activity and the ligated DNA was precipitated by using *n*-butanol, and purified using phenol extraction and ethanol wash. The purified DNA was dried using Speedi-vac and re-suspend in water or buffer solution for storage or further experimental use.

*Transmission electron micrsocopy*

Sample preparation:

10 µl of each DNA sample (500 ng/µl) was mixed with 40 µl of benzyldimethylalkylammonium chloride (BAC) using a droplet method for 10 ~ 50 minutes, and a carbon grid was suspended on the surface of the mixed drop for 10 minutes. The excess solution was removed from the grid by filter paper, and the sample was stained in a staining solution containing 0.5 mM uranyl acetate, 0.5 mM HCl and 90% ethanol by dipping the grid into in for 20 seconds. The excess stain was removed by filter paper and the grid was further washed using 90% ethanol for 15 seconds. The grid was air-dried on filter paper and ready for visualization.

Electron microscopic visualization:

DNA samples were visualized using a LEO 912 transmission electron microscope using conventional brightfield and darkfield method. Sample images were photographed using esiVision Pro software from Soft Imaging System (Image Sys) and saved as TIFF images.

## 2.3 Results

### 2.3.1 Thermal unfolding analysis of unligated three-way junction DNA

The 3WJ DNA was produced by mixing the three oligonucleotides 01S1, 02S1, and 03S1 (Table 3.2.1) in a 1:1:1 ratio in the solution containing 1 M NaCl, 10 mM Tris and 5 mM phosphate, pH 7. The mixed sample (sample A1) was pre-heated at 80℃ to avoid any possible non-specific folding patterns to assume a randomly coiled conformation, and cooled to room temperature to ensure the specific annealing. Sample A1 was analyzed by UV spectrophotometer to observe the hyperchromic shift as the function of the temperature. The melting profile showed a single transition with a melting temperature of approximately 36.9℃ (Figure 2.3.1). The transition represented the dissociation of 3WJ DNA sample A1 into three single stranded oligonucleotides.

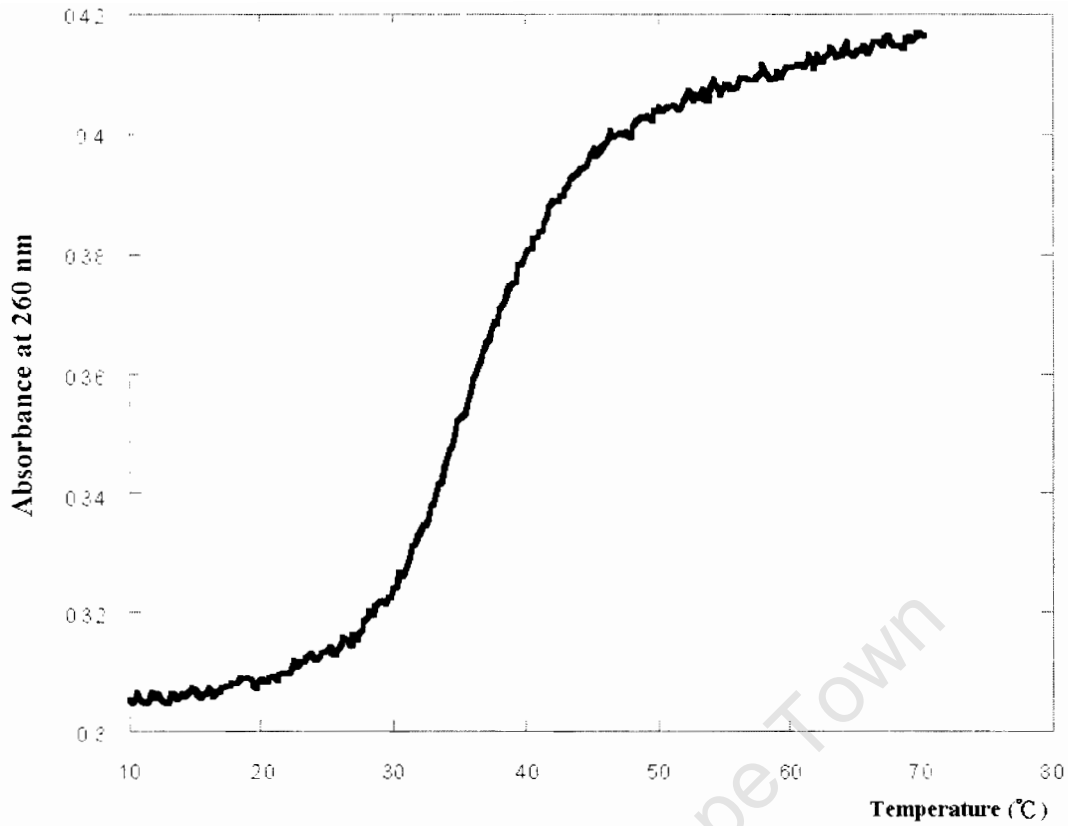


Figure 2.3.1 The UV thermal unfolding analysis (at 260nm) as function of temperature of the sample A1 in 1 M NaCl, 10 mM Tris and 5 mM phosphate buffer, pH 7.



### 2.3.2 DNA three-way junction ligation

The 5'-end of oligonucleotides 01S1, 02S1, and 03S1 were phosphorylated using T4 polynucleotide kinase (refer to method). These phosphorylated oligonucleotides were mixed to form 3WJ DNA (S1 3WJ DNA) as previously described. The ligation process was carried out at the room temperature after the phosphorylation step. The ligated phosphorylated 3WJ DNA (sample A2) was checked using native gel electrophoresis in comparison with the unligated sample A1. The size of the ligated

product was too large to be separated using PAGE (data not shown). And the size of the ligated sample was determined in a separate experiment using 0.5% agarose gel (Figure 2.3.2). The result showed the size of the ligated 3WJ DNA was over 30Kb.


Figure 2.3.2 A 0.5% agarose gel separating unligated and ligated three-way junction DNA.

### 2.3.3 Thermal unfolding analysis of ligated three-way junction DNA structures

Ligated sample A2 after purification was re-dissolved in the same buffer used for example A1 for the thermal unfolding analysis. The thermal unfolding analysis was performed using the same conditions and methods described previously. The UV melting profile of sample A2 showed a single extended transition with the melting temperature approximately at 74.9°C (Figure 2.3.3).

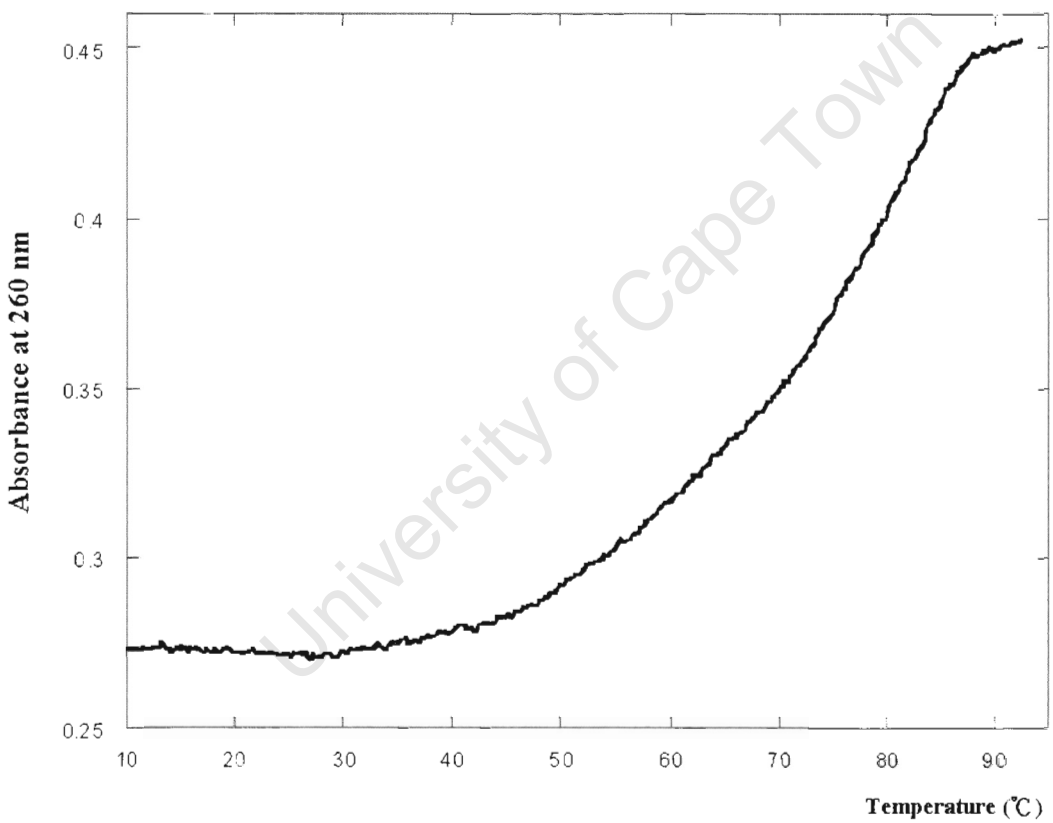




Figure 2.3.3 The UV thermal unfolding analysis (at 260nm) as function of temperature of the sample A2 in 1 M NaCl, 10 mM Tris and 5 mM phosphate buffer, pH 7.

### 2.3.4 Electron microscopy observation on ligated three-way junction DNA

The gel electrophoresis was not the appropriate method for the determination of the ligated DNA structure. Sample A2 was analyzed using transmission electron microscopy to observe the structures/pattern. The electron micrographs of sample A2 showed a large network created by ligated 3WJ DNA (Figure 2.3.4). The structure of the DNA network in sample A2 observed was irregular, but the pattern of the network was created by linkage of polygonal shapes such as pentagonal or hexagonal rings created by three-way junction DNA. Figure 2.3.5 showed both pentagonal and hexagonal ring structures that were observed as the underlying linkage pattern in the 3WJ DNA network.

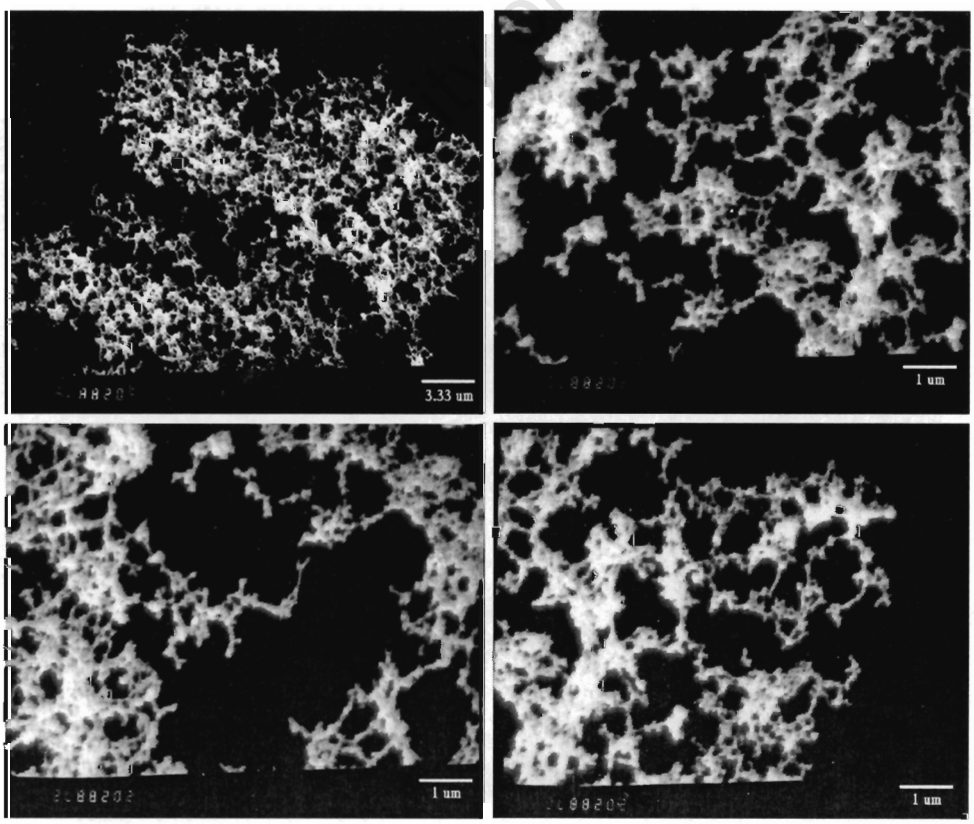


Figure 2.3.4 The electron micrograph of ligated three-way junction DNA sample A2.

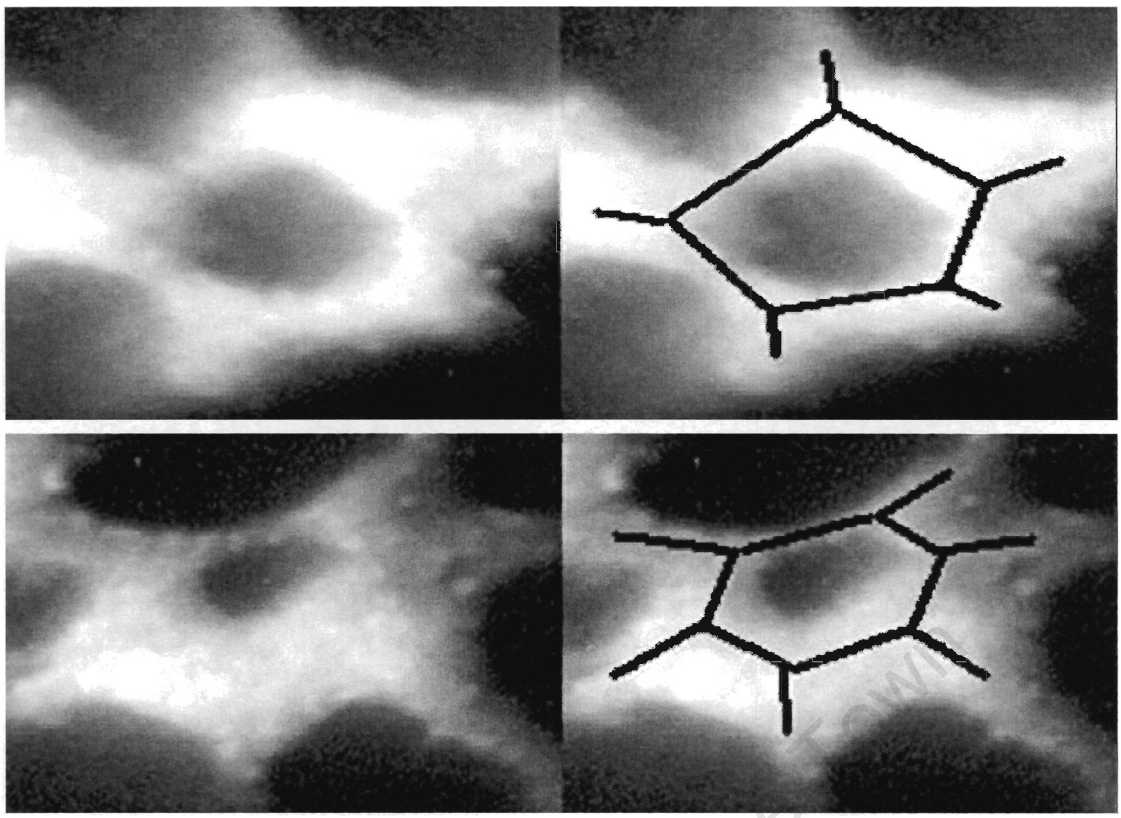

Figure 2.3.5 The electron micrograph of the pentagonal (top) and hexagonal (bottom) rings as the linking pattern observed in DNA network.



### 2.3.5 Control in size of three-way junction DNA network

*Time series experiment*

To investigate the relationship between the ligation time and the size of the ligated structure, an experiment was set up to allow ligating the same amount of three-way junction DNA for different length of time. The three-way junction DNAs were ligated for 5, 10, 20, 30 and 60 minutes. The ligation of each sample was stopped by heating the sample to 80℃ for 5 minutes. These samples were purified and the structures produced were checked by using native gel electrophoresis (Figure 2.3.6).

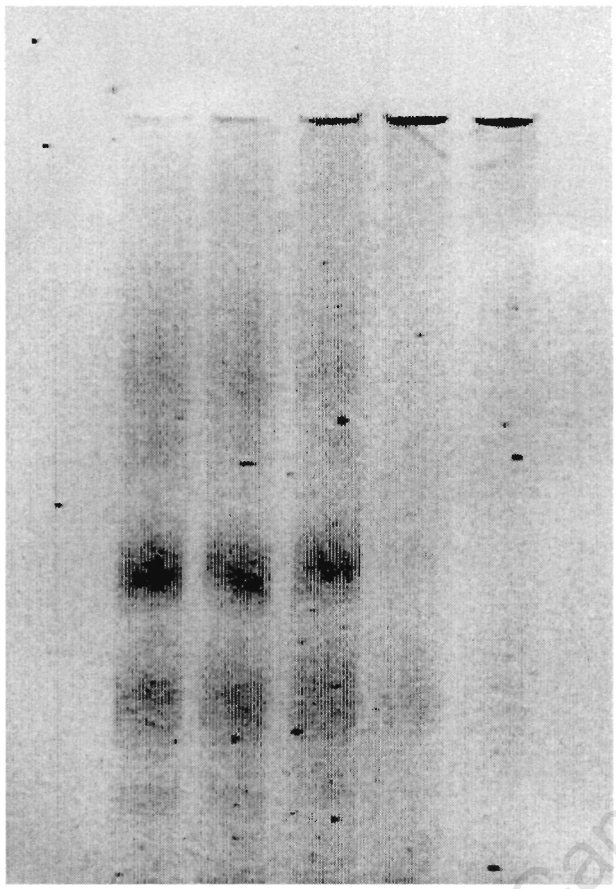


Figure 2.3.6 Ligation of three-way junction DNAs for different length of time (6% gel). Lane 1: ligation time of 5 minutes; lane 2: 10 minutes; lane 3: 20 minutes; lane 4: 30 minutes; lane 5: 60 minutes.



The gel result showed a decreasing in small fragments and an increasing in large fragments with time increment (at the top of the gel, the increasing intensity is a sign for larger and larger networks).

*Experiment using different number of sticky ends*

A set of oligonucleotides with blunt ends (01B, 02B and 03B, Table 2.2.1) was synthesized as candidates for the control of the size of 3WJ DNA network. Starting

with the first set of oligonucleotides, these blunt ended oligonucleotides were mixed in different amount to generate different number of sticky ends in the 3WJ DNA mix (ie. mixing 01B, 02B and 03S1 to generate a 3WJ DNA with a sticky end on one arm only). Hence to observe the effect of changing the network size, and these 3WJ DNA were ligated in different ratios. Table 2.3.5 shows the mixing ratio of different number of sticky ends in oligonucleotides present in each ligation experiment.

| Sample in lane | Oligonucleotide ratio | | |
|---|---|---|---|
| | 1 SE | 2 SEs | 3 SEs |
| 1 | 1 | - | - |
| 2 | 2 | 1 | - |
| 3 | 1 | 1 | - |
| 4 | 1 | 2 | - |
| 5 | - | 1 | - |
| 6 | - | 2 | 1 |
| 7 | - | 1 | 1 |
| 8 | - | 1 | 2 |
| 9 | - | - | 1 |
| 10 | 3 | - | 1 |
| 11 | 1 | - | 1 |
| 12 | 1 | - | 3 |
| 13 | 3 | 2 | 1 |
| 14 | 3 | 1 | 2 |
| 15 | 2 | 3 | 1 |
| 16 | 1 | 1 | 1 |
| 17 | 2 | 1 | 3 |
| 18 | 1 | 3 | 2 |
| 19 | 1 | 2 | 3 |

Table 2.3.5 The ligation samples with different number of sticky ends of 3WJ DNA mixed in different ratios.

The ligated DNA of each experiment was analyzed using 6% native PAGE to observe the DNA network size. The result is shown in Figure 2.3.7.

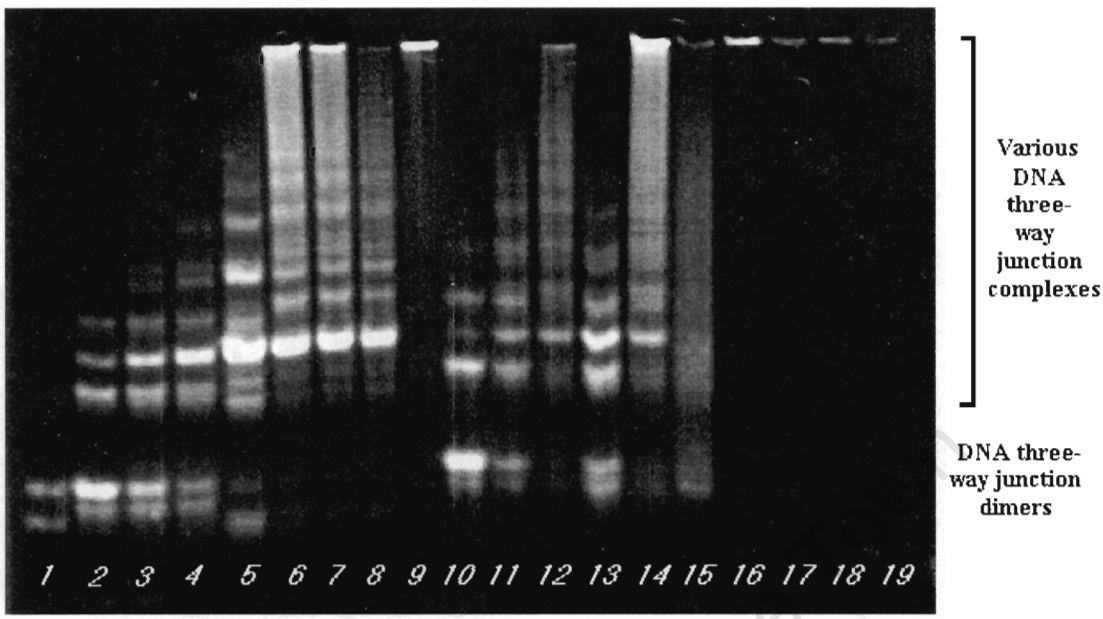


Figure 2.3.7 The native PAGE of the ligated samples mixed in different sticky ends ratios.

In the gel, lane 1 contains the sample with one sticky end (1SE) in each 3WJ DNA, and the ligated DNA was the smallest among all the samples; lane 2 contains the sample with 1SE 3WJ DNA and two sticky ends (2SEs) 3WJ DNA in 2:1 ratio, and the ligated DNA showed after additional larger fragments compared to the first sample; lane 3 and lane 4 contain the same samples as lane 2 but with 1SE to 2SEs 3WJ DNA mixing ratio of 1:1 and 1:2 respectively. The result showed the same bands already present in lane 2 but an increase in fragment size from lane 3 to lane 4; lane 5 contains the sample with 2SEs in each 3WJ DNA, and the ligated DNA showed yet

fragments larger than previous samples; lane 6 to lane 8 contain the samples with 2SEs and 3SEs 3WJ DNA mixed in a ratio of 2:1, 1:1 and 1:2 respectively. The result showed similar pattern to those in lane 2 to lane 4, but in addition much larger fragments which remained in the well; lane 9 was the sample with 3SEs 3WJ DNA only, and the result was identical to the data shown in 2.3.2. This was a DNA network that couldn't be separated by gel electrophoresis; lane 10 to lane 12 represents the bands of the samples of 1SE and 3SEs 3WJ DNA mixed in the ratio of 3:1, 1:1, and 1:3 respectively. The fragment patterns showed an increase in fragment size from lane 10 to lane 12, and the fragment sizes were in general larger than in lane 2 to lane 4 but smaller than in lane 6 to lane 8; lane 13 to lane 19 contain samples of 1SE, 2SEs, and 3SEs 3WJ DNA mixed in different ratio (refer to Table 2.3.5). These samples showed various DNA fragments but most of them were too large to be separated and remained in the wells.



The next experiment was to mix the three-way junction DNA with 2SEs and 3SEs in 4:3 ratio and ligate them for different length of time. The time each sample spent before it was stopped to ligate further was identical to the time series experiment. The ligated samples were analyzed using 6% PAGE and were found too large to be separated (data not shown). These samples were then examined using transmission

electron microscope. The results are shown in Figure 2.3.8.

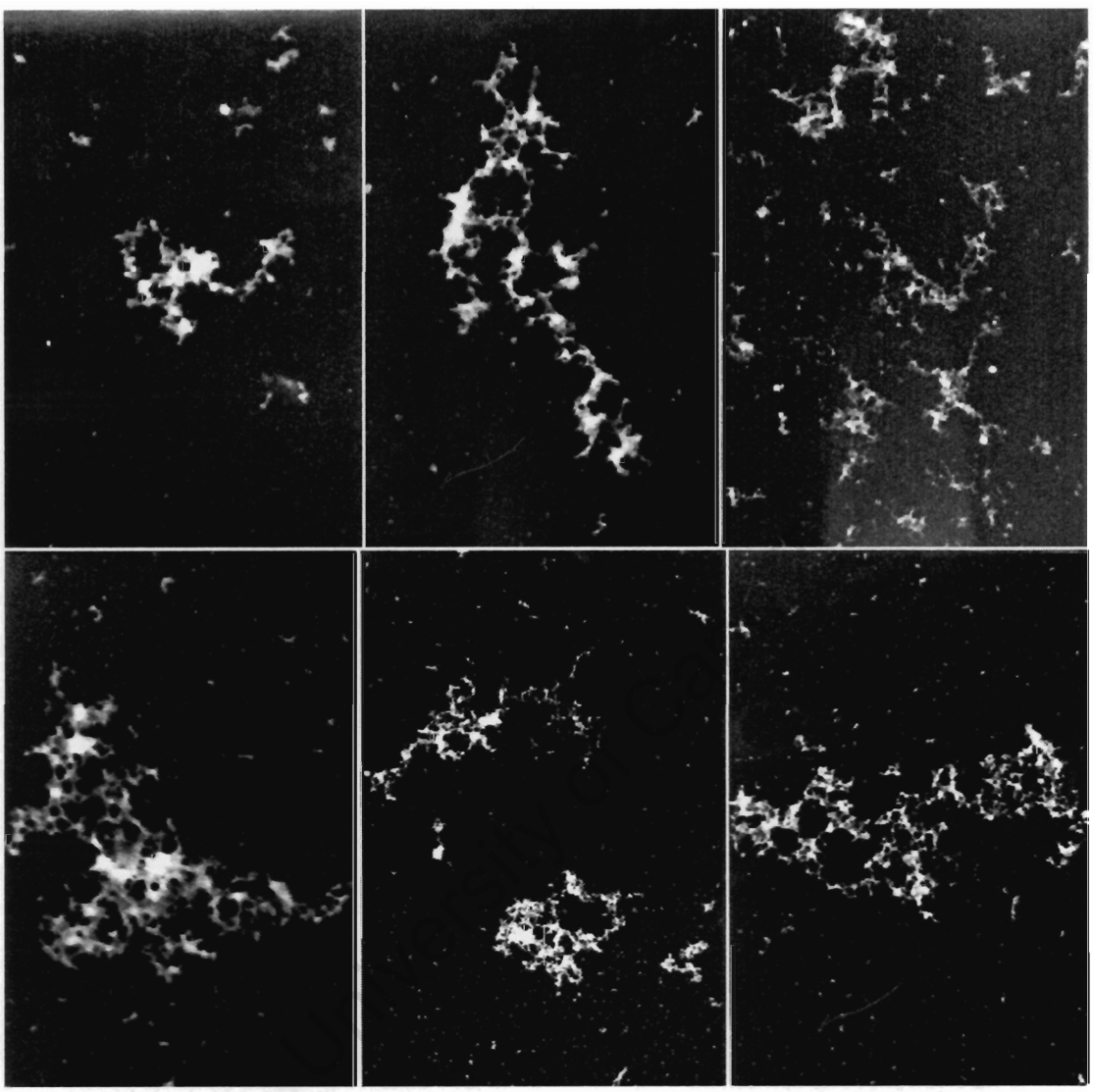

Figure 2.3.8 The electron micrograph of three-way junction DNA with 2SEs and 3SEs mixed in 4:3 ratio at different ligation time. Top-left: 5 minutes ligation time (1 in 25000); top-middle: 10 minutes (1 in 25000); top-right: 20 minutes (1in 16000); bottom-left: 30 minutes (1 in 25000); bottom-middle and right: 60 minutes (1 in 16000)

Two sets of oligonucleotides with different sequences of sticky ends (01S2, 02S2, 03S2 and 01S3, 02S3, 03S3) were synthesized to investigate the parameters that

control the size of ligated DNA networks. These oligonucleotides were phosphorylated for the ligation procedure and the phosphorylated oligonucleotides were pre-mixed in 1:1:1 ratio separately to form the three individual 3WJ DNA (S2 and S3 3WJ DNA) with three sticky ends. These 3WJ DNAs were then mixed in different ratio again to form different sizes of DNA networks (data not shown).

## 2.4 Discussion

The formation of 3WJ DNA is spontaneous and the structure formed is stable at room temperature (Tm ~ 36.9℃). The highly cooperative transition of the 3WJ DNA indicates that the melting start in all three arms and not preferentially from any particular arm.

Comparing the thermal unfolding process of unligated and ligated 3WJ DNAs, it is obvious that the stability was increased in ligated networks as the consequence of the ligation. The melting point is shifted from 36.9℃ to 74.9℃. This observation is supported by the results of the gel electrophoresis experiment where large structures are observed. This interpretation is further supported by analyzing the ligated structure using transmission electron microscope. The large DNA network made by three-way junction DNA was observed. The frame of the DNA network was based on the joining of pentagonal and hexagonal DNA rings that in turn are made by three-way junction DNA. The joining of these polygonal rings leads to a topological system that is three-dimensional and therefore resulted in a non-planar structure of a DNA network. The growth of a DNA network can be controlled by using ligation time variation and variation of the number of sticky ends in a 3WJ building unit. The size of ligated 3WJ is directly proportional to the ligation time. This is only valid when sticky ends in three-way junction DNAs are still available to be ligated. Once all

three-way junction DNAs are ligated, the ligation time will no longer effect the size.

The size of DNA network is also affected by the number of the sticky ends in a 3WJ that is unit building block for the networks. Ligation of three-way junction DNA containing 1 sticky end only, the structure produced can only be a three-way junction DNA dimer. With an increased number of the sticky ends in a single three-way junction DNA, the size of the network produced increases. Therefore the three-way junction DNA with 1 sticky end can be used as the inhibitor to control the size of DNA network.

A three-way junction DNA with two sticky ends provides two ligation sites when ligating, where a three-way junction DNA with three sticky ends provides three. Theoretically, by mixing these two DNAs in a ratio of 4:3 (2SEs to 3SEs), a family of structure could be formed (hybridization between 8 sticky ends and 9 sticky ends) and the linking pattern could be studied. The structure created remains a mixture of irregular patterns. The random hybridization between mixed three-way junction DNAs is more favourable than a single ordered linking pattern.

The number of DNA networks created using three-way junction DNA is large and

produces many variants. The design and the use of the sequences within the DNA network are important when one aims at specific applications, which will be further discussed in chapter 5.

# Chapter 3 Opto-mechanical hexagonal DNA nanoswitch

## 3.1 Introduction

*Hexagonal DNA nanoswitch construction*

Molecular mechanical devices made by DNA utilize the native or modified specific properties of DNA, and use them as the driving forces to run the process (refer to chapter 1). In this case, an opto-mechanical hexagonal DNA nanoswitch assembled from three-way junction DNAs utilizes conformational change from B- to Z-form as the drive of a mechanical switch mechanism. The device consists of six DNA three-way junctions that contain an unique linking sequence each to connect them in a particular way to form a two-dimensional hexagonal DNA ring structure. Two of the six DNA three-way junctions are specially designed to contain fluorescent and quencher groups respectively. The fluorescent and quencher molecules are used as indicators for different switching states. The device contains a particular section that allows the induction of a conformational change of a linking sequence when the environmental conditions change. This conformational change is based on one of the unique property of selected DNA sequences that can change helical handedness from a right-handed to a left-handed conformation. The particular sequence is sensitive to the salt concentration in the environment. When the cation concentration increases to

a certain level the sequence is forced to change into another conformation that is more stable under such conditions. The switching mechanism in the ring is driven by this conformational change. The quencher and fluorescent group are designed to face each other in the initial state so that the fluorescence is quenched. This represents the "OFF" state. With changing salt concentration from low to high, the conformation of a particular sequence changes its helical handedness causing the fluorescent group to move away from the quencher. This move causes the increase in fluorescence intensity of the system. This represents the "ON" state.

Therefore six sets of three-way junction DNAs are required for this construction. Each set is designed to contain at least one sticky end (SE), and sequences of each SE in a set are identical. Set 1 and 2 are designed to contain one SE with a $(CG)_3$ sequences that is responsible for B-form to Z-form DNA conversion, and another SE to link it with set 4 and 3 respectively. Set 3 is designed to contain SEs that link to set 2 and 6, where as set 4 is designed to connect with set 1 and 5. Set 5 and 6 are designed to contain one SE to link with set 4 and 3 respectively. A fluorescein group and a quencher are attached to set 6 and set 5 respectively as indicators for the different switching states. These sequences are designed in such a way that corresponding SEs are hybridized. It will generate an open ended hexagonal ring

structure with the fluorescein group and the quencher facing each other on the open side of the ring and the sequences that cause the change to the Z-form DNA is on the opposite side of the indicators (Figure 3.1.1).

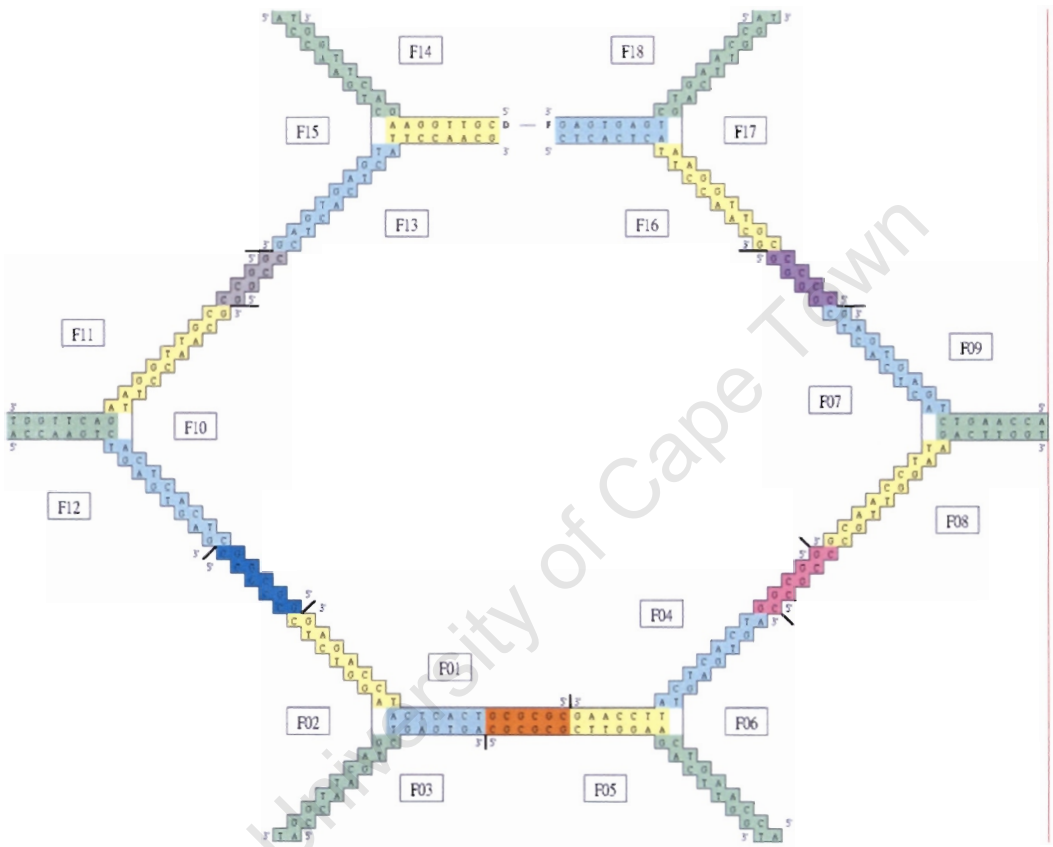


Figure 3.1.1 An overview of a hexagonal nano-switch consists of six sets of 3WJ DNA. (The fluorescent and the quencher groups are attached to F18 and F14 respectively)

The construction method is based on the ligation directed by outer strands to inner strands.

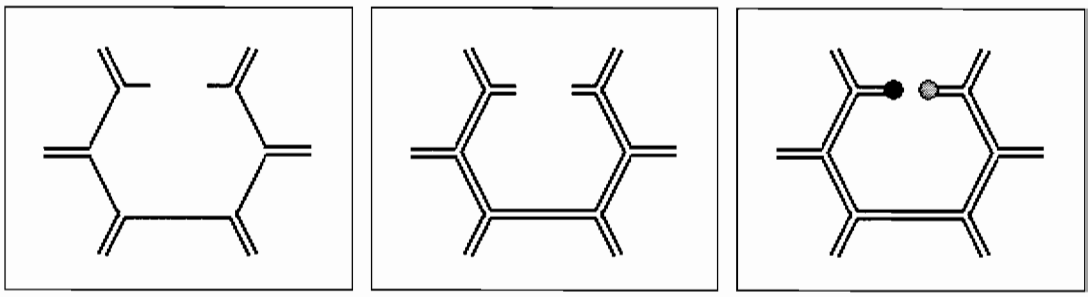

Figure 3.1.2 The schematic diagram demonstrating the construction of hexagonal DNA from outer strand to inner strand. (Left: the combination of outer strands through ligation; middle: the hybridization of inner strands with outer strands; right: addition of strands containing the fluorescent and the quencher group)

The first step requires a single SE ligation. A single SE ligation requires only one SE that is capable to be ligated, and the principle behind this step is the phosphorylation state of SEs. When creating a set of 3WJ DNA, the formation is done by mixing a phosphorylated ssDNA with SE sequences, an unphosphorylated ssDNA with other SE sequences, and a blunt end ssDNA. This generates a 3WJ DNA with two SEs that one of them is capable to be ligated. By ligating this 3WJ DNA with another 3WJ DNA containing corresponding SE (unphosphorylated), an outer strand contains specific SE sequences can be obtained after ligation by using denaturing PAGE (Figure 3.1.3).

The second step is a directed inner strand ligation by outer strands. This ligation is done by ligating two sets of 3WJ DNA first by hybridizing corresponding phosphorylated ssDNA with outer strands, and then ligating the ligated sets of 3WJ DNA by the final outer strand (Figure 3.1.4). The construction is completed by the

addition of two ssDNA containing fluorescein and quencher groups. The switching process is recorded based on the fluorescence intensity change as the structure is converted from B-form to Z-form.

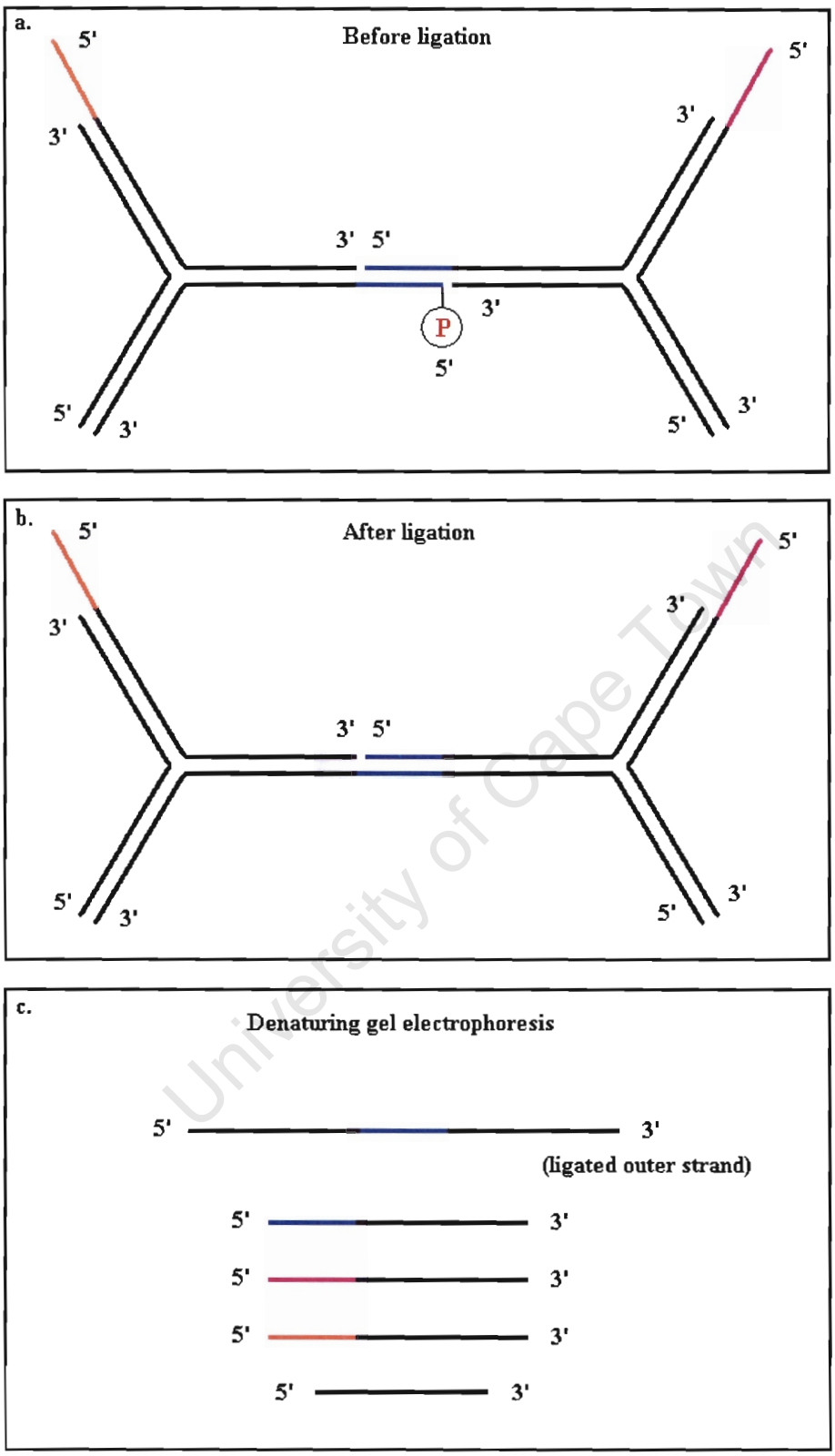


Figure 3.1.3 The outer strand ligation using the phosphorylated and unphosphorylated sticky ends.

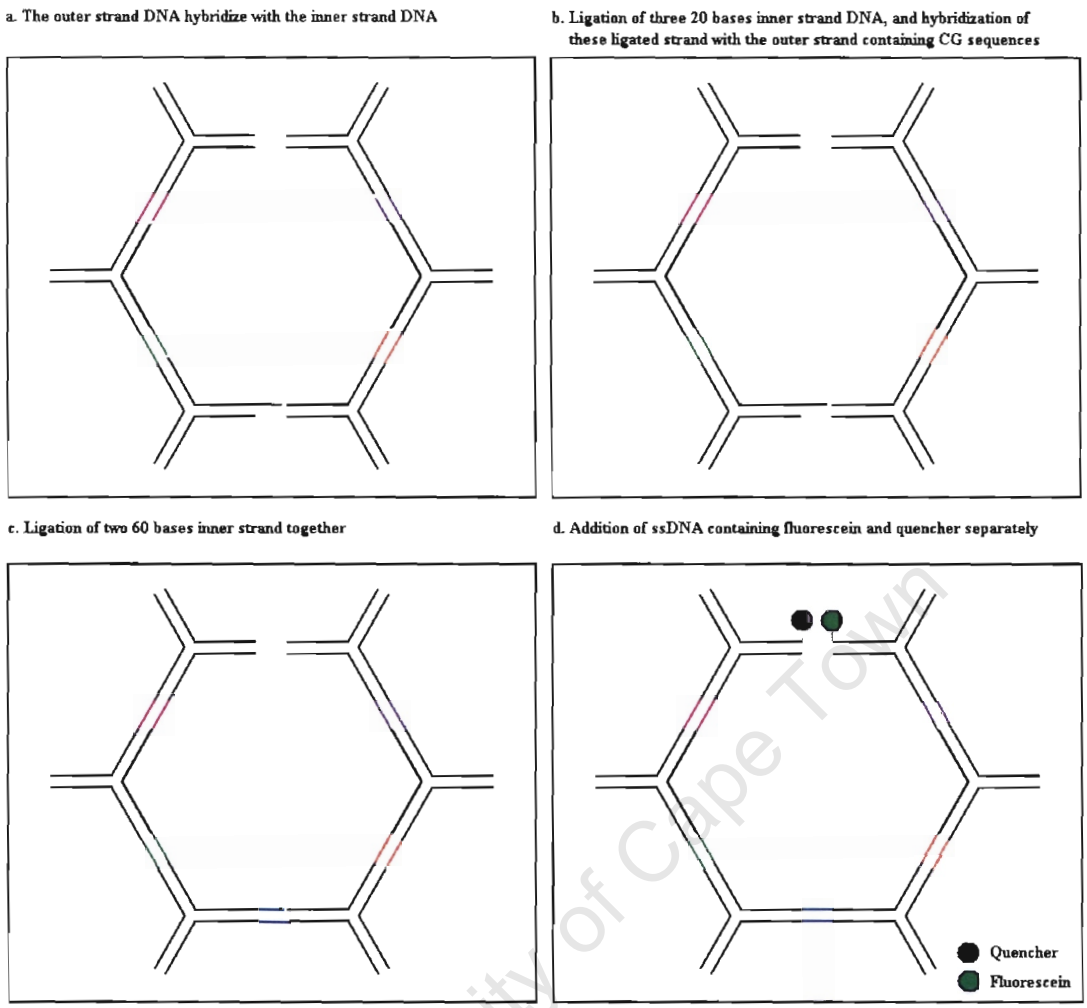


Figure 3.1.4 The schematic diagram of ligation using outer strands to ligate the inner strands with addition of strands containing the fluorescein group and the quencher. a. the outer strands hybridize with the inner strand DNA; b. ligation of inner strand; c. ligation of two ligated inner strands by adding the last outer strand; d. the addition of strands containing the fluorescein group and the quencher.



*Fluorescence intensity analysis*[97]

Fluorescence is a phenomenon that registers the change in wavelength between absorbed light energy at a specific wavelength and the emitted light at a longer wavelength. The electrons of this molecule are excited by a photon and moved to a

higher energy level. When returned to the ground level, this molecule emits light at a longer wavelength. The light emission is measured with a fluorometer. The instrument is capable of exciting fluorescent molecules at a specific wavelength and records the amount of light emitted at certain wavelength range (emission band). Accordingly, in this case, the amount of light emitted by the fluorescent group in the hexagonal DNA nanoswitch can be measured. The fluorescein group in the hexagonal DNA is fluorescence green which can be excited at 495 nm and the emission maximum is approximately at 525 nm. The shift from B- to Z-form of the hexagonal DNA nanoswitch is dependent on the environmental cation concentrations, therefore the fluorescence intensity of the hexagonal DNA nanoswitch is measured at different cation concentrations.

## 3.2 Materials and methods

*Oligonucleotide synthesis*

Oligonucleotides listed in Table 3.2 were purchased from Inqaba Biotech (South Africa). These oligonucleotides were purified using a cartridge method and the amount of each oligonucleotide was measured by UV spectroscopy at the wavelength of 260nm and the corresponding OD reading of each strand was given (Table 3.2). All oligonucleotides were checked using denaturing gel electrophoresis to check for the remaining level of failure sequences and they were found to be of high purity. The oligonucleotide concentrations were calculated using the same method as describe in chapter 2 and the stock solutions were made up to a final concentration of 100 μM in sterile Milli-Q water and stored in -20℃ for experimental use.

| Name | Sequence (5' to 3') | ε ($M^{-1}$ $cm^{-1}$) |
|---|---|---|
| F01 | CGCGCGTCACTCATCCAGAG | 204400 |
| F02 | CCGCCCTCTGGAGACTTGGT | 195100 |
| F03/06 | ACCAAGTCTGAGTGA | 171300 |
| F04 | GGCGGTCACTCATTCCAAG | 198300 |
| F05 | CGCGCGCTTGGAAGACTTGGT | 218700 |
| F07 | GGGGCTCACTCATTCCAACG | 205700 |
| F08 | CCGCCCGTTGGAAGACTTGG | 214600 |
| F09/12/15/18# | ACCAAGTCTGAGTGAG | 182800 |
| F10 | GGCGGCTCACTCATTCCAACG | 213100 |
| F11 | GGCCCGTTGGAAGACTTGGT | 211300 |
| F13 | GGCCCTCACTCATTCCAACG | 197500 |
| F14* | CGTTGGAAGACTTGGT | 173500 |
| F16 | CTCACTCATTCCAACG | 159700 |
| F17 | CCCCCGTTGGAAGACTTGGT | 203100 |

* contained dabcyl quencher at 5'-end of F14; # contained fluorescence green at 3'-end of F18

Table 3.1 Details of oligonucleotides synthesized from Inqaba Biotech (South Africa).

*Polyacrylamide Gel Electrophoresis (PAGE)*

Denaturing gel electrophoresis:

The denaturing polyacrylamide gel was made to 20% contain polyacrylamide with the same reagents as the native gel, but in addition it contains a fixed concentration of urea (final concentration of 7M). The electrophoresis was performed at room temperature with high voltage (150~200V) for 2 hours. The denaturing PAGE samples were mixed with denaturing sample loading buffer containing either urea or formamide in the same ratio as in native gel. The gel was stained in a stains-all solution containing water and formamide in the ratio of 1:1 for 45 minutes, and the de-stain procedure was done by placing the gel in water and expose it to light for several hours. Digital recording was performed by visualizing stained DNA bands on a normal light box. The recorded images were scanned and saved as a Microsoft TIFF image.



*Oligonucleotide excision from denaturing gel*

The gel was placed on the TLC plate after gel electrophoresis and UV light was applied to the gel to identify the specific bands that were identified to be excised. Gel bands were excised using a metal blade and each excised gel piece was placed in an Eppindorf tube containing 0.3 M sodium acetate at pH 5.2 to extract the DNA

contained in the gel piece. The amount of sodium acetate required for DNA extraction is subject to the size of the excised gel piece (the standard ratio is 250 µl acetate for a 1 cm long of gel piece). Eppindorf tubes were shake at 37℃ over night, and the supernantant of each sample was kept for phenol extraction. Phenol extraction purifed samples were further washed using ethanol and dried using a "speedi-vac". The dried samples were re-dissolved in Milli-Q water or an appropriate buffer solution for further experimental use.

*Fluorescence spectroscopy*

The fluorescence emission analyses were carried out using a Perkin Elmer luminescence spectrometer LS50B and the absorbance was recorded by FL WinLab software as a function of the wavelength. The sample was initially excited at 495 nm and the emission was recorded from 500 to 650 nm. The sample volume required was 500 µl the slitwidth is 3 nm and the scanning speed is100 nm per minute, 10 scans were accumulated for each sample. The fluorescence intensity in a.u. versus the wavelength was plotted using the Microsoft Excel program.

## 3.3 Results

### 3.3.1 Hexagonal DNA nanoswitch assembly

The assembly of the hexagonal DNA nanoswitch was carried out according to the flow chart presented in Figure 3.3.1. The first step in the construction was to ligate the outer strands of the nanoswitch. The oligonucleotides F01, F02, F04, F05, F07, F08, F10, F11, F13 and F17 were phosphorylated using T4 polynucleotide kinase. The phosphorylated oligonucleotides were mixed in stochiometric amounts of the corresponding oligonucleotides (refer to Figure 3.3.1). These mixed oligonucleotides were heated to 65℃ and cooled to room temperature. This resulted in six sets of the three-way junction DNAs. In each set, the three-way junction DNA contained the phosphorylated sticky end. Each set was mixed with the complementary set containing an unphosphorylated sticky end. The ligation was carried out after the hybridization. The ligated products (40 bases in length) were checked for completion of the ligation by using 20% denaturing gel electrophoresis (Lane 1 to 4 in Figure 3.3.2). The ligated fragments were excised from the gel and purified for the next step. The next step in the construction was the ligation of the inner strands. This ligation was done by hybridizing the purified ligated fragments (Los 1&4 and Los 3&5 in Figure 3.3.1) with the complementary ssDNAs (Lis 1 and 2 in Figure 3.3.1

respectively). The ligated products were extracted and checked using denaturing gel (Lane 5 to 6 in Figure 3.3.2). These ligated fragments (60 bases length) were purified and mixed with all the outer strands. The mixed sample (FL1 in Figure 3.3.1) was further ligated to generate the final inner strand (120 bases, data not shown). The construction was completed by addition of ssDNA containing the fluorescent (at 3'-end of F18) and the quencher (at 5'-end of F14) groups.

The structure of the hexagonal DNA nanoswitch was examined using transmission electron microscope. The electron micrograph showed a two-dimensional hexagonal DNA ring with a gap on one side.

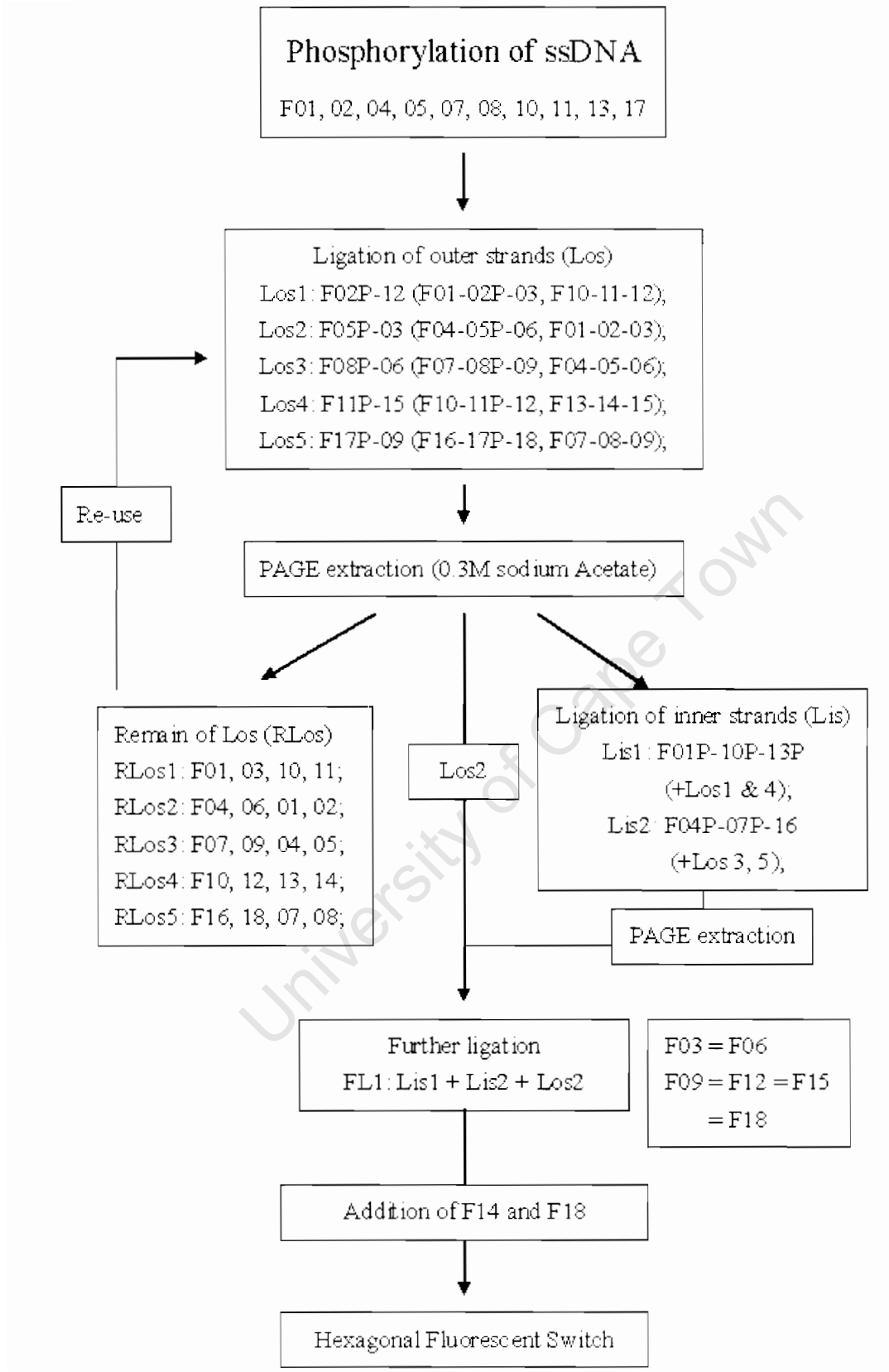


Figure 3.3.1 The flow chart desmonstrating the construction of the hexagonal DNA nanoswitch.

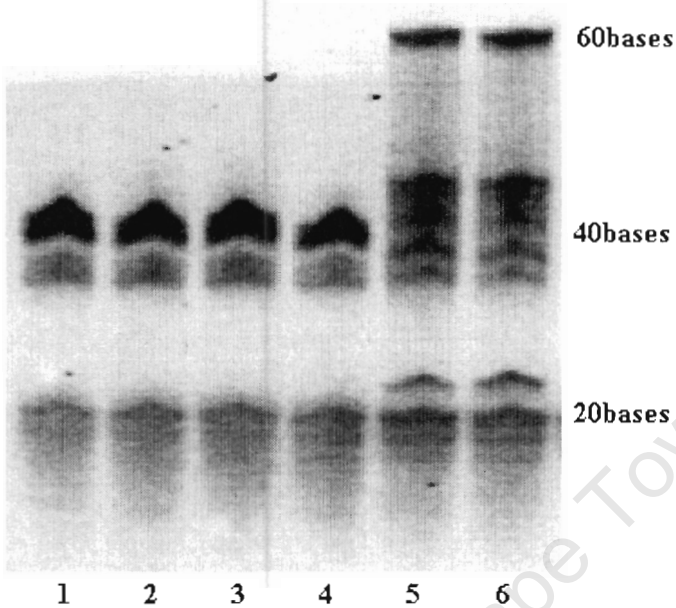




Figure 3.3.2 A 20% denaturing gel showing ligation of outer strand and inner strand DNAs. Lane 1 to 4: Los 1, Los 3, Los 4 and Los 5 (Los 2 not shown); Lane 5 and 6: Lis 1 and Lis 2.

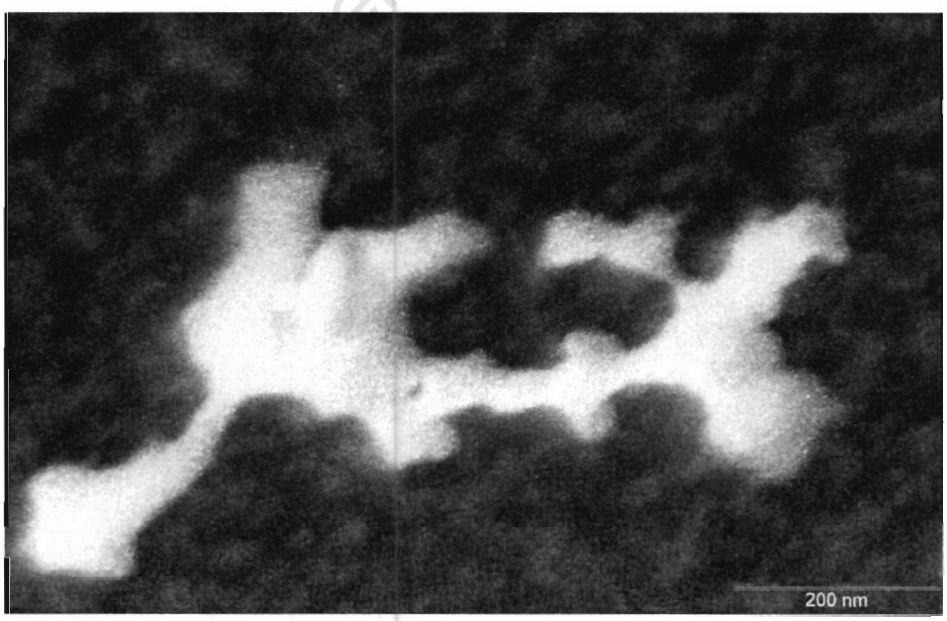


Figure 3.3.3 The electron micrograph of a hexagonal DNA nanoswitch.

### 3.3.2 Fluorescence intensity measurement upon salt concentration gradient

The hexagonal DNA nanoswitches were mixed with a set of different $NaClO_4$ solutions with the sodium concentration increasing in 0.5 M interval from 1 M to 5 M. The samples were excited at 495 nm and the fluorescence emissions were recorded from 500 to 650 nm. The fluorescence intensity measurements were first made with the blank solutions of different $NaClO_4$ concentrations and with the solutions containing the fluorescein group only. The results showed the fluorescent emission was not dependent on $NaClO_4$ concentration.

The fluorescence emission intensities were first measured for five samples with 1 M $NaClO_4$ concentration increase in regular intervals. The results are shown in Figure 3.3.4.

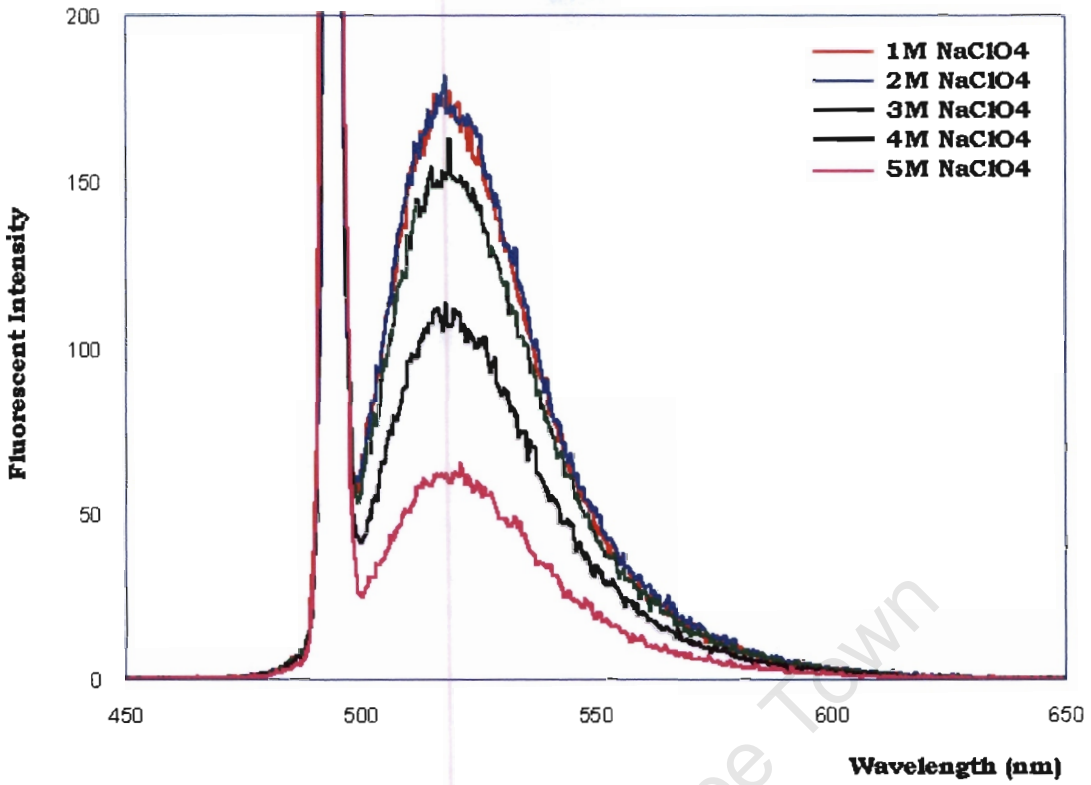


Figure 3.3.4 The fluorescence emission intensity change of the hexagonal DNA nanoswitch as a function of the $NaClO_4$ concentration.

The fluorescence intensity change of the hexagonal DNA nanoswitch was found to decrease with increasing cation concentrations. The emission peak was found to stay at 521 nm. A decrease in fluorescence occurred at 3 M $NaClO_4$ and was lowest at 5 M $NaClO_4$. A further measurement was made with samples that increase in 0.5 M $NaClO_4$ intervals (Figure 3.3.5).

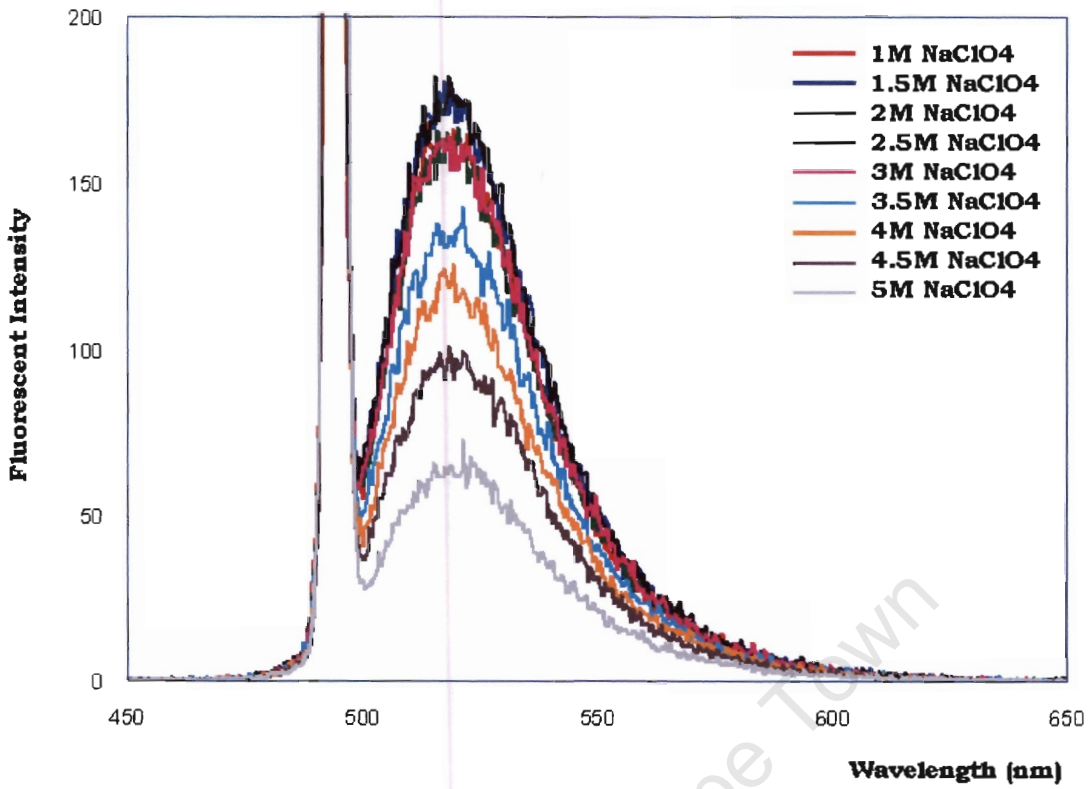


Figure 3.3.5 The fluorescence intensity change of the hexagonal DNA nanoswitch upon the $NaClO_4$ concentration increases in 0.5 M increments.

## 3.4 Discussion

The assembly of the hexagonal DNA nanoswitch is based on the sticky end sequences that were designed for each set of three-way junction DNAs. The sticky end sequence(s) of each set of the three-way junction DNA is different from any another, which results in the specific linkage between different DNA sets. The way to assemble this nanoswitch was chosen as to increase the specificity of each ligation and to avoid the occurrence of possible non-specific secondary structures. The switching mechanism is based on the $(CG)_3$ sequence opposite of the open gap. This hexagonal ring is free of torsion. Theoretically, by design, the initial state of the hexagonal DNA nanoswitch is intended in the closed state (the fluorescein group and the quencher should be aligned next to each other). When the environmental cation concentration increases, the nanoswitch then shifts to the open state (the fluorescein group and the quencher move apart from each other). The fluorescent emission measurement showed a different result. This strongly suggests that the initial state of the hexagonal DNA nanoswitch is the open state. With increasing cation concentration, the nanoswitch is twisted to the closed state. We can reasonably assume that the initial state is a distanted hexagonal ring (the distance between the fluorescent and the quencher group is further in the initial ring structure) with wide open ends that approach each other when the $(CG)_3$ sequence changes its

conformation. The fluorescence intensity change of the nanoswitch and the percentage of the fluorescence intensity change at different $NaClO_4$ concentration can be calculated at 521 nm (Table 3.4.1).

| Concentration | Fluorescence | Δ F.I. (a.u.) | △% F.I. |
|---|---|---|---|
| 1.0 M | 160.68 | 0 | 0.00 % |
| 1.5 M | 168.52 | -7.84 | 0.00 % |
| 2.0 M | 160.63 | 0.05 | 0.03 % |
| 2.5 M | 174.59 | -13.91 | 0.00 % |
| 3.0 M | 161.88 | -1.2 | 0.00 % |
| 3.5 M | 137.46 | 23.22 | 14.45 % |
| 4.0 M | 116.44 | 44.24 | 27.53 % |
| 4.5 M | 95.563 | 65.117 | 40.53 % |
| 5.0 M | 60.945 | 99.735 | 62.07 % |

Table 3.4.1 Table of the fluorescence intensity change and the percentage of fluorescence intensity change of DNA nanoswitch at 521nm.



The percentage of the fluorescence intensity change amounts to 62.07% when the sodium concentration changes between 1 M and 5 M. The fluorescence intensity change of the hexagonal DNA nanoswitch is shown to be concentration dependent as expected. The plot that depicts the fluorescence intensity change of the nanoswitch at different sodium concentrations, is shown in Figure 3.4.1.

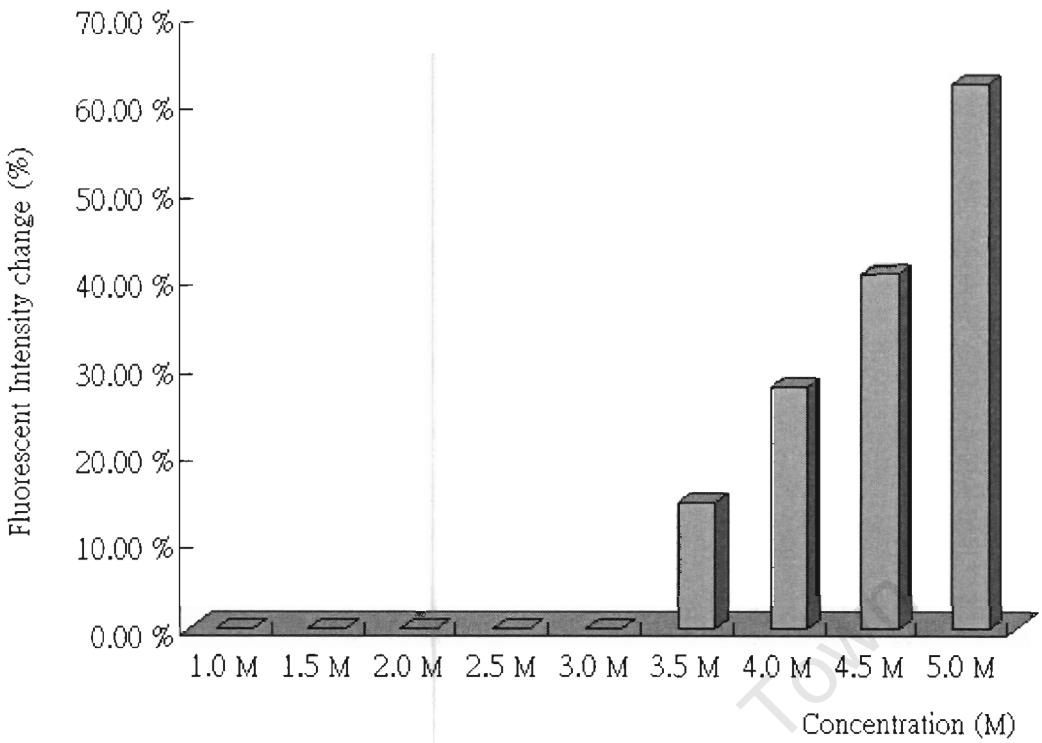


Figure 3.4.1 The plot represents the percentage of fluorescence intensity change at increasing $NaClO_4$ concentrations.

The potential application using this hexagonal DNA nanoswitch will be discussed in chapter 5.

# Chapter 4 DNA nanostructures made by hairpin loop

## 4.1 Introduction

### 4.1.1 Meta-stable state systems using DNA hairpin loop

DNA can be used as a tool to carry out specific tasks such as functional molecular motors or walking devices. The principle forces that drive these devices originate at the interfaces between different DNA structures, they are termed intermolecular interactions. We have employed a novel strategy to demonstrate this important principle. This strategy is called "strand displacement strategy" (SDS). This strategy is modeled on the biological enzyme-substrate binding mechanism[98]. According to this strategy a DNA sequence (substrate) is designed in such a way that it is able to interact with a target DNA structure (enzyme). This interaction results in a new combined structure and each of the separate initial structures is undergoing a conformational change. The new structure still is a meta-stable state intermediate (enzyme-substrate complex). The DNA which causes the structural conversion is also called the "fuel" strand. The "fuel" strand can be removed from its complex by interacting with another DNA strand that binds the fuel strand with higher affinity than the target DNA structure to form a fully complementary double helix DNA (product). After the removal of the fuel strand, the target DNA structure returns to its

initial conformation. This structure is then ready for the next cycle. The process can then be repeated many times as the target DNA structure always has to return to its initial state.

In this study, a 34 base ssDNA is designed to form a hairpin loop structure that represents the target DNA structure (enzyme). This ssDNA contains alternating $(CG)_4$ sequences at the both 5'- and 3- ends that are complementary to each other. These repeat sequences form the stem structure of the hairpin loop structure. The sequences flanking these CG sequences are designed to contain $(CTG)_6$ triplet repeats. These repeats are known to self-associate into secondary structure elements to increase the stability of the hairpin loop structure (Figure 4.1.1).

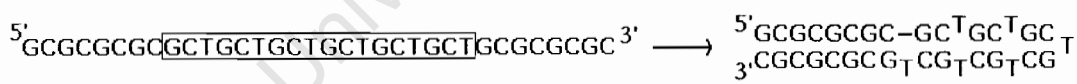


Figure 4.1.1 Hairpin loop DNA structure showing the base pairing of alternating CG sequences and the interaction between triplet repeats.

The section of unpaired sequences $(CTG)_6$ flanked by CG sequences is designed as the interacting site. The fuel strand is a 16 nucleotide ssDNA that hybridizes with the loop sequences with a few mispairs. This fuel strand is designed to bind to the loop

section with lower affinity than the remover strand. The binding of the fuel strand to the loop section results in two mismatches. These mismatches were deliberately introduced so as to create a less stable interaction in order to facilitate strand displacement when the perfect complementary single strand is added. This single strand competes for the binding of the fuel strand with the hairpin loop DNA structure. After removing the fuel strand, the mismatched binding DNA structure returns to its initial state. This mechanism is demonstrated in Figure 4.1.2.



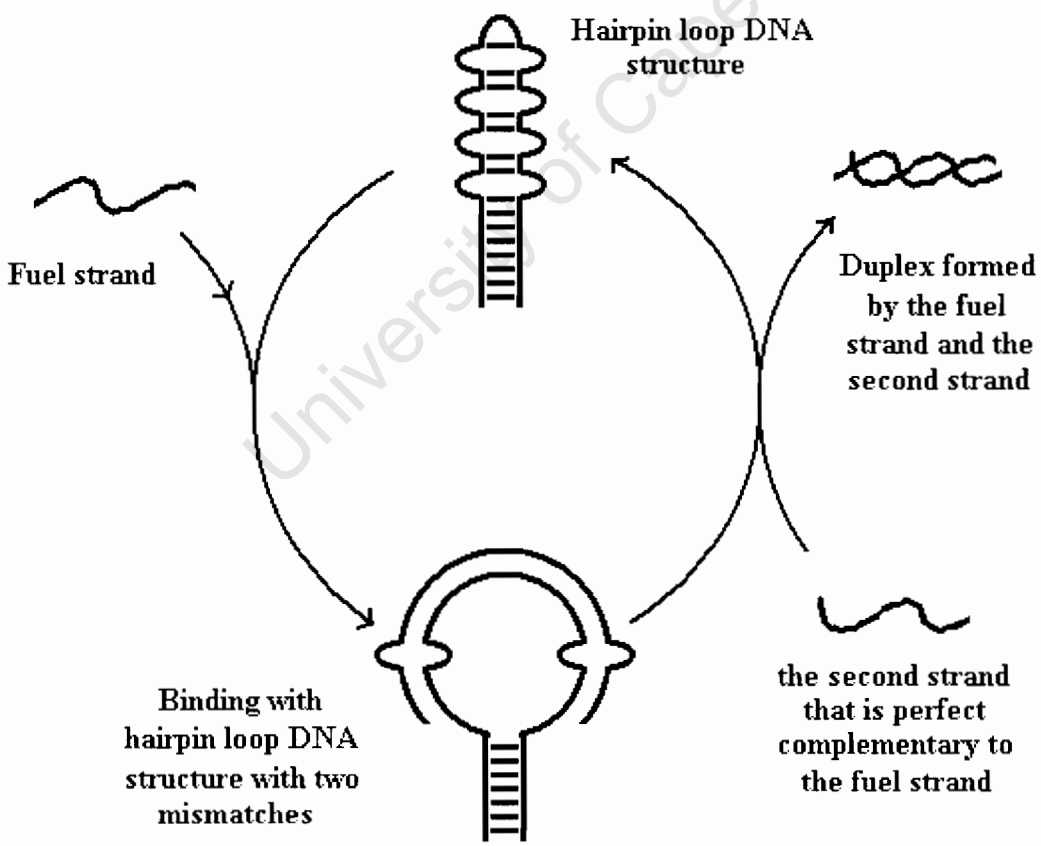


Figure 4.1.2 Formation of a partially mismatching stem-loop DNA structure from the fuel strand and the hairpin loop DNA structure, and the fuel strand is removed by addition of the complementary strand.

Varying the approach we challenged the hairpin loop DNA structure using a different fuel strand. This results in a conformational change of the target DNA structure that includes breaking the hairpin loop DNA structure. The fuel strand in this system is designed to bind partially to the hairpin loop DNA structure at the alternating CG sequences as well as to the unpaired loop section. This results in breaking of the initial stem structure and in the formation of a dsDNA which has overhangs at both 5' and 3' ends. Again this intermediate complex contains a few mispairs. A single strand DNA is then added to be complementary to this fuel strand and as its perfect complementary acts to remove it from the dsDNA structure. This result in the formation of a short duplex and the hairpin loop DNA structure is then restored (Figure 4.1.3).

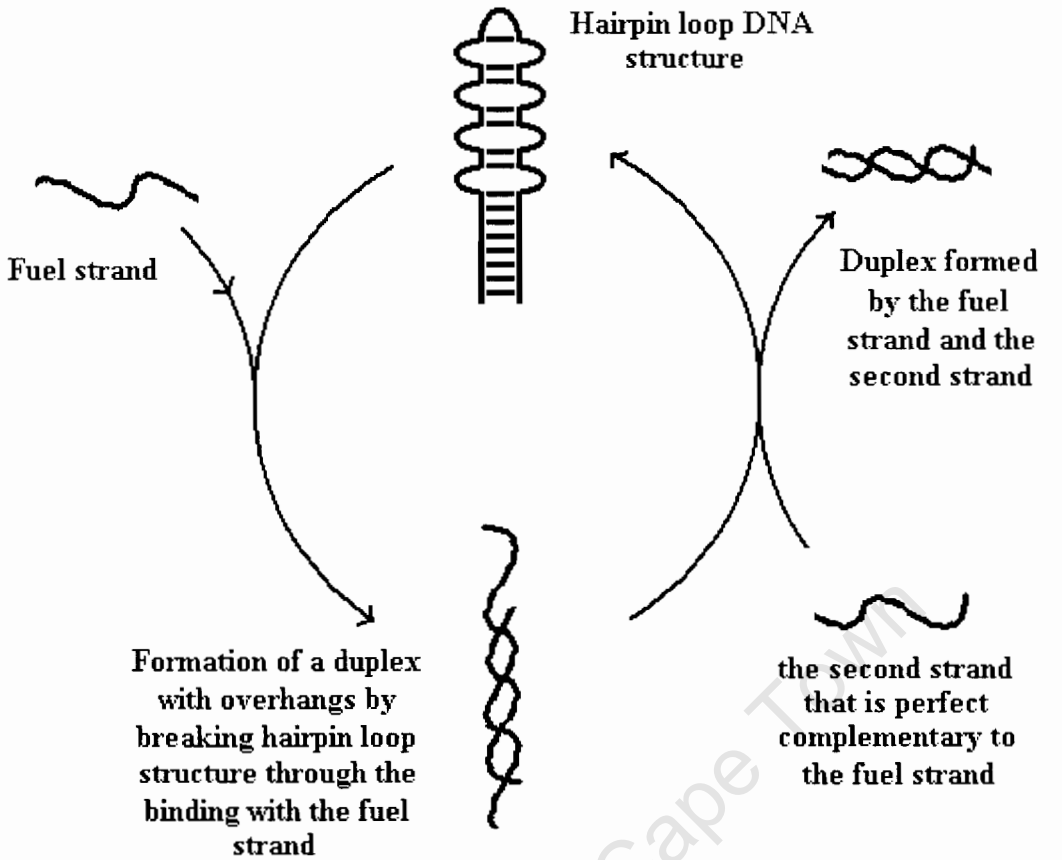


Figure 4.1.3 Formation of a double helix with a 3'extension that replaces the initial hairpin loop DNA structure followed by the removal of the fuel strand by a perfectly complementary second single strand.



### 4.1.2 Linkage of the DNA hairpin loop using single strand extensions of the stem

A novel way of organizing hairpin loop DNA structures is now possible based on the interactions described above. The aim of this approach is to be able to orientate consecutive hairpin loop DNA structures "on top" of one another. The hairpin loop DNA structure used in the previous experiment is modified to contain two SEs at the 5`- and 3`- ends of the stem sequences. This results in the design of a ssDNA, responsible for hairpin loop formation, containing 6 sections of various sequences

(Figure 4.1.4a).

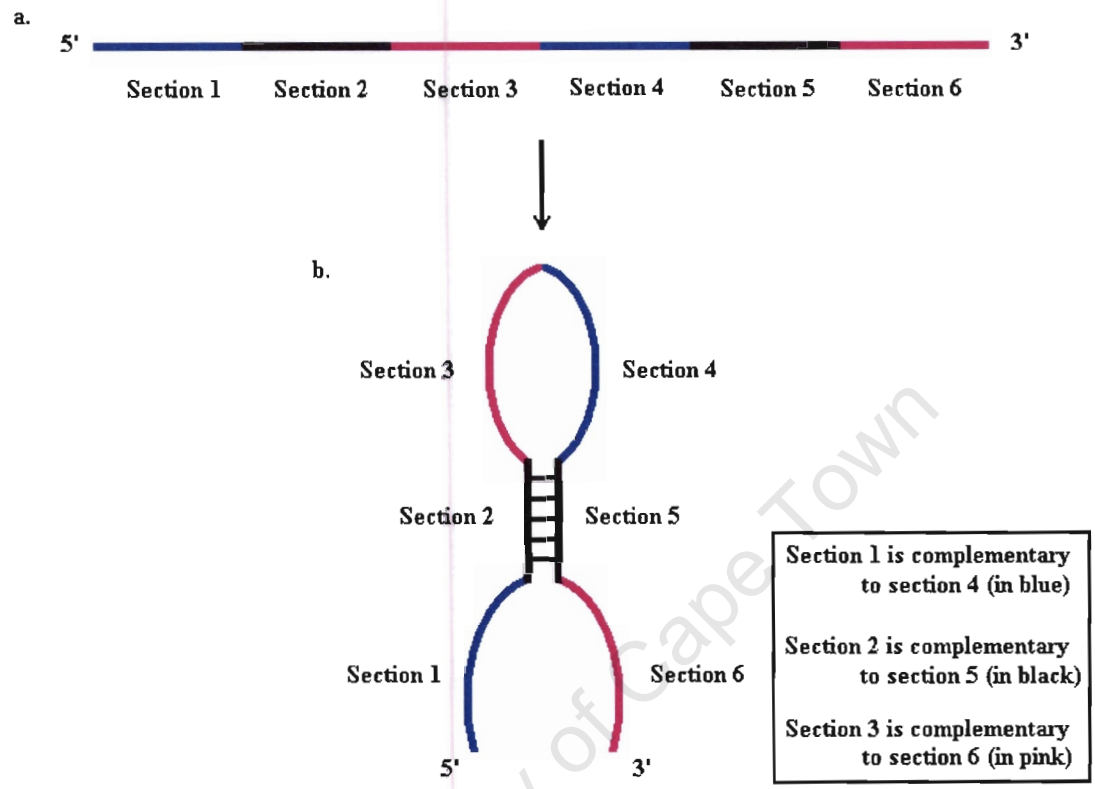


Figure 4.1.4 A schematic diagram of the hairpin loop DNA structure containing 6 consecutive sections of sequences that are complementary to specific sections (a), and form a structure that contains extensions at the both 5'- and 3'- ends (b).



Nucleotides in the section 1 and 6 are designed to be complementary to nucleotides in section 4 and section 3 respectively (and they do not self-associate), while sequences in sections 2 and 5 are designed to be complementary to each other. When the hairpin loop structure forms, it creates a folded DNA structure with two single strand extensions (4.1.4b). These extensions are capable to hybridize with the unpaired sequences in sections 4 and 3 in an anti-parallel fashion. Hence, it is possible to create

a chain of hairpin loop DNA structures connected to each other in head (loop) to tail (extensions) manner (Figure 4.1.5). Literally each one is standing on the shoulders of the previous one.

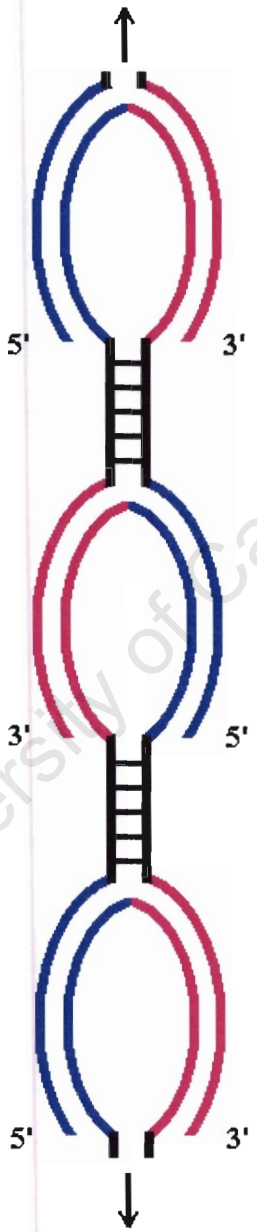


Figure 4.1.5 A schematic diagram of the linked hairpin loop DNA structure using single strand extensions. The linking process is bi-directional.

The length of these connected structures is dependent on the amount of DNA structure

present in the sample. To control the length of these linked structures, a single stranded DNA is introduced to bind either in the single stranded loop section or to the single stranded extension regions to stop further linkage. This results in hairpin loop DNA structures which are no longer capable of annealing with each other (Figure 4.1.6).

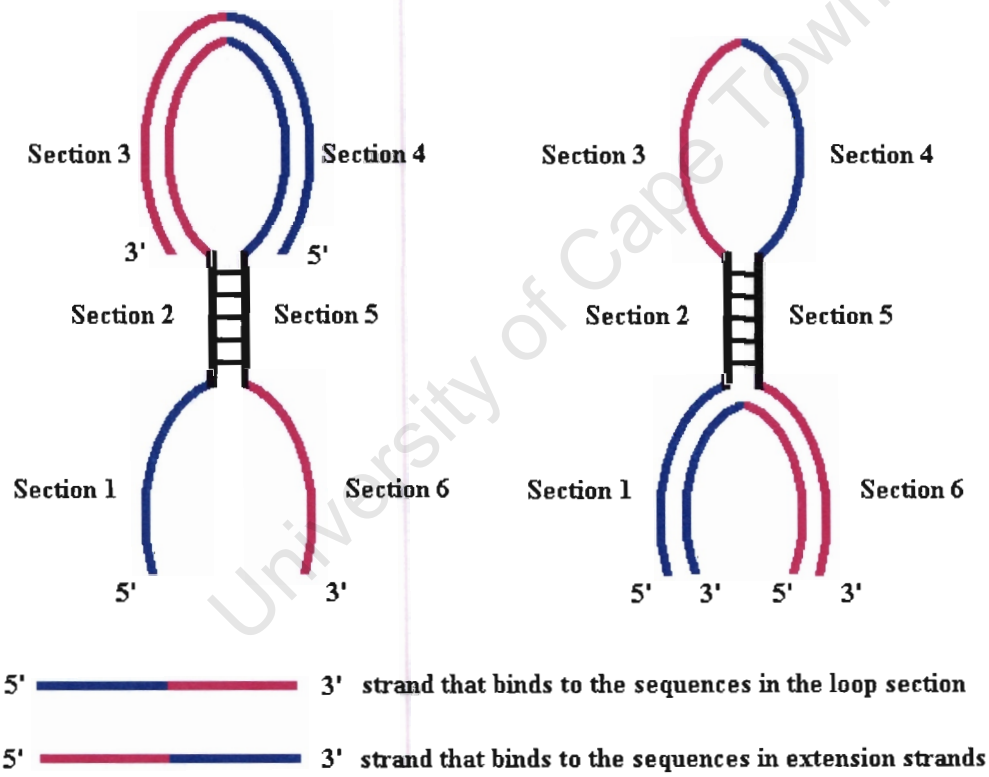


Figure 4.1.6 A schematic diagram showing the linkage of hairpin loop DNA structures can be stopped by blocking the sequences in the loop section (left) or the at the extension strands (right).

To test this model, a 48 base ssDNA is designed to contain 6 sections of sequences (8 bases each). The complementary sequences in sections 2 and 5 are designed to contain

CG sequences only. The sequences of the extension and the loop section are designed with a 50% GC content. Two ssDNA sequences (16 bases each) are designed that contain the complementary sequences to the extension ends or the loop section. These two sequences are used to stop single strand interactions and act to break the linkage between hairpin loop structures. The sequences of these two stop strands are complementary, and therefore the simultaneous addition of both strands to the hairpin structures at the same time has no effect on further growth. Rather, these sequences will result in dsDNA helices. Therefore the "stop process" should be carried out using one strand at a time.

The sizes of these structures created in the systems described above are analyzed using non-denaturing PAGE. The conformational changes between these meta-stable intermediates are observed by using the temperature gradient UV spectroscopy (section 4.3).

## 4.2 Materials and methods

### Nucleic acid synthesis

Oligonucleotides were synthesised by phosphoramidate chemistry using a Beckman 1000M DNA synthesizer. The products were further purified by DMT-on and DMT-off reverse-phase HPLC using an acetonitrile gradient. The sequence details of these oligonucleotides were summarized in Table 4.1. The extinction coefficient of theses oligonucleotides were calculated using nearest-neighbour model methods, and listed as in Table 4.2.1. These oligonucleotides were checked by 20% denaturing gel electrophoresis for the remaining level of failure sequences and they were found to be of high purity. The stock solutions of these oligonucleotides were diluted to a final concentration of 100 μM using sterile milli-Q water.

Table 4.2.1: Details of oligonucleotides synthesized from oligonucleotide synthesis laboratory in University of Cape Town

| Name | Sequence (5' to 3') | ε ($M^{-1}$ $cm^{-1}$) |
|---|---|---|
| Oligo A | GCGCGCGCGCTGCTGCTGCTGCTGCT-GCGCGCGC | 316800 |
| Oligo B | AGCAGTAGCAGCAACA | 192100 |
| Oligo C | TGTTGCTGCTACTGCT | 151900 |
| Oligo D | AGCAGCAGCAGCGCGCG | 186500 |
| Oligo E | CGCGCGCTGCTGCTGCT | 155600 |
| LOL01 | AAGACCAGGGCGGCGGCACGATGT-CTGGTCTT CCGCCGCCACATCGTG | 495200 |
| LOL02 | AAGACCAGACATCGTG | 185400 |
| LOL03 | CACGATGTCTGGTCTT | 158600 |



**UV spectroscopy**

UV melting scans, or absorbance changes due to temperature variation, were performed using a Unicam SP17000 Ultraviolet spectrophotomer as previously described. Aliquots of the DNA stock solutions were diluted to a final concentration of 0.75 μM in 1M NaCl and of 10 mM sodium cacodylate, pH 7.0. Three temperature scans were performed per sample of the isolated sequences at 260 and 272 nm (for the

metastable state DNA nanostructures and the linkage of hairpin loop structures respectively) to start with and then the various combinations were subjected to the same temperature cycles. The temperature was increased from 20 $^{0}$C to 110 $^{0}$C with a scan rate of 1 $^{0}$C per minute.

**Native Gel electrophoresis**

All samples were pre-heated to 85 $^{0}$C for 5 minutes before mixing to establish a uniform and reproducible starting conformation. They were eventually diluted to 1.5μM DNA in 89mM tris-borate-buffer and 100mM NaCl prior to loading. All samples were loaded into the wells of a 10% non-denaturing gel and the electrophoresis was performed at 70V at 4 $^{0}$C for 2 ~ 3 hours. The gel was stained with ethidium bromide for 10 minutes before digital recording. (Visualization is performed by placing the gel on 254 nm UV light box and the image is recorded digitally)

## 4.3 Results

### 4.3.1 Meta-stable states mechanisms

*The first mechanism: UV melting analysis*

The starting conditions was established prior to the UV melting experiments by pre-heating the 34mer oligonucleotide A to 85°C for 5 minutes. This step was carried out to break potentially non-specific folding patterns to assume a randomly coiled conformation. The sample was then slowly cooled to room temperature to form the specific hairpin loop structure (cf Figure 4.1.1). The UV melting scan of the hairpin loop DNA structure showed a single high temperature hyperchromic effect (Tm ~80°C) (Figure 4.3.1a). The initial slope is due to contributions from the loss of some self-structure within a stretch of a $(CAG)_6$ repeats that constitutes the loop section. The unfolding of the GC-rich helical stem resulted in a pronounced co-operative transition at high temperature. In the next heating cycle, a stochiometric amount of oligonucleotide B was added to oligonucleotide A. After a second melting scan, this sample had shown that the thermal unfolding of the hairpin loop DNA structure is fully reversible. According to sequence design, the binding of oligonucleotide B to the loop section of oligonucleotide A results in 14 matching and 2 mismatched base pairs. The thermal unfolding of the combined oligonucleotide A and B mixture occurs in two separate steps. The first step is represented by a low-temperature transition due to

the dissociation of oligonucleotide B from the loop sequence of oligonucleotide A. The second step occurs as a high-temperature transition due to the destabilisation of the stem of oligonucleotide A (Figure 4.3.1b). In the next step of the reaction cycle, the 16mer oligonucleotide C at low temperature was added to this (A+B) complex. This resulted in the pulling of the mismatched strand B from the loop upon heating which results in a small hypochromic effect. The two 16mers are perfectly complementary and their mutual binding will form a stable 16mer helical duplex (cf. Figure 4.1.2). The thermal melting of this duplex results in a hyperchromic effect at about 60℃ in Figure 4.3.1c. This is followed by the unfolding of the intra-molecular stem structure of strand A as a high-temperature hyperchromic effect (Tm ~ 80℃). The system has now differentiated into a perfect complementary W-C double helix of 17 base pairs while the hairpin loop DNA structure has returned to its initial state. This reformed structure (A) is now available to bind to the next oligonucleotide B to restart the thermodynamic cycle. The solution now contains the two complexes, oligonucleotide A and oligonucleotide B complex as well as an oligonucleotide B and oligonucleotide C duplex complex in the correct stochiometric amounts. This system shows three consecutive hyperchromic effects in the corresponding UV melting curve. These three effects are the caused by: (1) the reversible dissociation of oligonucleotide B from the loop of strand A at low temperature. (2) the reversible

thermal unfolding of the double-helical 17mer at intermediate temperature and finally (3) the reversible unfolding of the helical stem of oligonucleotide A (Figure 4.3.1d). On addition of more strand C to the system the UV melting curve shows only two transitions (Figure 4.3.1e). This is due to the fact that the hyperchromic effect associated with the increased amount of the 17mer helix increases due to the rise in the combined concentration of strands B and C respectively while the concentration of strand A in the system remains unchanged. In each repeating cycle, the melting curves obtained are similar to each other with the only difference in the hyperchromic effect observes due to an increasing fraction of the short double helix DNA accumulating in the system (data not shown) as the concentration of A relatively to the combined concentration of B and C decreases.

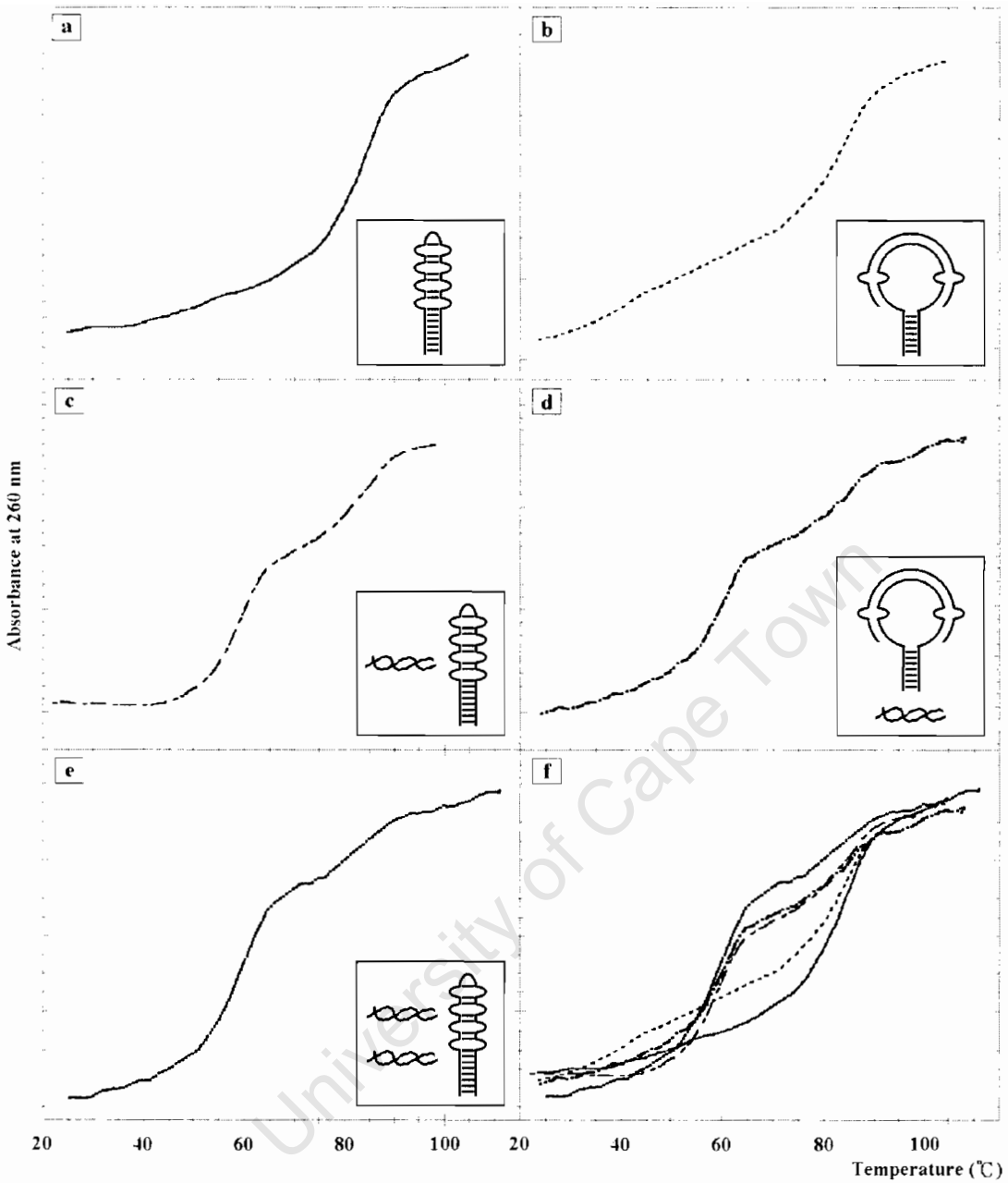




Figure 4.3.1 UV thermal unfolding analysis (absorbance at 260nm as function of temperature) of folded single strands and their combinations as they appear in the intermediate steps of the first mechanism. (Panel **f** shows the progressive changes observed in panels **a** to **e**)

*The second mechanism: UV melting analysis*

The first step in the thermodynamic cycle of the second proposed mechanism involves

the binding of the complementary strand (oligonucleotide D) to the hairpin loop structure (oligonucleotide A). This resulted in the opening of the hairpin loop structure followed by the formation of a helical segment consisting of the 5'-section of oligonucleotide A and full length oligonucleotide D with a 3'-single-strand extension of the remaining part of oligonucleotide A (cf. Figure 4.1.3). The 3'- half of oligonucleotide D binds to the 5'-section of oligonucleotide A (initially contributing to the stem of the hairpin-loop structure) and continues to bind into the loop sequence of oligonucleotide A. The corresponding UV melting curve (Figure 4.3.2b) of this complex shows a slightly broader transition which is believed to represent the melting of the duplex section of the complex formed by the association of oligonucleotide A with oligonucleotide D. Due to the heterogeneity of the sequences that form the helix the transition width is extended (the cooperativity is deminished) but the Tm remains largely unchanged compared to the melting of the hairpin loop region (Figure 4.3.2a). In the next step of the thermodynamic cycle the perfect complementary strand (to oligonucleotide D) represented by oligonucleotide E is added to the system. In the presence of the oligonucleotide A/oligonucleotide D complex, oligonucleotide E will compete with oligonucleotide A for the binding to oligonucleotide D upon heating (Figure 4.3.2c). The UV melting scan of the new system shows a single merged transition resulting from the superposition of the unfolding of the straight double helix

and the unfolding of the reformed hairpin loop (Tm of about 80°C). The various steps along the thermodynamic cycle are either dominated by the double helix with the single strand extension (A/D) or by the double helix formed by the two complementary strands (D/E). The release of the single strand sequence D from the complex (A/D) is driven by the combined formation of the complex (D/E) and the reformation of the hairpin loop structure of A. Repeated cycles showed a similar set of transitions as the first cycle (data not shown).

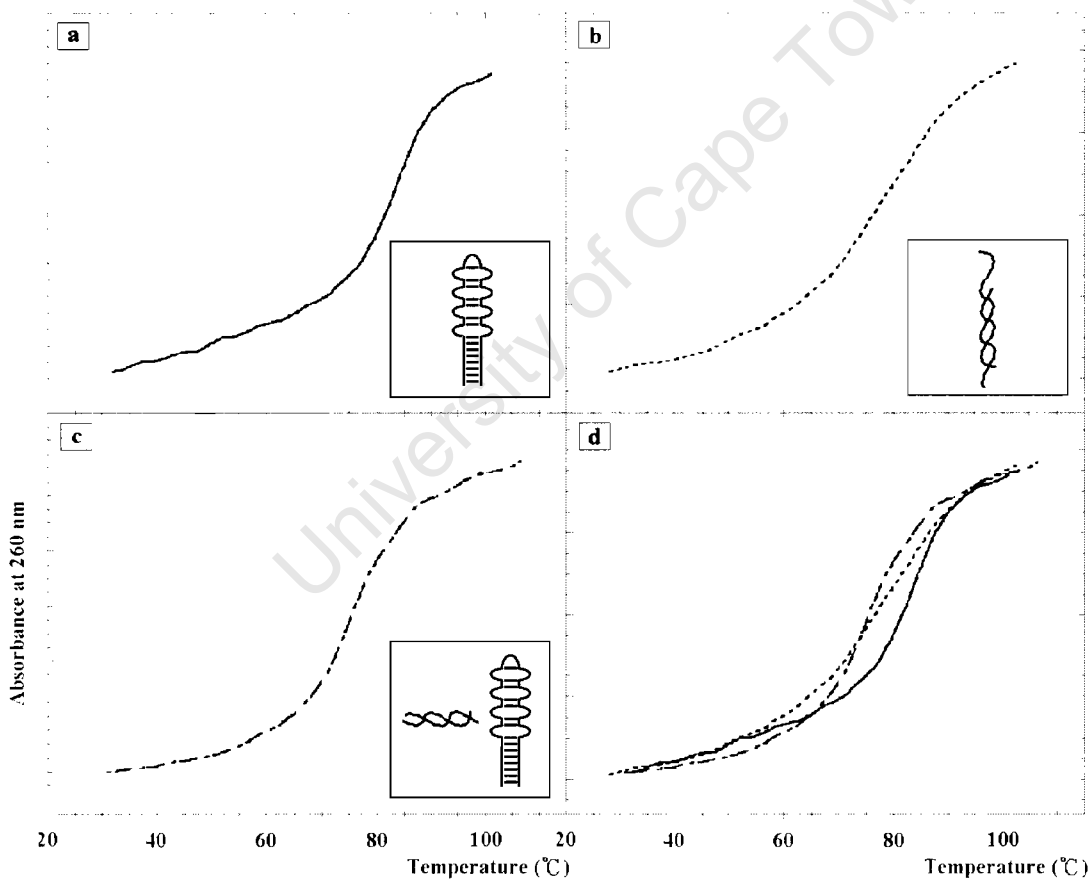


Figure 4.3.2 UV thermal unfolding analysis (absorbance at 260nm as function of temperature) of folded single strands and their combinations as they appear in the intermediate steps of the second mechanism. (Panel **d** shows curves **a**, **b**, and **c** plotted together)

*The first mechanism: Gel electrophoresis*

In order to obtain further independent confirmation of the molecular species present in the various systems analysed previously using UV melting analysis, gel electrophoresis was used to analyse the various stages (systems) obtained on both the first and the second mechanisms. According to the reaction cycle proposed to occur in the first mechanism we should be able to identify the hairpin loop structure of sequence A, the coiled single strands B and C, the mismatch complex of sequences A and B combined, the double helix formed by the interaction of sequences B and C, and the various combinations of these molecular species and/or their complexes (Figure 4.3.3). The native PAGE gel should allow for discrimination between these various species due to their different speed of migration for a given set of experimental conditions. The two short single strands (oligonucleotide B and C respectively) are expected to travel at equal speed and slightly ahead of the double helix formed by their combination. Oligonucleotide A is a hairpin loop structure and so will lag behind the short double helix in speed. The mismatched complex of oligonucleotide A with B will travel the shortest distance in the PAGE gel. Under conditions where there is a surplus of species B over A, two bands should be observable, one representing the complex and another representing the coiled single strand B.

Similar observations are expected for the combination of the complex of A and B in the presence of sequence C before heating. The banding pattern changed after heating to show bands representing the short double helix and the free hairpin loop sequence. All samples were pre-heated before loading (see methods) in order to ensure conformational reproducibility.

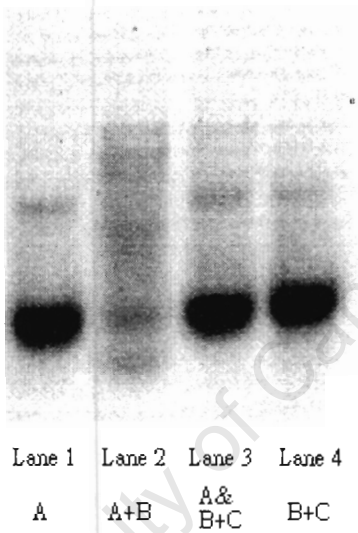


Figure 4.3.3 Non-denaturing PAGE gel photograph of oligonucleotide A and various combinations of oligonucleotides A, B and C involved in the first mechanism proposed (see text). Lane 1 (from left): the stem-loop DNA structure of oligonucleotide A; lane 2: the mismatched complex of oligonucleotides A and B; lane 3: the hairpin loop DNA structure A and the 17mer duplex B,C; lane 4: the 17mer duplex B,C.



*The second mechanism: Gel electrophoresis*

Non-denaturing PAGE gel electrophoresis was used, as performed to assay the first mechanism, to determine the various oligonucleotide combinations and species present in the various stages of the thermodynamic cycle involved in the second

mechanism. The results are shown in Figure 4.3.4. The single strands of oligonucleotides D and E (in analogy to oligonucleotides B and C in the first mechanism) were the most mobile entities, followed by oligonucleotide A (hairpin loop DNA structure). The helix with the 3'-extension will be slightly slower than the hairpin loop sequence as compared to the strand displacement helix that originated from the addition of oligonucleotide E to the complex of oligonucleotide A with oligonucleotide D. All molecular species can be identified as individual intermediates which can be found in various combinations. Hence, native gel electrophoresis is a very useful method which can be employed for the identification of the range of molecular (oligonucleotide) species present at the various stages of a thermodynamic reaction cycle.

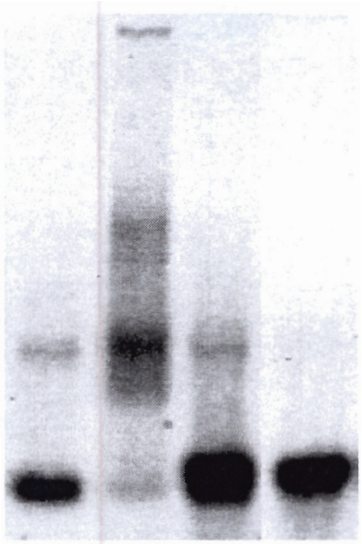


Figure 4.3.4 Non-denaturing PAGE gel photograph of oligonucleotide A and various combinations of oligonucleotides A, D and E involved in the second mechanism proposed (see text). Lane 1 (from left): the stem-loop DNA structure A; lane 2: the duplex with overhangs A,D; lane 3: the stem-loop DNA structure A and the 18mer duplex D,E; lane 4: the 18mer duplex D,E.



### 4.3.2 Linkage of the DNA hairpin loop structures (on the shoulder of giants)

*UV melting analysis*

The larger structures formed by linking DNA hairpin loop structures together using single strand extensions were at the 5'- and 3'- ends of a standard sequence analyzed using UV melting analysis. It was necessary to initially determine the characteristics of the linking phenomenon. The formation of the DNA hairpin loop structure with single strand extensions (LOL01) was performed using the same pre-heating procedure described in the previous section. The UV absorbance spectrum of this

structure ranged from 220 to 320 nm at both low (~20°C) and high (~100°C) temperatures. This was required in order to obtain the optimal wavelength for further UV melting analysis. The optimal wavelength for this structure was shown by plotting the absorbance difference between high temperature and low temperature scans as the function of wavelength (Figure 4.3.5) and was found to be 272 nm (the maximum peak of the curve).

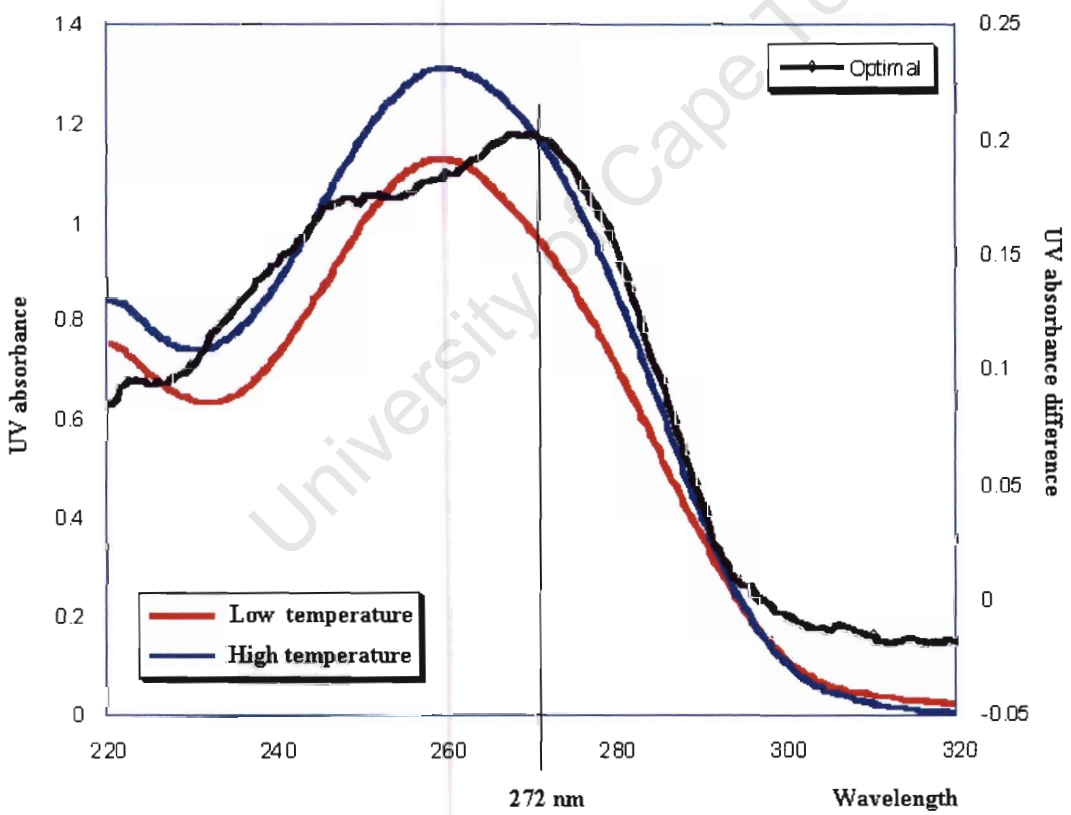


Figure 4.3.5 The UV absorbance spectrum of the DNA hairpin loop structures with single strand extensions (LOL01) in 1M NaCl, 10mM Na-cacodylate, pH 7.0 at low and high temperatures from 220 to 320 nm. The optimal wavelength was found to be 272 nm (vertical line).

The linking phenomenon was then characterised using a UV melting analysis at 272 nm. Figure 4.3.6 showed the melting profile of the sample containing LOL01 only.

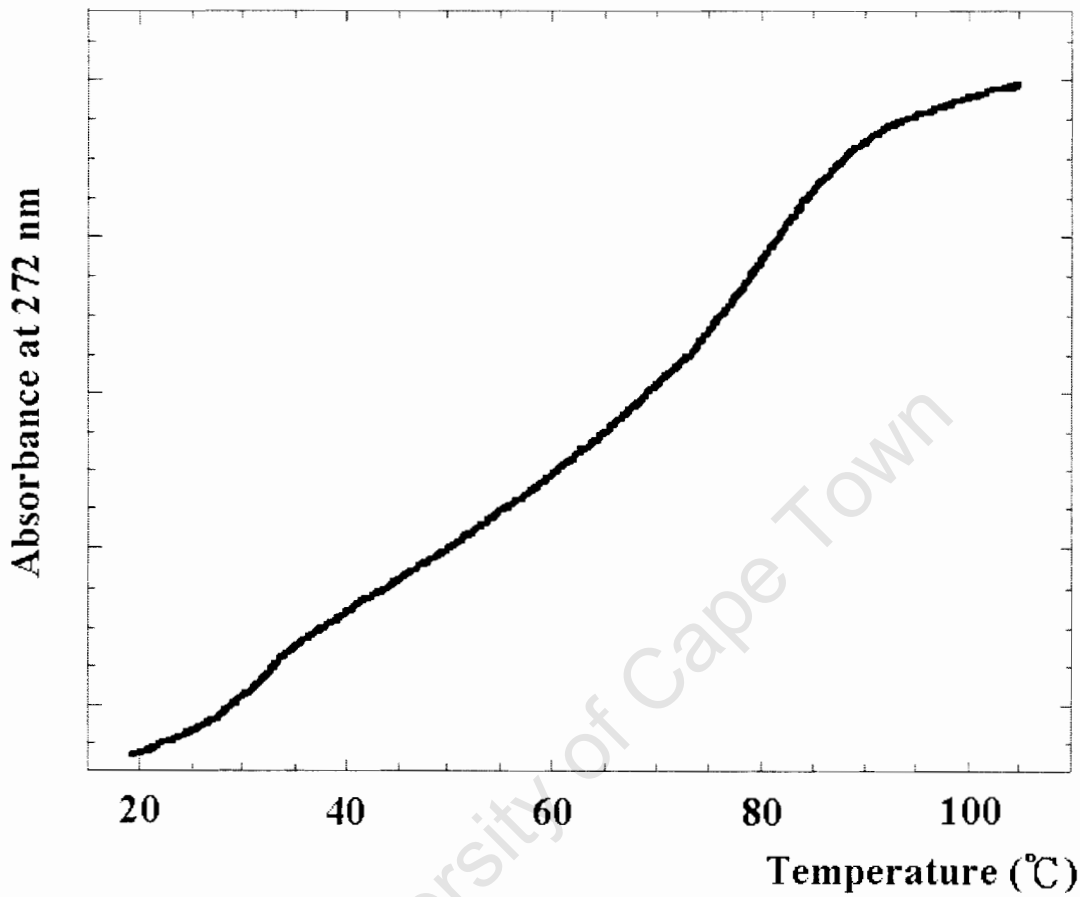




Figure 4.3.6 The UV melting curve of LOL01 in 1M NaCl, 10mM Na-cacodylate, pH 7.0 at 272 nm.

The first transition in the UV melting curve (cf. Figure 4.3.6) is the result of binding between single strand extensions and hairpin loop structures. The second transition observed is the result of the melting of stem loop structure in the DNA hairpin loop. The linking of DNA hairpin loop structures together is controlled by competitive binding of ssDNAs either to single strand extensions or to single strand loop sections

(cf. Figure 4.1.6). UV melting analysis was performed to characterise hybridization of the ssDNA to the single strand loop sequence. This analysis was performed on the sample containing LOL01 only (Figure 4.3.7a). Stochiometric amounts of LOL02 binds to single stranded loop sequences added to the sample. The addition of single stranded loop sequence to this system resulted in the thermal unfolding. This was evident by the shift of the first transition to a higher melting temperature (Figure 4.3.7b). This transition represented the melting of LOL02 after the addition of the single stranded loop sequence. The further addition of LOL01 to this sample showed additional binding between single strand extensions and hairpin loop sequence (Figure 4.3.7c). The thermal unfolding changed into a three-step process. These three steps included: (1) the first transition due to a linkage between LOL01 sequences, (2) the second transition due to the interaction between LOL01 and LOL02, and the last transition (3) due to the melting of the GC rich stem loop structure. Finally the addition of LOL02 resulted in the loss of the linking characteristic between LOL01 structures (Figure 4.3.7d).

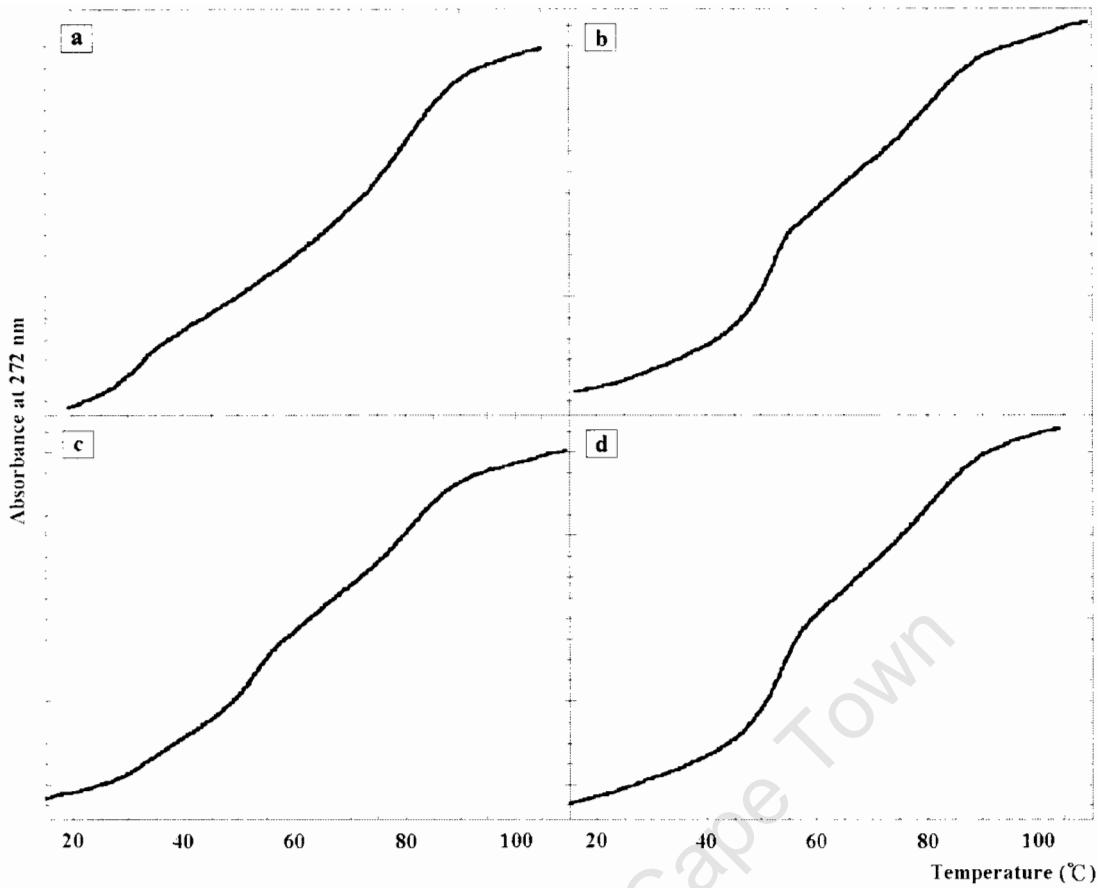


Figure 4.3.7 UV melting analysis of the sample containing LOL01 only (a) with addition of equal concentrations of ssDNA in the following order: LOL02 (b), LOL01 (c) and LOL02 (d).



The further analysis on the relationship between LOL01 and LOL02 was carried out using increasing concentrations of LOL02 (different ratios). The thermal unfolding processes are shown in Figure 4.3.8.

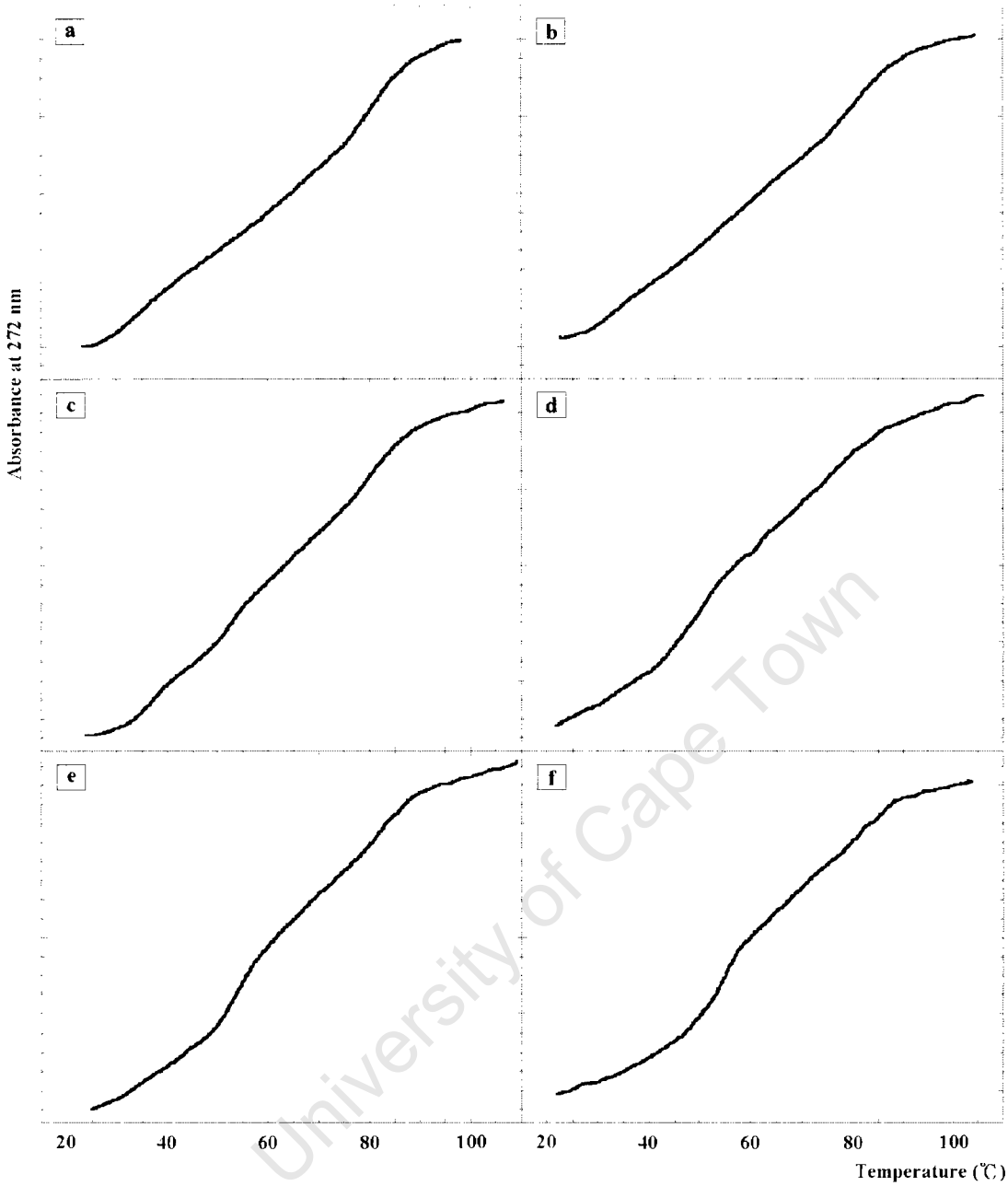




Figure 4.3.8 The thermal unfolding process of LOL01 with increasing concentration of LOL02. (LOL02 concentration in **a**: 0 μM; **b**: 0.2 μM; **c**: 0.4 μM; **d**: 0.6 μM; **e**: 0.8 μM; **f**: 1 μM)

Further analysis investigated the binding of the ssDNA (LOL03) to the single strand extensions. The thermal unfolding process between LOL01 and mixtures of LOL01 and LOL03 are shown in Figure 4.3.9.

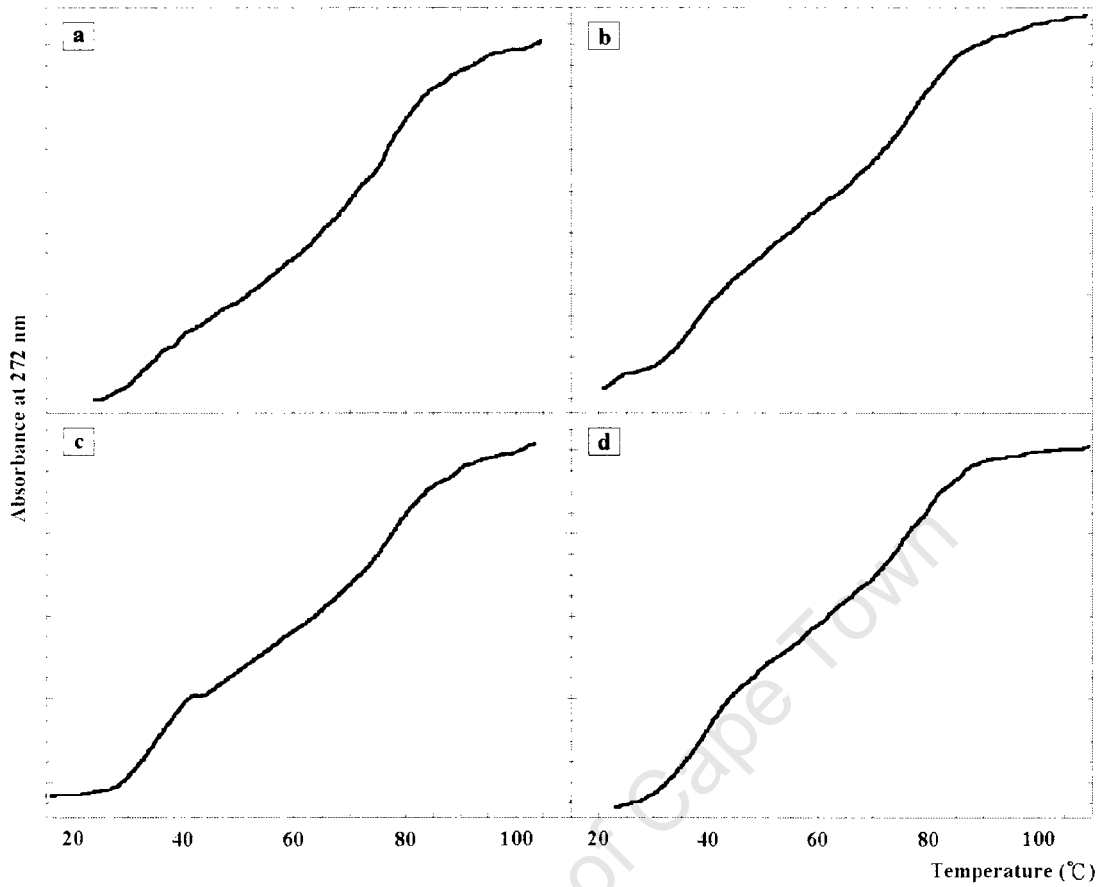


Figure 4.3.9 The thermal unfolding process of the sample containing LOL01 only (a) with addition of equal concentrations of ssDNA in the following order: LOL03 (b), LOL01 (c) and LOL03 (d).



The binding of LOL03 to LOL01 at the single strand extensions resulted in the formation of a three-way junction. This complex was not as stable as the complex formed by single strands binding to the hairpin loop. A concentration gradient experiment in which a constant amount of LOL01 is combined with an increasing amount of LOL03 was also performed. The results (Figure 4.3.10) obtained were similar to those found previously (Figure 4.3.9).

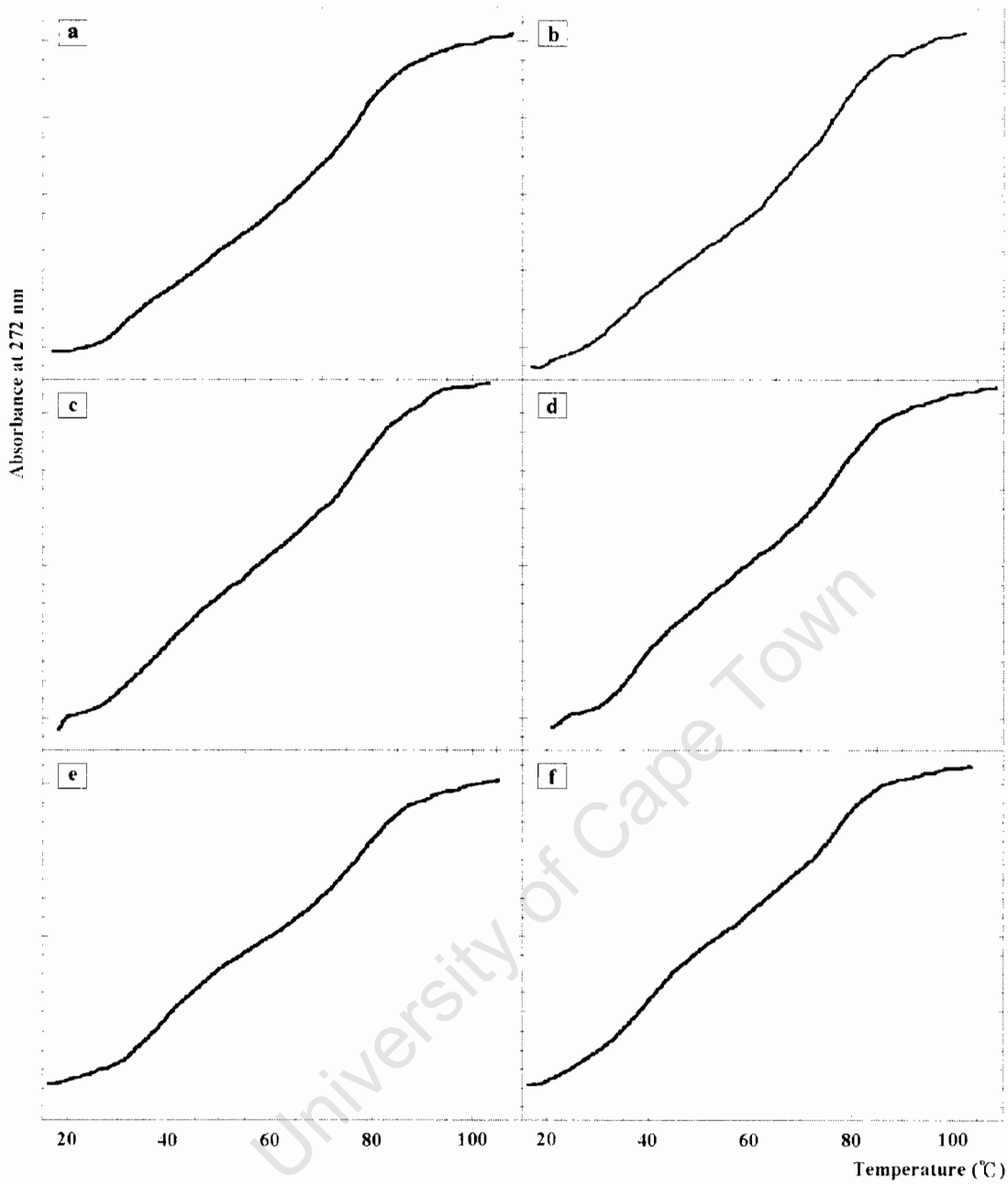




Figure 4.3.10 The thermal unfolding of LOL01 as a function of increasing LOL03 concentration. (LOL03 concentration in **a**: 0 μM; **b**: 0.2 μM; **c**: 0.4 μM; **d**: 0.6 μM; **e**: 0.8 μM; **f**: 1 μM)

*Gel electrophoresis*

Further independent analysis of the linking process between the various DNA hairpin

loop structures was performed using native PAGE gel electrophoresis. The first optimisation step for this process was to investigate the relationship between the size and amount of DNA hairpin loop present in the system using native PAGE gel electrophoresis. Samples containing different amounts of LOL01 were then heated to 85℃ and cooled to room temperature prior to gel electrophoresis. This was to induce the formation of linked DNA hairpin loop structures. The presence and size of these structures were analysed using 4% native (PAGE) gel electrophoresis (Figure 4.3.11). The DNA material was found to accumulate in the sample wells as a function of increased DNA concentration. This DNA material, present in the sample wells, was suggested to be large DNA structures which were not resolvable by PAGE. An alternative approach was to limit the linking process by using a LOL02 sequence which could bind to the loop sequence. This was undertaken by the addition of LOL02 DNA to the LOL01 material in varying ratios. The result showed that with the increasing concentration of LOL02, additional LOL01-LOL02 complexes were created (Figure 4.3.11).

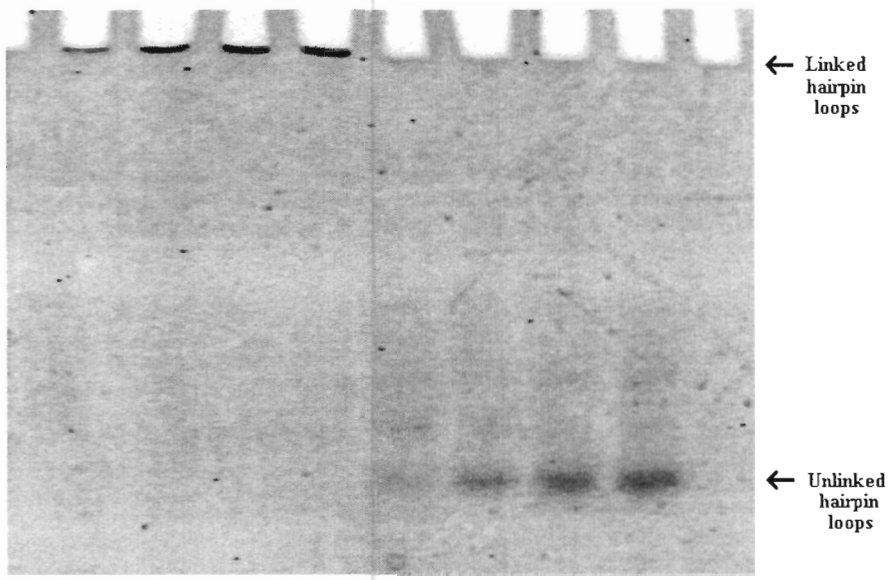


Figure 4.3.11 A 4% native PAGE gel showing the DNA structures formed in the presence of varying amounts of LOL01 (Lane 1 to 4, from left) and that the linking process was interrupted with the increasing amounts of LOL02 present in the LOL01 system.

Experiments using LOL03 with LOL02 in various combinations in order to test the ability of these structures to block the linkages between LOL01 structures were performed. LOL01 was first mixed with LOL02 and LOL03 individually in order to observe the complexes formed. LOL01 was then mixed with LOL02 and LOL03 in different orders of addition and the complexes obtained were analysed using gel electrophoresis (Figure 4.3.12). The combined complex created by adding LOL02 first and then LOL03 second, resulted in both strands binding to LOL01 instead of forming a duplex between each other (LOL02 and LOL03) (Figure 4.3.13, lane 4), This duplex between LOL02 and LOL03 occurs when all strands are mixed together at the same time.

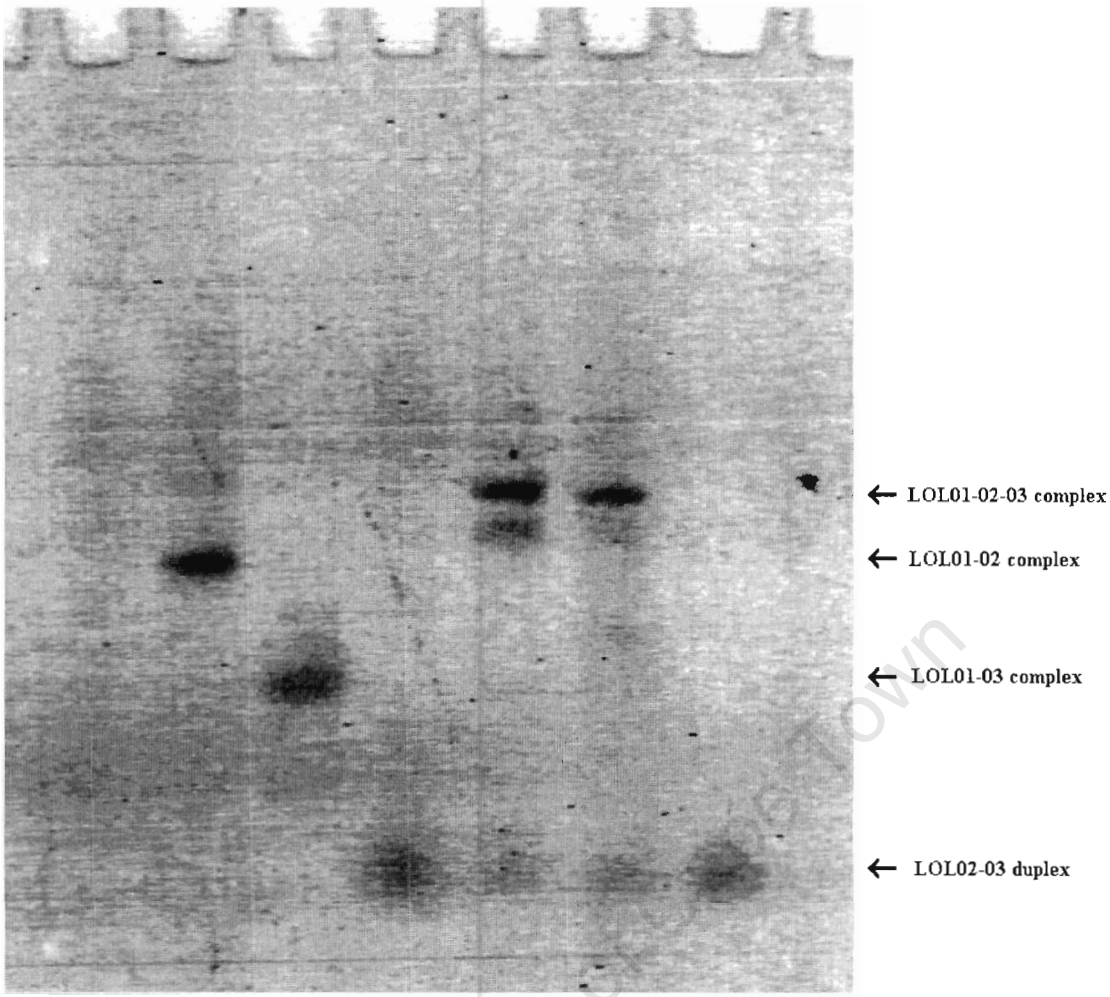


Figure 4.3.12 A 4% native PAGE gel showing the complexes formed by combining LOL01, LOL02 and LOL03. Lane 1: LOL01 only (structure was too large to be resolved); Lane 2: LOL01 and LOL02; Lane 3: LOL01 and LOL03; Lane 4: LOL01, LOL02 and LOL03 mixed at the same time; Lane 5: LOL01-LOL02 complex followed by addition of LOL03; Lane 6: LOL01-LOL03 complex followed by addition of LOL02; Lane 7: LOL02 and LOL03 duplex.

A further experiment was conducted to test the efficiency of using LOL02 to block the formation of linear complexes between LOL01 structures. LOL01 and LOL02 were mixed in different ratios and the products obtained were analysed using non-denaturing PAGE. The results of this analysis are shown in Figure 4.3.14. The size of the structures formed was found to be dependent on the amount of LOL02

added. This was interpreted to be a consequence of binding of LOL02 to the loop sequence.

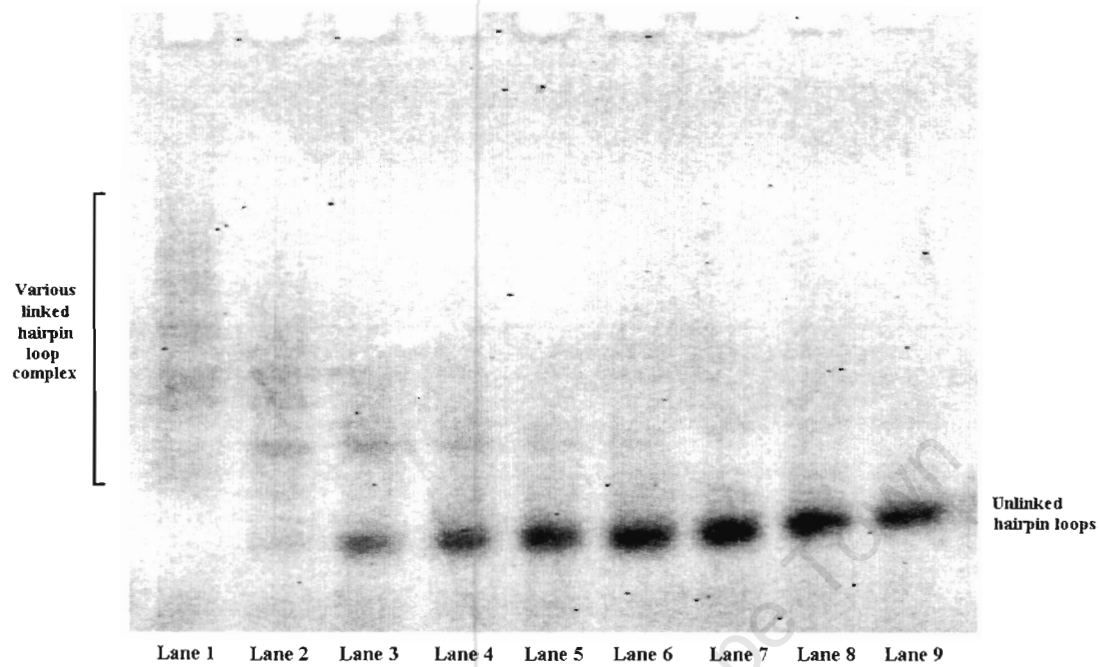


Figure 4.3.13 Non-denaturing PAGE gel electrophoretic analysis of the products obtained from mixing LOL01 (0.5μM) with LOL02 in different ratios. Lane1: LOL01 only; lane 2: LOL01 to LOL02 in a ratio of 5:1; lane 3: in 5:2; lane 4: in 2:1; lane 5: in 5:3; lane 6: in 5:3.5; lane 7: in 5:4; lane 8: in 5:4.5; and lane 9: in 1:1 ratio.

The results indicate that as the amount of LOL01-LOL02 complex increased the corresponding size of LOL01 complexes decreased (Figure 4.3.14). A similar result was observed when LOL02 was replaced with LOL03. The binding of LOL03 to LOL01 blocked the linking of hairpin loop due to single strand extensions. This result is shown in Figure 4.3.14.

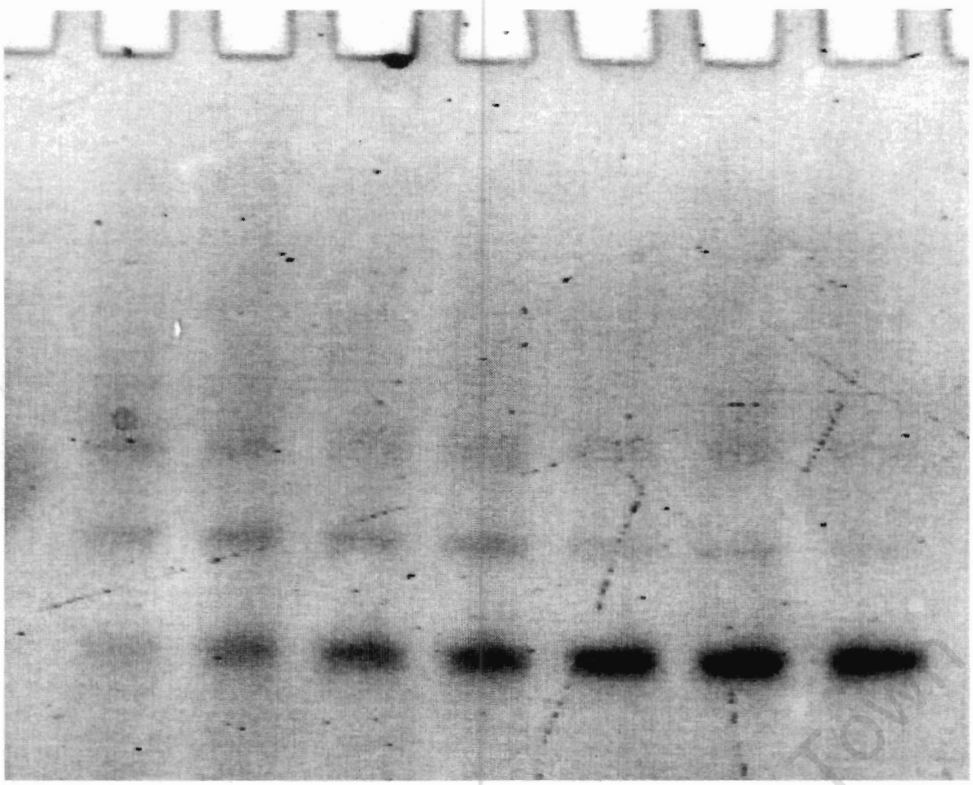


Figure 4.3.14 Gel electrophoresis experiment of mixing LOL01 (0.5μM) with LOL03 in different ratios. Lane 1: LOL01 to LOL03 in a ratio of in 5:2; lane 2: in 2:1; lane 3: in 5:3; lane 4: in 5:3.5; lane 5: in 5:4; lane 6: in 5:4.5; and lane 7: in 1:1 ratio.

## 4.4 Discussion

### 4.4.1 Meta-stable state systems using DNA hairpin loop formation

The formation of different DNA nanostructures that represented different meta-stable states can be described in terms of the free energy changes that occur when one meta-stable state is changed to another. The free energy change between DNA nanostructures determines which DNA nanostructure is thermodynamically favourable under a given set of conditions. Figure 4.4.1 depicts the free energy changes $\Delta\Delta G$ (in a.u.) that occur along the reaction coordinates for the first and the second mechanism respectively (cf Figure 4.1.2 and 4.1.3).

The initial state of the folded hairpin loop structure is set as $\Delta G$ equal to zero, the addition of the oligonucleotide B or D respectively as seen in step 1 will require a small activation energy to allow the rearrangement into the (A+B) or (A+D) complexes. These newly formed helical complexes are more favorable than the initial state situation. In step 2, the addition of the 'fuel' strands C or E resulted in the formation of a perfectly matching double helix (oligonucleotide B and C) or (oligonucleotide D and E) respectively. These double helices form after overcoming another activation energy barrier. This addition allows the reformation of the initial state (hairpin loop structure) of oligonucleotide A to occur. The addition of the mismatching oligonucleotide B or the stem binding oligonucleotde D can reinitiate

the cycle (cf. Figure 4.1.2 and 4.1.3).

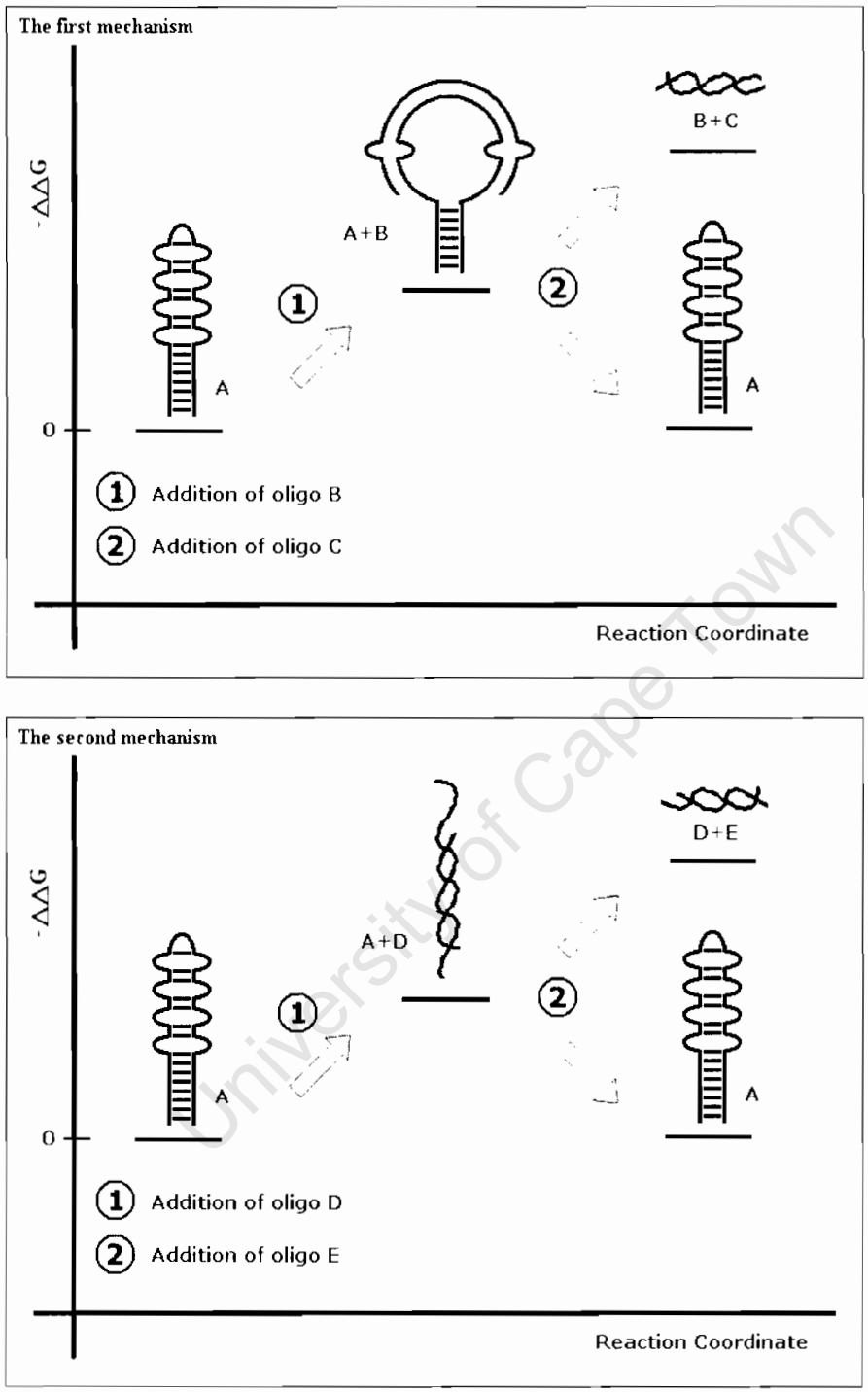




Figure 4.4.1 The changes in free energy level when moving along the thermodynamic cycle upon the addition of the different single strands to the initial hairpin-loop structure.

Figure 4.4.2 depicts the combination of the first and the second mechanism that comes about when the two 'fuel' strands B or D respectively are added to the same solution at a suitable point in the thermodynamic cycle. Figure 4.4.3 demonstrates the free energy changes that occur between consecutive steps around the full thermodynamic cycle.

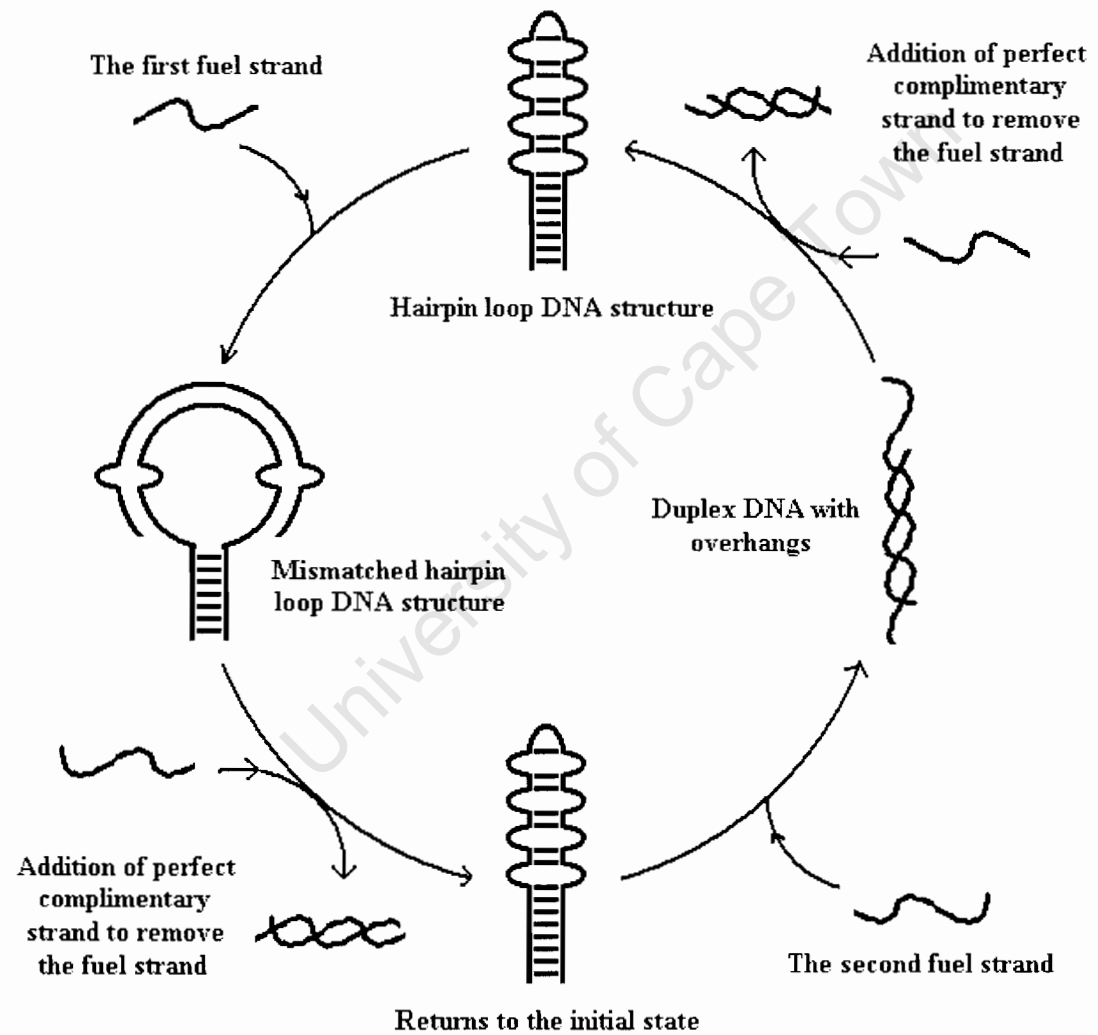


Figure 4.4.2 The combined first and second mechanisms presented as a thermodynamic cycle driven with two additions of two different fuel strands (C and E)

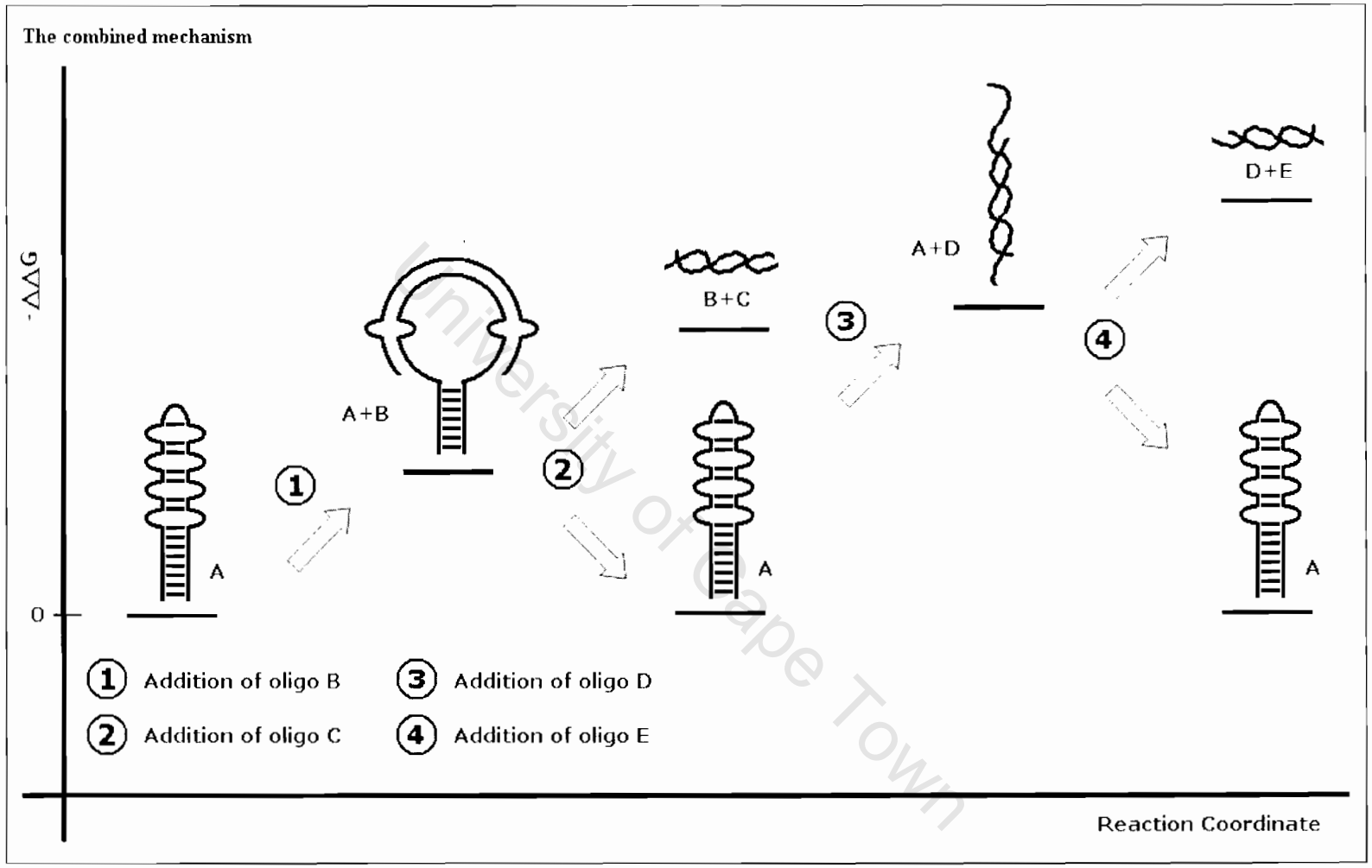


Figure 4.4.3 The free energy change in the combined mechanism

In this experiment, oligonucleotides are designed to interact with each other in a cyclic sequential fashion. The process resembles an enzyme-mediated turnover from a substrate to a product. The key-starting element is a meta-stable hairpin loop structure, which we called 'the enzyme' that binds a 16mer ssDNA (substrate), to its single stranded loop sequence (binding site). The 16mer ssDNA binds to the loop sequence that consists of 6 triplet repeats $(CAG)_6$ to form a double helix containing two mismatches (the "enzyme-substrate" complex). $(CAG)_6$ repeat sequences were chosen as they are implicated in the length-dependent expansion of gene sequences. These expansions are likely to involve unusual DNA structures. The 16mer ssDNA can reversibly dissociate from the loop at elevated temperatures but this does not cause the denaturation of the hairpin loop stem. On addition of a perfectly complementary sequence to the 'substrate' sequence, a 16mer linear double helix 'product' is formed and the 'enzyme' hairpin returns to its initial conformational state. The intermediate meta-stable helical complex is formed that can again be challenged by the second 17 mer ssDNA.



### 4.4.2 Linkage of the DNA hairpin loop with single strand extensions

Linear DNA chain created by linking DNA hairpin loop with single strand extensions is a novel method that can be used to build unusual DNA nanostructures. This unique

orientation of DNA hairpin loop structures is carried out by hybridizing the single strand extensions at the ends of the stem-loop to the single strand loop sequence in the middle. The respective sequences in these sections are complementary to each other and this result in the formation of self-assembled linear aggregates. The linking process is spontaneous and the size of the linked structure is directly proportional to the concentration of the DNA hairpin loop present in the system. The structural topology is not yet known as binding in loop sequence creates a three-way junction. The linkage can be influenced by introducing ssDNAs that compete either with the single strand extension or with the single strand loop sequence. The consequence of this result in a size reduction of the linked structures, and the size of linked structures can be controlled by the amount of ssDNAs added to the system.

The binding to loop sequence of ssDNA to block the linkage between two DNA hairpin loops shows better efficiency than the binding achieved using single strand extensions. This is possibly because the three-way junction created at the single strand extensions resulted in less stable structure.

The structures formed from the interactions between DNA hairpin loop structures and single strand DNA, or between DNA hairpin loop structures using single strand

extensions, are based on the sequence complementarity of the two species. The potential applications for the design of new nanostructures will be discussed in the next chapter.

# Chapter 5 Potential applications using DNA nanotechnology

## 5.1 Potential future applications using DNA network

Large DNA networks are built using uniform DNA building blocks. These DNA building blocks are chosen to ensure sequences that the highest stability for the DNA network structure. These sequences used here are therefore designed accordingly. This sequence design aims at combinations of different DNA structures that can appear in a single DNA building block (discussed in chapter 1). These combinations result in different properties of the building blocks. The shapes of the network units created by these building blocks are determined by the shape of these DNA building blocks, as well as by the interaction between them. Each compartment of the network contains more than one double helix. In a topology like this, it is impossible to carry out the biological functions of the DNA like transcription or replication as the processes are always started by separating the double strand of the DNA. In order to make these structures useful biologically, the reactions have to occur with in the spaces provide by a single compartments and repeated many times. This requires extra structural features located within a compartment, and will not be discussed here. In our cases, a DNA network is created based on the branched three-way junction DNA. In this network, due to the topological considerations, the compartments

created by the junction are basically hexagonal in shape[99]. The linkage between three way junction DNA is random as the consequence of identical sticky ends in each arm, which resulted in a mix of pentagon and hexagon compartments in the DNA network. The potential applications using this DNA network are not limited by these non-identical compartments. The distance between two branch points is exactly two helical turns, resulting in defined size irrespective of the sequence information. Using selected sequences will enable us to design the DNA network with biological function such as multiplying a binding site of a particular transcription factor. The sequence that binds the transcription factors can be introduced in each branched arm. The sequence will become recognizable by transcription factors after ligation, and each compartment will have at least five binding sites for a transcription factor. The binding of transcription factors will not be hindered as the space provided by each compartment is enough to accommodate these proteins without structural hindrance (Figure 5.1.1).

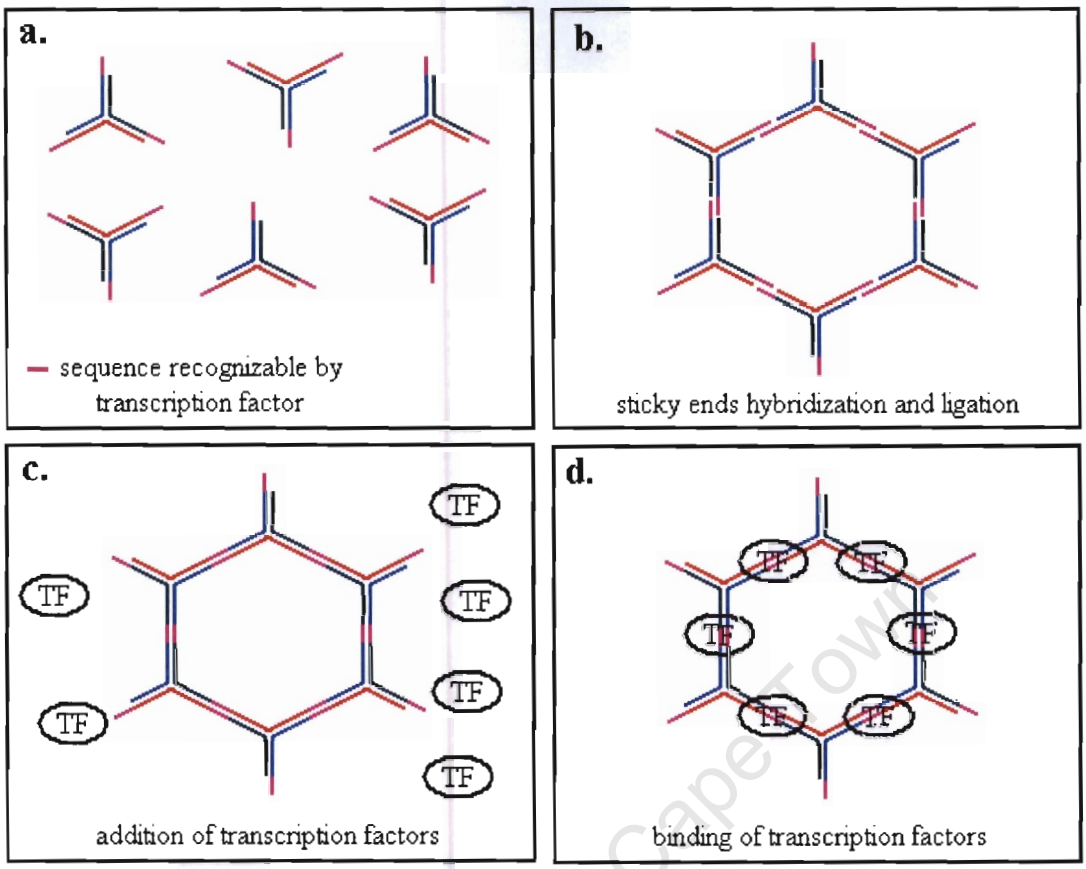


Figure 5.1.1 Schematic diagram of three-way junction DNA network binding with transcription factors (TF). a) three way junction DNA with sticky end sequence recognizable by transcription factor; b) sticky ends hybridization and ligation; c) addition of transcription factors after ligation; d) binding of transcription factors to DNA network. (This drawing is not according to scale)



## 5.2 Potential future applications using hexagonal DNA nanoswitch

Molecular detection using the interaction of fluorescent groups and quenchers is a popular technique in single mismatch detection and PCR product amplification. In our case, the hexagonal DNA nanoswitch made by sequential arrangement of three-way junction DNA can be used as a detective tool in this research. In single mismatch detection, the detective tool has to be very sensitive in order to pick up the difference

between two correct hybridized ssDNA. For a hexagonal DNA nanoswitch carrying out this task, the fluorescent group and quencher will be arranged juxtapositioned to each other when the correct strand is hybridized to the opening end of the nanoswitch. This requires the fluorescent group and the quencher attached to the single strand extensions at both opening end of the nanoswitch. The initial state of the nanoswitches is set to be the "ON" state, where the fluorescent groups and the quenchers are far apart. A solution containing a matching ssDNA will hybridize to both single strand extensions and arrange the fluorescent group and the quencher to align next to each other. This result in the fluorescent energy transfer and no light emission will take place. This hybridization turns the nanoswitch to a "OFF" state, which indicates the correct strand is bound (Figure 5.2.1). To increase the sensitivity of this detection, the hybridization process has to occur at a certain temperature. This temperature is set to allow the correct hybridization to occur. Accordingly if a ssDNA containing mismatches is added, the hybridization will not occur at this temperature and the nanoswitch will stay "ON" state to indicate the incorrectness.

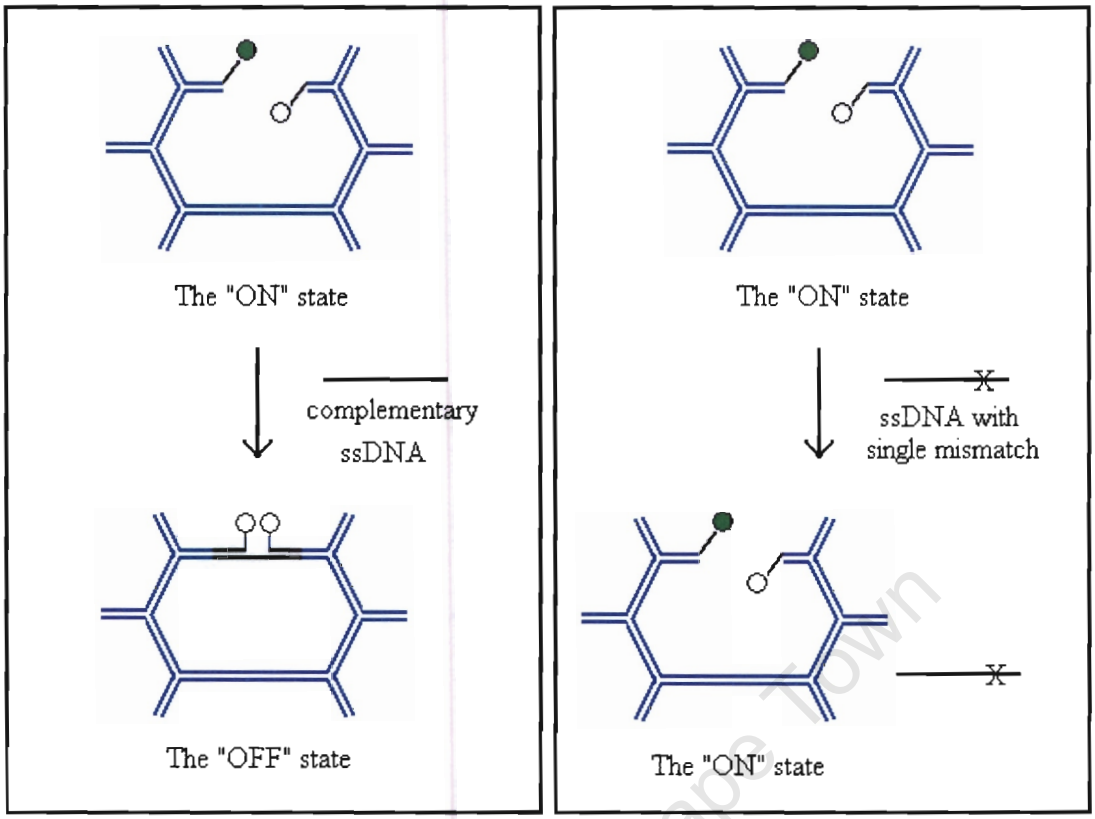


Figure 5.2.1 A schematic diagram of single mismatch detection using hexagonal DNA nanoswitches at a fixed temperature. Change from the "ON" state to the "OFF" state when complementary ssDNA is added (left). The hexagonal DNA nanoswitch stays the "ON" state when a ssDNA with a single mismatch is present.



The further modification of this nanoswitch can be made by selecting the ssDNA containing specific sequences. This is done by mixing the nanoswitch with a solution containing a mixture of ssDNAs with different sequences. In this case, only the ssDNA that consists of the perfect complementary sequence will be picked up by these nanoswitches, and therefore be selected out from the other ssDNAs (Figure 5.2.2). This selection can also be used in checking the correct PCR amplified product.

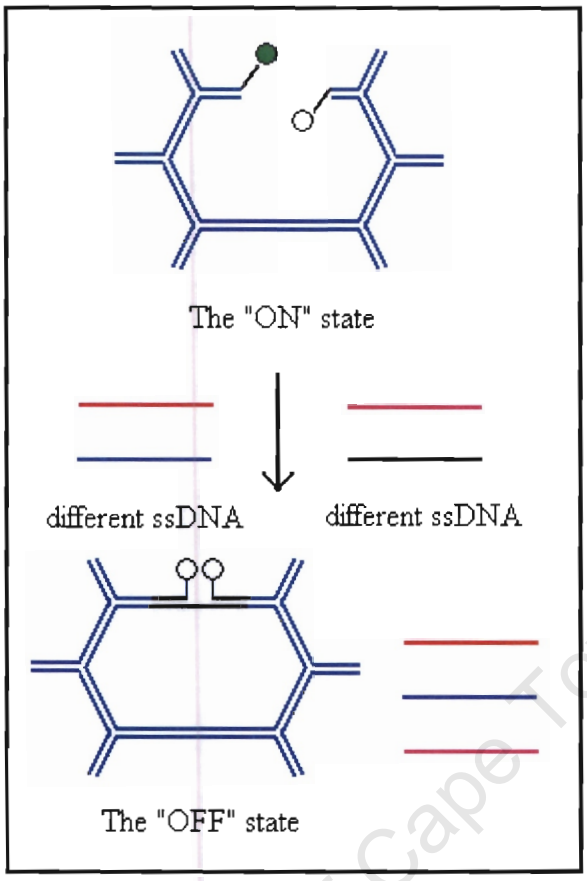


Figure 5.2.2 The schematic diagram demonstrating the ssDNA separation using hexagonal DNA nanoswitches.

The non-biological use of these nanoswitches can be applied in terms of computer memory system. In these nanoswitches, the "ON" state represents the state "1", where the "OFF" state represents as the state of "0". This results in a binary memory system created by using these nanoswitches in different states. Changing between these two states is driven by two concentrations. The memorial state of each nanoswitch can be read out by amount of fluorescence detected in a fluorimeter (Figure 5.2.3).

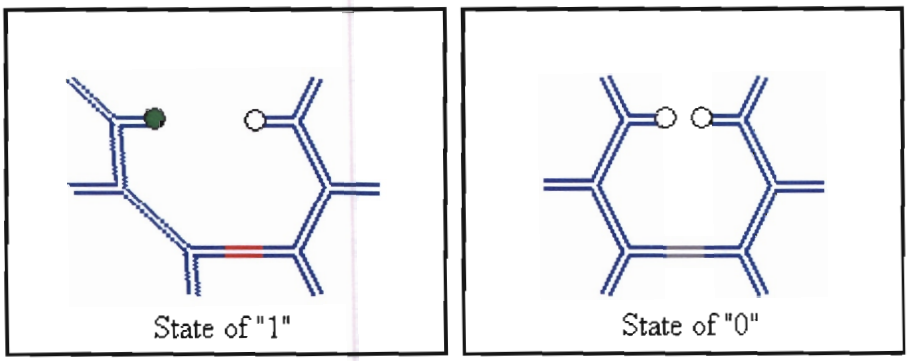


Figure 5.2.3 The schematic diagram of a binary memory system using hexagonal DNA nanoswitches. The "ON" state represents the state of "1" (left); the "OFF" state represents the state of "0" (right).



**5.3 Potential future applications using DNA nanostructures**

From the study of meta-stable DNA nanostructures it is evident that the secondary interactions between different DNA strands constitute the essential driving force behind these nanostructures. The stability and identity of a meta-stable nanostructure is dependent on these interactions. Changing from one meta-stable state to another requires an activation energy which acts to move from the current conformation and to facilitate the transition into the next state. The activation energy (used in chapter 4 and here) is supplied as heat. The conformational change of a DNA nanostructure is thermodynamically driven and is reversible.

Different fuel strand designs allow for the creation of different levels of interactions between the fuel strands and the binding sites present on DNA nanostructures. The first design parameter concerns the length and the sequence of the fuel strand. The

length of the fuel strand refers to the number of base pairs formed when hybridizing to a DNA binding site in a nanostructure. A higher number of base pairs between the fuel strand and the DNA nanostructure results in a more stable complex being formed. In terms of sequence contribution, a higher GC% in the fuel strand makes it more thermodynamically favorable for the fuel strand to bind the DNA nanostructure as compared to a strand of identical length but of lower GC content. The second design parameter concerns the the introduction of mismatches into the fuel strand. Mismatches between the fuel strand and the DNA nanostructure result in a lower general stability of the complex. The consequence of this is that the interaction will be more thermodynamically more favorable between the second fuel strand and the DNA nanostructure when present in the system. This is because the sequence of the second fuel strand is perfectly complementary to the DNA nanostructure. A third possibility is to create unusual DNA structures within the DNA nanostructure itself that are specific for different fuel strands. Through the addition of different fuel strands in stages, the DNA nanostructure can undergo different sequential conformational changes. Each can then be tailored to perform a particular task (described in example below). These conformational changes are interchangeable and are not necessarily sequential.

A number of potential practical uses can be derived from the above design. One

obvious use for this system is to utilize DNA to convey specific macromolecules. The concept of DNA based macromolecules conveyance involves two major steps: loading and releasing. What is important to establish is under which conditions the loading or releasing stages of this process will take place. As in the mechanisms that are driven by changing meta-stable DNA nanostructure, a hairpin loop DNA structure undergoes a conformational change when interacting with different DNA strands. It can be designed for example as a transporter structure which can carry out the loading and releasing of specific macromolecules (such as protein or DNA). The design of the unpaired DNA sequence in the loop section is critical to the successful development of this process. During the loading process, the DNA nanostructure is designed to be specifically recognizable by the target (macromolecule). This is done by including a specific sequence in the loop section that is specific for the target recognition. This sequence is not recognizable by the target until a complementary strand is hybridized to it. This complementary strand is the fuel strand and the hybridization acts as to increase the level of loading specificity. The binding of the fuel strand (Fuel(+) strand) to the DNA nanostructure enables the complex to bind the target. This step concludes the loading stage. After the target binds to the DNA nanostructure, the entire structure converts into a new conformation that is more thermodynamically favorable than the DNA nanostructure-Fuel(+) strand complex and the stand-alone target.

To release the loaded target, it is necessary to destabilize this intermediate complex. This is achieved by introducing a different fuel strand (Fuel(-) strand) that causes the dissociation of the Fuel(+) strand from the DNA nanostructure and the target. This dissociation is based on the fact that the binding affinity of the Fuel(+) strand for the Fuel(-) strand is higher than to the DNA nanostructure or to the target after the activation barrier is overcome. Once the Fuel(+) strand is removed from the intermediate complex, the DNA nanostructure is no longer recognizable by the target. This result in the release of the target from the DNA nanostructure, and the DNA nanostructure is then available for the next loading process. The entire conveyance system is demonstrated in Figure 5.3.1. In this system, the Fuel(-) strand and target have no interactions with the DNA nanostructure. Therefore in absence of the Fuel(+) strand no loading occurs.

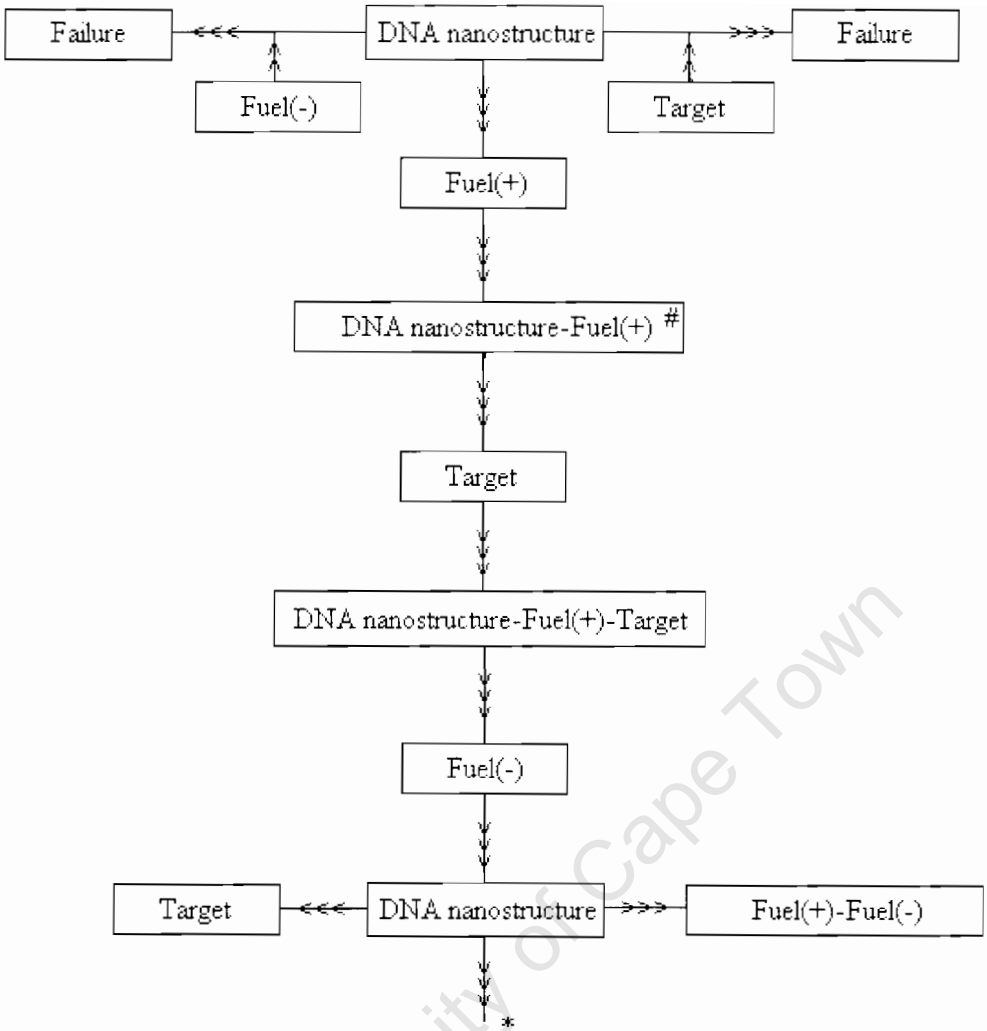


Fuel(+): the fuel strand that makes vector target-recognizable;
Fuel(-): the fuel strand that removes Fuel(+) from vector;
DNA nanostructure is not recognizable by target and not associated with Fuel(-);
# DNA nanostructure-Fuel(+) is recognizable by target;
* Cycle restarts;



Figure 5.3.1 A flow chart showing the target-conveyance system based upon meta-stable state DNA nanostructures.

An example of how this system can be used is in separating a specific protein from a mixture of proteins. The DNA hairpin loop can be used as a DNA nanostructure in this situation. The sequence of the DNA hairpin loop region is designed to bind this protein specifically. The Fuel(+) strand is a ssDNA that is designed to contain

complementary sequences to the DNA nanostructure (Figure 5.3.2, top). The Fuel(+) consists of three region. The first section is composed of a sequence complementary to the target sequence, the second section consists of a sequence that binds to the unpaired sequence adjacent to the target sequence in order to stabilize binding. The last section contains a sequence that is complementary to the Fuel(-) strand. The fuel(-) strand is designed to contain two sections of sequence. One section is identical to the unpaired sequence adjacent to the target sequence, whereas the other sequence is complementary to the remaining unpaired Fuel(+) strand sequence. When the Fuel(+) strand is added, it binds to the loop sequence to create a double helix section within the loop that allows the protein to bind (Figure 5.3.2, bottom left). This combined complex can be extracted from the mixture and transferred to a new environment. The release of protein into the new environment is accomplished by addition of the Fuel(-) strand to the combined complex. The binding of Fuel(+) and Fuel(-) strands forms a dsDNA complex with a single strand extension (Figure 5.3.2, bottom right). This dsDNA complex is thermodynamically favourable as the number of base pairs in the new structure is higher than that found in the target sequence binding complex. The unpaired bases in the single strand extension function as the protein binding sequence. Furthermore, the protein is not able to bind with the duplex either and therefore is released from the complex.

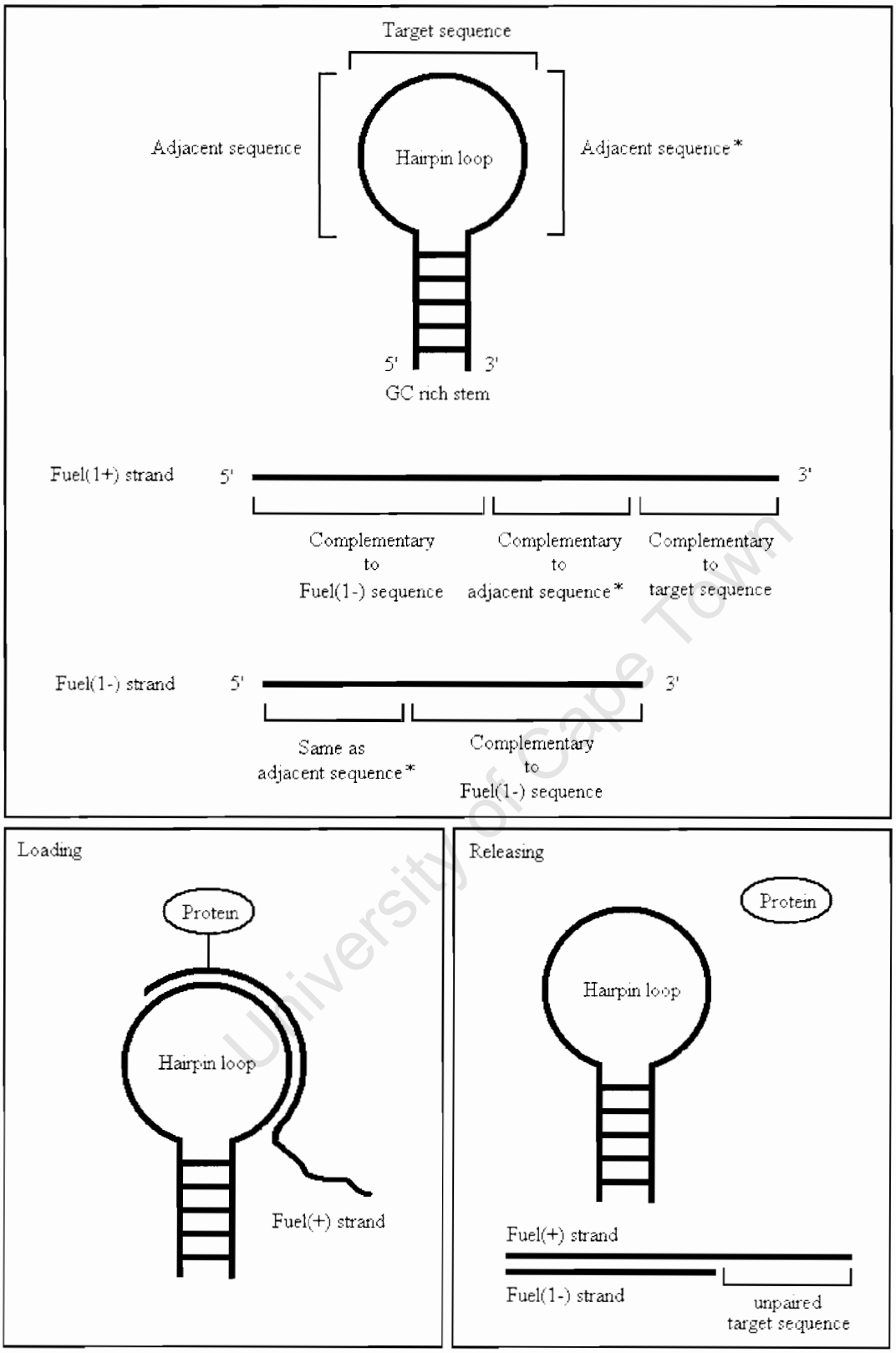


Figure 5.3.2 A schematic diagram of a protein conveyance system. Top) Design of DNA hairpin loop and Fuel(+)/(-) strands; bottom left) to complex when the protein is loaded; bottom right) the duplex that is formed when the protein is released. (This drawing is not according to scale).

The conveyance system discussed above is for a single target protein only. This system can be further modified to bind and release multiple targets. To convey multiple targets using a single DNA nanostructure, the unpaired sequence of the DNA nanostructure has to be designed to contain different sequence binding sections for the different targets. Different Fuel (+)/(-) strands have to designed so as to release the specific target. The loading process is identical to that occurring in the single target convey system. The addition of the first Fuel (1+) strand to the corresponding target 1 results in the target1 being loaded onto the system. This target 1 is then released after the addition of the Fuel(1-) strand, and the DNA nanostructure is then ready to convey the next target protein. The second Fuel(2+) strand and the target 2 can be added to this system. The Fuel(2+) strand binds at different binding site of the DNA nanostructure and facilitates the target 2 loading to this site of the complex. The addition of the Fuel(2-) strand releases the target 2. The DNA nanostructure now can either load target 1 or target 2 or target 3 if applicable (Figure 5.3.3). The only difference in this conveyance system is that it requires Fuel(3+) strand, and binding of Fuel(3+) to the DNA nanostructure must be at a different binding site.

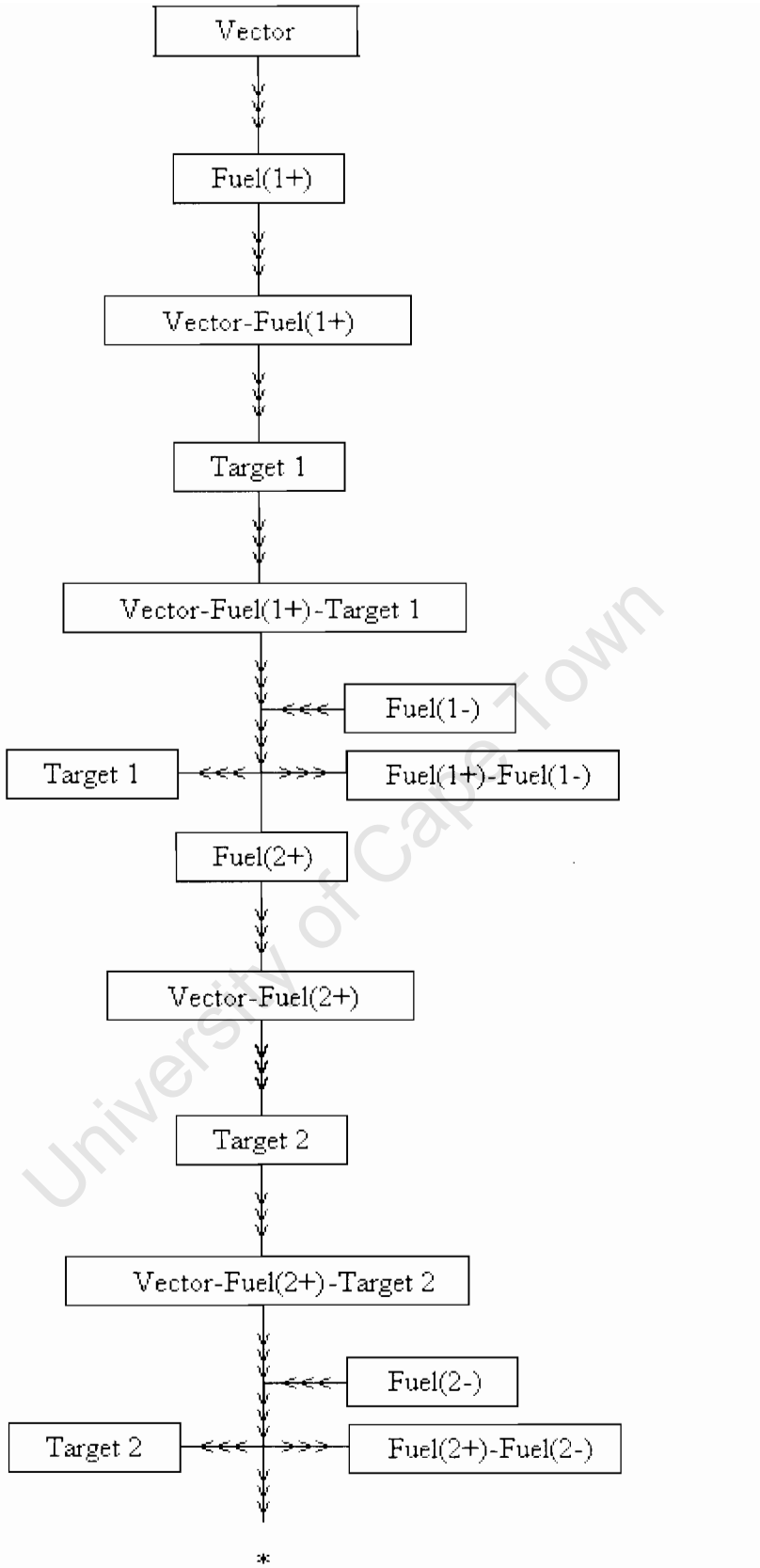




Figure 5.3.3 The flow chart showing a multiple targets-convey system.

In the next example we demonstrate this process by modifying the previous system. The DNA hairpin loop sequence is now designed to contain three hairpin loop sections of different sequences that are specific for three individual proteins. These sequences are folded in the coverleaf structure like a t-RNA. When Fuel(1+) strand is added and hybridized with the target 1 sequence, the target protein can bind to this sequence and be separated from the other proteins and then released by addition of Fuel(1-) strand. The DNA hairpin loop now is ready to carry target 1 protein again, or it can carry target 2 or target 3 for separation (Figure 5.3.4).

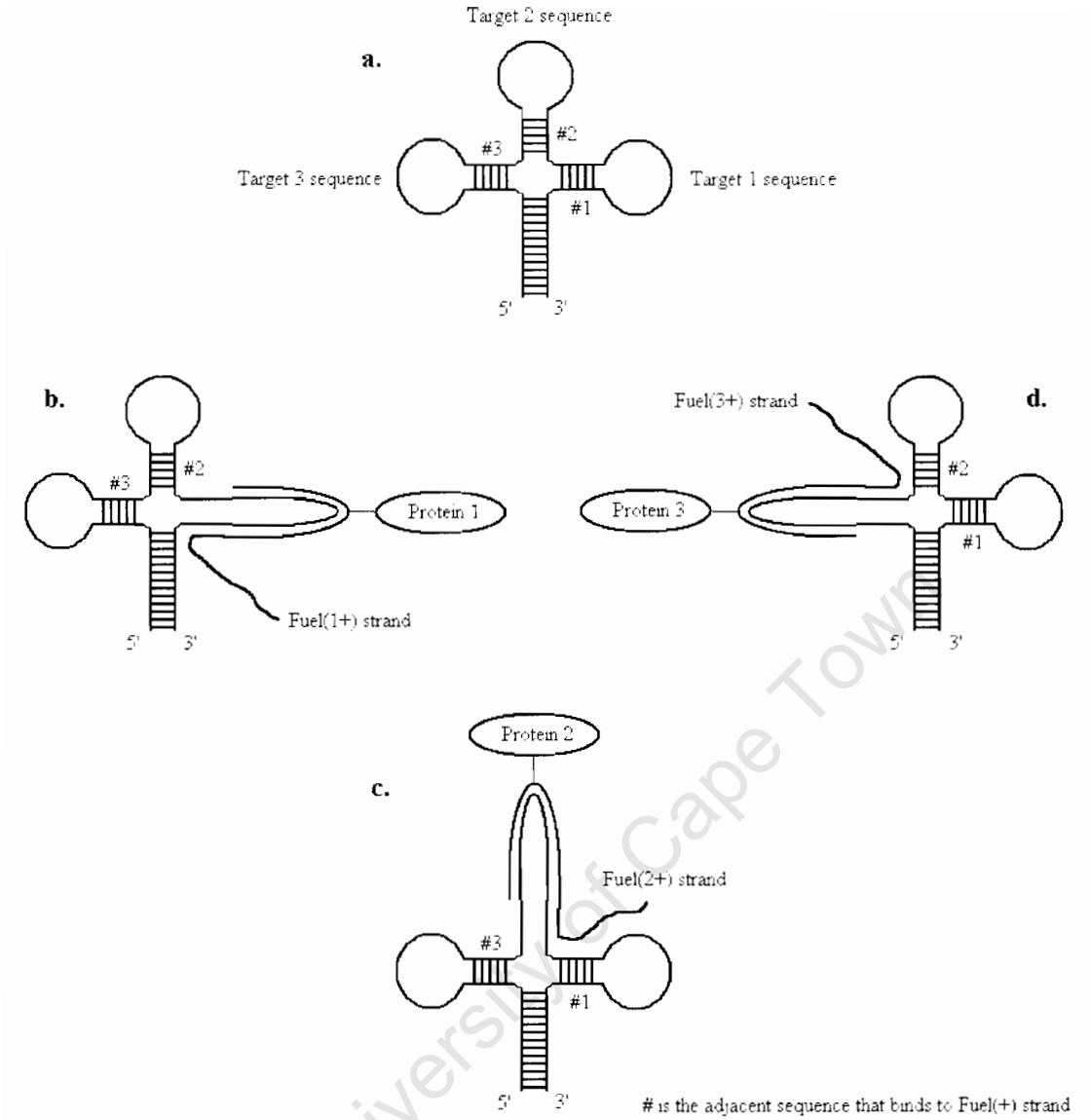


Figure 5.3.4 The schematic diagram shows modified hairpin loop structure carrying different protein when different Fuel(+) strands are added. a.) modified hairpin loop structure (cloverleaf structure); b.) Protein 1 loading; c.) Protein 2 loading; d.) Protein 3 loading.



**"On the shoulder of giants"**

Using linked DNA hairpin loops by hybridizing single strand extensions with another loop sequence can be used to create DNA nanowires. The feature of DNA nanowire using linked DNA hairpin loops requires a fitting design of the loop sequence. This

new design of loop sequence now contains 4 sections of selected sequences (Figure5.3.5, left). The first and the last sections are designed to bind to two ssDNAs. These two ssDNA sequences are attached with gold nanoparticles at their 5'- ends. The remaining middle two sections consist of sequences that are complementary to the sequences single strand extenstions. The linkage of this new hairpin loop DNA creates two unpaired sections below the binding of the loop sequence to the complementary single strand extenstions. These two unpaired sections are complementary to two ssDNA with gold nanoparticles attached, and this hybridization constitutes the DNA nanowire (Figure 5.3.5, right).

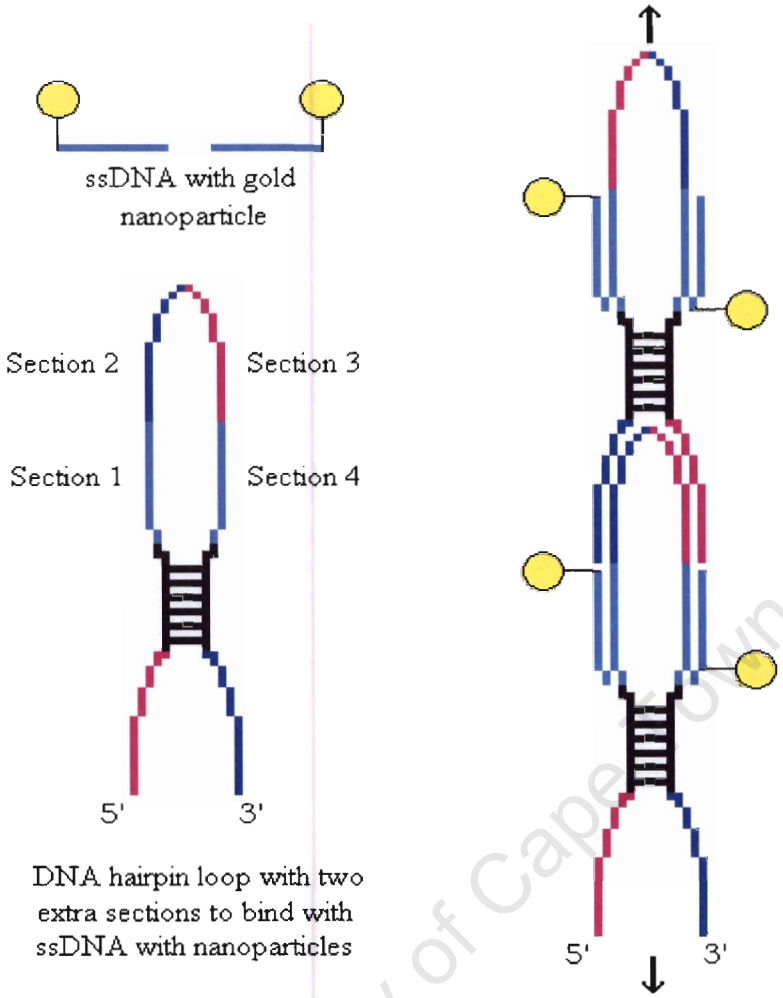


Figure 5.3.5 The schematic diagram of a new DNA hairpin loop with two extra sections that bind to two ssDNA with gold nanoparticles attached.

The conductivity of this DNA nanowire can be tuned by designing the linking sequences between hairpin loops. This is done by attaching limited number of gold nanoparticles through ssDNA hybridization. There is a modification required on changing the sequences of single strand extensions prior to the hybridization. Changing these sequences resulted in the DNA hairpin loop being now unable to self-assemble. Instead, the addition of another DNA hairpin loop with complementary single strand extensions containing sequences that are complementary to the single

strand loop sequence can initiate the linking process. The single strand loop sequence of the second DNA hairpin loop is designed to be complementary to the single strand extensions of the first DNA hairpin loop. This resulted in the linked structures between these two hairpin loops occurring in an alternating arrangement (Figure 5.3.6). The size of the linked structure is dependent on the amount of DNA hairpin loops present.

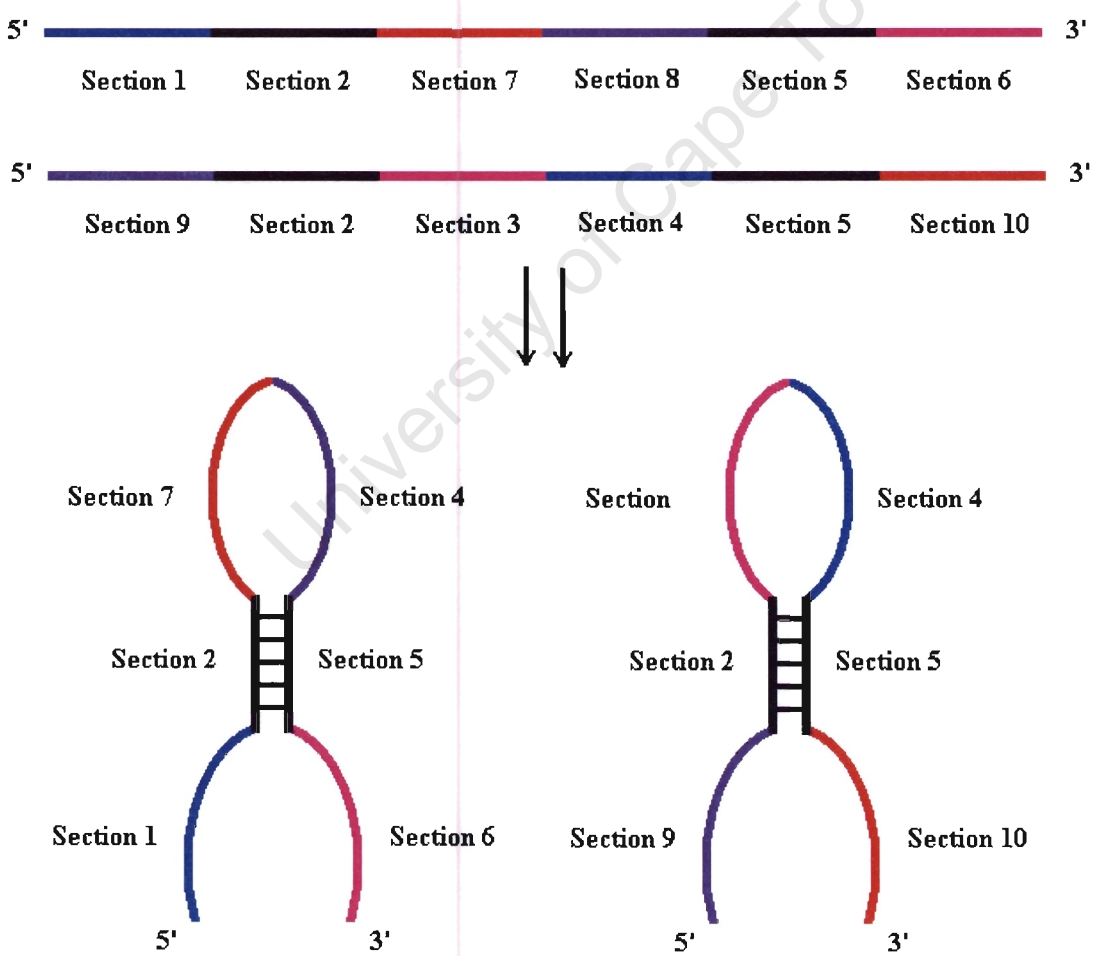


Figure 5.3.6 A schematic diagram illustrating the modified DNA hairpin loop structures in both hairpin loop and extension sequences.

The sequence of each structure is designed to be complementary to the loop section of the corresponding DNA structure. This results in the structural orientation of two structures in an alternating arrangement (Figure 5.3.7).

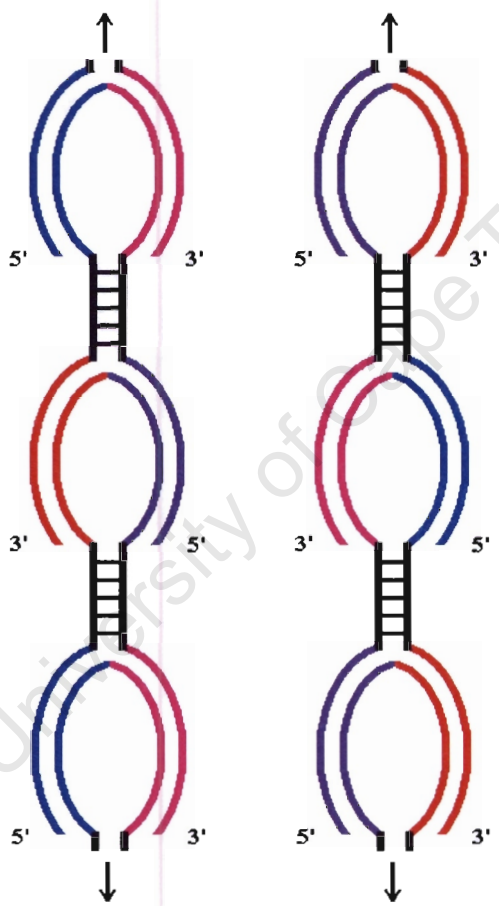


Figure 5.3.7 The extension of the DNA hairpin loop structure using different sequences in an alternating pattern.

The two approaches can be combined when some modifications are made in this design. The modification can be made using the combination of the nanowire and this alternating linking DNA hairpin loops. It needs the change of the sections of the loop

sequence of the second DNA hairpin loop that binds to ssDNA with the nanoparticle to another sequence. The ssDNA that binds to this sequence is therefore not attached with a gold nanoparticle. The consequence of this design result in gold nanoparticles in every second hairpin loop in the linkage (Figure 5.3.8a), and reducing the conductivity over the entire nanowire.

The nanowires can be grown from a common base. This is done by introducing a piece of single strand DNA containing sections of sequences that are complementary to different single strand extensions' sequences. This result in a two-dimensional DNA structure consisted of DNA nanowires in an elongated fashion (Figure 5.3.8b).

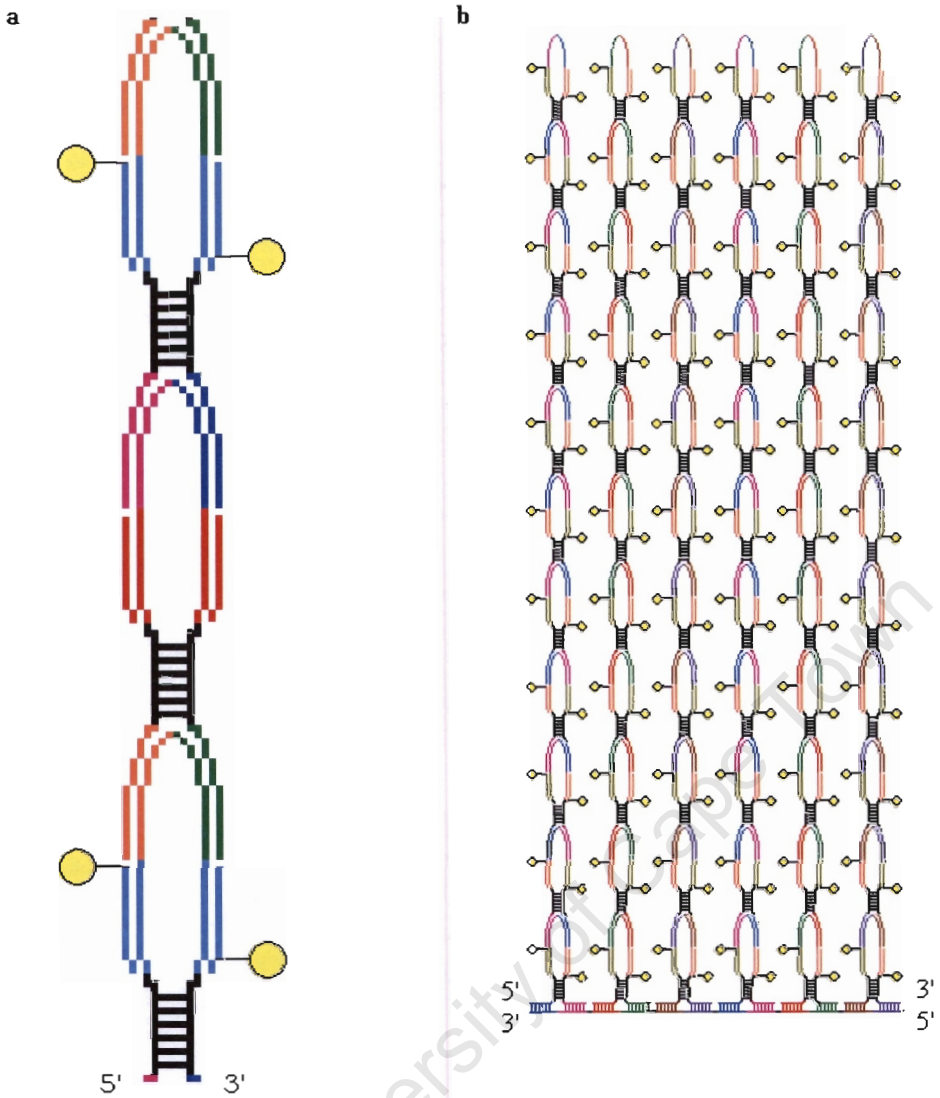


Figure 5.3.8 The schematic diagram of DNA nanowire using alternating DNA hairpin loop linkage (a). A two-dimensional DNA structure containing DNA nanowires in an elongated fashion (b).

## 5.4 Conclusion

DNA sequences and/or structures have been found with many unique properties. By exploiting these properties, many nanostructures or devices can be made from DNA. We have studied these structures and devices, and we will apply what we learnt to create various new structures made from DNA.

In this work, we have shown how large DNA networks can be constructed using three-way junction DNA. We have controlled the growth of the DNA network using different kinds of sticky end sequences and different number of sticky ends as part of the DNA three-way junction building block. The size of the DNA network appears to be determined by these factors. We then constructed a opto-mechanical hexagonal DNA nanoswitch by using six sets of three-way junction DNA containing different sticky ends sequences. The switching mechanism of the nanoswitch is based on the conformational change of a sequence from the right handedness to the left handedness. This shift is driven by change in the environmental cation concentrations. The occurrence of the shift is detected by the fluorescent intensity change (FRET). The shift from the right handedness to the left handedness results in a relocation of the quencher relative to the fluorescence emitter resulting in a 62.07% decrease in fluorescent intensity. This is sufficient to make the nanoswitch a tool for the detection of conformational changes. Next, we have demonstrated how meta-stable state DNA

nanostructures based on a DNA hairpin loop can mimic the enzyme-substrate binding mechanism. This system uses a DNA hairpin loop as the "enzyme" to bind with the so called "Fuel strand" that acts as the substrate. This substrate binds to the "enzyme" to make the whole complex undergo a conformational change. The substrate is then dissociated from the enzyme by addition of a second ssDNA whose sequence is complementary to the fuel strand sequence. The DNA hairpin loop is then returned to its initial state for the next cycle of binding and release. This system can be used as a protein-conveyance system that enables the protein loading and releasing. The target can be any macromolecule that associates with the DNA nanostructure in a way that the target bound complex is thermodynamic favourable compared to the stand-alone target. The loading process requires the aid of a fuel strand. The release of this target is accomplished by the addition of a ssDNA that has higher affinity to the fuel strand. This addition results in a formation of a dsDNA by the fuel strand and the complementary strand. This results in the target being released from the complex. This system can be applied to the separation of specific proteins. This system can also be modified to convey different targets using a single DNA nanostructure. Finally, we have used a DNA hairpin loop with single strand extensions to generate an extended DNA chain. This is done by designing a DNA hairpin loop with single strand extensions with sequences that are complementary to its loop sequence. This results in

an unlimited linkage between DNA hairpin loops. This linkage can be controlled by introducing a ssDNA that either binds to the loop sequence or to the single strand extensions. An application of this linked DNA chain can be used to create DNA nanowires. By changing the loop sequence to hybridize with the ssDNA attached to the gold nanoparticles, a nanowire with a fixed conductivity is created. The resistance of this nanowire is tunable by changing the number of hybridized ssDNA with gold nanoparticles along the chain. This results in a resistance difference between two DNA nanowires with the same length. The integration of these DNA nanowires can be done by introducing a ssDNA with sections of sequences that are complementary to different single strand extensions. This results in a formation of large DNA structures consisting of different DNA nanowires in an elongated fashion.

The fundamental principle of a DNA based nanotechnology is the sequence design. Through variations of this design, many nanostructures can be made from DNA. Although we are only at the beginning of this interesting research filed now, details need to be discovered and problems need to be overcome. But it is already clear that there lies a great future potential.

## References


1. E. Schrodinger, *What Is Life? With Mind and Matter and Autobiographical Sketches*. Canto ed Cambridge University Press, 1967).

2. R.P. Feynmann, "There Is Plenty Room at the Bottom," *www.its.caltech.edu/~feynman/plenty.html* (1959).

3. G. Binnig, H. Rohrer, Ch. Gerber and E. Weibel, "Surface Studies by Scanning Tunneling Microscopy," *Phys. Rev. Lett.* 42 (1982): 57.

4. G. Binnig, C.F. Quate and Ch. Gerber, "Atomic Force Microscope," *Phys. Rev. Lett.* 56 (1986): 930-33.

5. J.M. Lehn, "Toward Complex Matter: Supramolecular Chemistry and Self-Organization," *Proc. Natl. Acad. Sci.* 99 (2002): 4763-68.

6. J.M. Lehn, "Toward Self-Organization and Complex Matter," *Science* 295 (2002): 2400-03.

7. J.M. Lehn, *Supramolecular Chemistry*. VCH (1995) Chapter 9, p 139.

8. M. Boncheva, D.H. Gracias, H.O. Jacobs and G.M. Whitesides, "Biomimetic Self-Assembly of a Functional Asymmetrical Electronic Device," *Proc. Natl. Acad. Sci.* 99 (2002): 4937-40.

9. L.A. Chrisey, G.U. Lee and C.E. O'Ferrall, "Covalent Attachment of Synthetic DNA to Self-Assembled Monolayer Films," *Nucleic Acids Res.* 24 (1996): 3031-39.

10. S. Zhang, "Fabrication of Novel Biomaterials through Molecular Self-Assembly," *Nature Biotechnology* 21 (2003): 1171-78.

11. C.M. Niemeyer, "Self-Assembled Nanostructures Based on DNA: Towards the Development of Nanobiotechnology," *Curr. Opin. Chem. Biol.* 4 (2000): 609-18.

12. G.M. Whitesides and B. Grzybowski, "Self-Assembly at All Scales," *Science* 295 (2002): 2418-21.

13. V.L. Colvin, "The Potential Environmental Impact of Engineered Nanomaterials," *Nature Biotechnology* 21 (2003): 1166-70.

14. B.J. Chen, K.J. Huang and L.Y. Chiang, "Acute and Subacute Toxicity Study of Water-Soluble Polyalkylsulfonated C-60 in Rates," *Toxicol. Pathol.* 26 (1998): 143-51.

15. D.B. Warheit, B.R. Laurence, K.L. Reed, D.H. Roach, G.A.M. Reynolds and T.R. Webb, "Comparative Pulmonary Toxicity Assessment of Single Walled Carbon Nanotubes in Rats," *Toxicol. Sci* 77 (2004): 117-25.

16. C.R. Lowe, "Nanobiotechnology: The Facbrication and Applications of Chemical and Biological Nanostructures," *Curr. Opin. Struct. Biol.* 10 (2000): 428-34.

17. R.K. Soong, G.D. Bachand, H.P. Neves, A.G. Olkhovets, H.G. Craighead and C.D. Montemagno, "Powering an Inorganic Nanodevice with a Biomolecular Motor," *Science* 290 (2000): 1555-58.

18. G.M. Whitesides, "The 'Right' Size in Nanobiotechnology," *Nature Biotechnology* 21 (2003): 1161-65.

19. V. Vijayanathan, T. Thomas and T.J. Thomas "DNA Nanoparticles and Development of DNA Delivery Vehicles for Gene Therapy," *Biochemistry* 41 (2002): 14085-94.

20. F. Crick, "Central Dogma of Molecular Biology," *Nature* 227 (1970): 561-63.

21. N.C. Seeman, H. Wang, X. Yang, F. Liu, C. Mao, W. Sun, L. Wenzler, Z. Shen, R. Sha, H. Yan, M.H. Wong, P. Sa-Ardyen, B. Liu, H. Qiu, X. Li, J. Qi, S.M. Du, Y. Zhang, J.E. Mueller, T. Fu, Y. Wang and J. Chen, "New Motifs in DNA Nanotechnology," *Nanotechnology* 9 (1998): 257-73.

22. N.C. Seeman, "DNA Is More Than Just the Secret of Life - Its Is Also a Versatile Component for Making Nanoscopic Structures and Devices.," *Scientific American* 290 (2004): 35-43.

23. N.C. Seeman, "DNA Engineering and Its Application to Nanotechnology," *Nanotechnology* 17 (1999): 437-43.

24. J.D. Watson and F.H. Crick, "Molecular Structure of Nucleic Acids: a Structure for Deoxyribose Nucleic Acid.," *Nature* 171 (1953): 737-38.

25. C. Bancroft, T. Bowler, B. Bloom and C.T. Clelland, "Long-Term Storage of Information in DNA," *Science* 293 (2001): 1763-65.

26. J. Marmur and P. Doty, "Determination of the Base Composition of Deoxyribonucleic Acid from Its Thermal Denaturation Temperature," *J. Mol. Biol.* 5 (1962): 120.

27. J. Marmur, "Heterogeneity in Deoxyribonucleic Acids: I. Dependence on Composition of the Configurational Stability of Deoxyribonucleic Acids," *Nature* 183 (1959): 1427-29.

28. L.A. Marky and K.J. Breslauer, "Calculating Thermodynamic Data for Transitions of Any Molecularity from Equilibrium Melting Curves," *Biopolymers* 26 (1987): 1601-20.

29. F.M. Ausubel, R. Brent, R.E. Kingston, D.D. Moore, J.G. Seidman, J.A. Smith, and K. Struhl, *Current Protocols in Molecular Biology*. Chapter 3.10 edJohn Wiley & Sons, 1987).

30. F.M. Ausubel, R. Brent, R.E. Kingston, D.D. Moore, J.G. Seidman, J.A. Smith, and K. Struhl, "Current Protocols in Molecular Biology," (1987): Chapter 3.14.

31. Y. Cao, R. Jin and C.A. Mirkin "DNA-Modified Core - Shell Ag/Au Nanoparticles," *J. Am. Chem. Soc.* 123 (2001): 7961-62.

32. S. Fujii, A.H. Wang, G. van der Marel, J.H. van Boom, and A. Rich, "Molecular Structure of (m5 dC-dG)3: The Role of the Methyl Group on 5-Methyl Cytosine in Stabilizing Z-DNA.," *Nucleic Acids Res.* 10 (1982): 7879-92.

33. S. Tyagi and F.R. Kramer, "Molecular Beacons: Probes That Fluoresce Upon Hybridization," *Nature Biotechnology* 14 (1996): 303-08.

34. J. Wang, D. Xu and R. Polsky, "Magnetially-Induced Solid-State Electrochemical Detection of DNA Hybridization," *J. Am. Chem. Soc.* 124 (2002): 4208-09.

35. T.F. Kagawa, M.L. Howell, K. Tseng and P.S. Ho, "Effects of Base Substituents on the Hydration of B- and Z-DNA: Correlations to the B- to Z-DNA Transition," *Nucleic Acids Res.* 21 (1993): 5978-86.

36. A. Rich and S. Zhang, "Timeline: Z-DNA: The Long Road to Biological Function.," *Nat. Rev. Genet.* 4 (2003): 566-72.

37. R. Liu, H. Liu, X. Chen, M. Kirby, P.O. Brown and K. Zhao, "Regulation of Csf1 Promoter by the Swi/Snf-Like Baf Complex.," *Cell* 106 (2001): 309-18.

38. J. Nickol, M. Behe and G. Felsenfeld, "Effect of the B--Z Transition in Poly(dG-m5dc). Poly(dG-m5dc) on Nucleosome Formation.," *Proc. Natl. Acad. Sci.* 79 (1982): 1771-75.

39. D.B. Haniford and D.E. Pulleyblank, "The in-Vivo Occurance of Z-DNA," *J. Biomol. Struct. Dyn.* 1 (1983): 593-609.

40. F.M. Pohl and T.M. Jovin, "Salt-Induced Co-Operative Conformational Change of a Synthetic DNA: Equilibrium and Kinetic Studies with Poly (dG-dC)," *J. Mol. Biol.* 67 (1972): 375-96.

41. L.J. Peck, A. Nordheim, A. Rich and J.C. Wang, "Flipping of Cloned $d(pCpG)_n.d(pCpG)_n$ DNA Sequences from Right- to Left-Handed Helical Structure by Salt, Co(III), or Negative Supercoiling.," *Proc. Natl. Acad. Sci.* 79 (1982): 4560-64.

42. A. Rich, A. Nordheim and A.H.J. Wang "The Chemistry and Biology of Left-Handed Z-DNA," *Ann. Rev. Biochem.* 53 (1984): 791-846.

43. P.S. Ho, "The Non-B-DNA Structure of $d(CA/TG)_n$ Does Not Differ from That of Z-DNA," *Proc. Natl. Acad. Sci.* 91 (1994): 9549-53.

44. M Vorlíckovă, J Kypr, S. Stokrová, and J Sponar, "A Z-Like Form of Poly(dA-dC).Poly(dG-dT) in Solution?" *Nucleic Acids Res.* 10 (1982): 1071-80.

45. D.B. Haniford and D.E. Pulleyblank, "Facile Transition of Poly[d(TG).d(CA)] into a Left-Handed Helix in Physiological Conditions," *Nature* 302 (1983): 632-34.

46. T.J. Thomas and R.P. Messner, "A Left-Handed (Z) Conformation of Poly(dA-dC).Poly(dG-dT) Induced by Polyamines," *Nucleic Acids Res.* 14 (1986): 6721-33.

47. H.H. Klump and R. Loffler, "Reversible Helix Coil Transitions of Left-Handed Z-DNA Structures," *Biol. Chem. Hoppe-Seyler* 366 (1985):

345-53.

48. H.H. Klump, "Thermodynamics of Left-Handed Helix Formation," *FEBS LETTERS* 196 (1986): 175-79.

49. S.M. Stirdivant, J. Klysik and R.D. Wells, "Energetic and Structural Inter-Relationship between DNA Supercoiling and the Right- to Left-Handed Z Helix Transitions in Recombinant Plasmid," *J. Biol. Chem.* 257 (1982): 10159-65.

50. L.J. Peck and J.C. Wang, "Energetics of B-to-Z Transition in DNA," *Proc. Natl. Acad. Sci.* 80 (1983): 6206-10.

51. H.H. Klump, E. Schmid and M. Wosgien, "Energetics of Z-DNA Formation in Poly d(A-T), Poly d(G-C), and Poly d(A-C) Poly D(G-T)." 21 (1993): 2343-48.

52. N.C. Seeman and N.R. Kallenbach, "DNA Branched Junctions," *Annu. Rev. Biophys. Biomol. Struct.* 23 (1994): 53-86.

53. R.D. Wells, "Unusual DNA Structures," *J. Biol. Chem.* 263 (1988): 1095-98.

54. L.S. Shlyakhtenko, E. Appella, R.E. Harrington, I. Kutyavin, and Y.L. Lyubchenko, "Structure of Three-Way DNA Junctions. 2. Effects of Extra Bases and Mismatches," *J. Biomol. Struct. Dyn.* 12 (1994): 131-43.

55. R. Assenberg, A. Weston, D.L.N. Cardy and K.R. Fox, "Sequence-Depedent Folding of DNA Three-Way Junctions," *Nucleic Acids Res.* 30 (2002): 5142-50.

56. E.A. Oussatcheva, L.S. Shlyakhtenko, R. Glass, R.R. Sinden, Y.L. Lyubchenko and V.N. Potaman, "Structure of Branched DNA Molecules: Gel Retardation and Atomic Force Microscopy Studies," *J. Mol. Biol.* 292 (1999): 75-86.

57. D.R. Duckett and D.M.J. Lilley, "The Three-Way DNA Junction Is a Y-Shaped Molecule in Which There Is No Helix -Helix Stacking," *EMBO J.* 9 (1990): 1659-64.

58. L.S. Shlyakhtenko, D. Rekesh, S.M. Lindsay, I. Kutyavin, E. Appella, R.E. Harrington and Y.L. Lyubchenko, "Structure of Three-Way DNA Junctions 1. Non-Planar DNA Geometry," *J. Biomol. Struct. Dyn.* 11 (1994): 1175-89.

59. F. Stuhmeier, J.B. Welch, A.I.H. Murchie, D.M.J. Lilley and R.M. Clegg, "Global Structure of Three-Way DNA Junctions with and without Additional Unpaired Bases: A Fluorescence Resonance Energy Transfer Analysis," *Biochemistry* 36 (1997): 13530-38.

60. N.B. Leontis, W. Kwok and J.S. Newman, "Stability and Structure of Three-Way DNA Junctions Containing Unpaired Nucleotides," *Nucleic Acids Res.* 19 (1991): 759-66.

61. M. Yang and D.P. Millar, "Conformational Flexibility of Three-Way DNA Junctions Containing Unpaired Nucleotdes," *Biochemistry* 35 (1996): 7959-67.

62. R.I. Ma, N.R. Kallenbach, R.D. Sheardy, M.L. Petrillo and N.C. Seeman, "Three-Arm Nucleic Acid Junctions Are Flexible," *Nucleic Acids Res.* 14 (1986): 9745-53.

63. Y. Li, Y.D. Tseng, S.Y. Kwon, L. D'Espaux, J.S. Bunch, P.L. Mceuen and D. Luo, "Controlled Assembly of Dendrimer-Like DNA," 3 (2004): 38-42.

64. N.C. Seeman, "Biochemistry and Structural DNA Nanotechnology: An Evolving Symbiotic Relationship," *Biochemistry* 42 (2003): 7259-69.

65. C. Mao, W. Sun and N.C. Seeman "Designed Two-Dimensional DNA Holliday Junction Arrays Visualized by Atomic Force Microscopy," *J. Am. Chem. Soc.* 121 (1999): 5437-43.

66. N.C. Seeman, "DNA in a Material World," *Nature* 421 (2003): 427-31.

67. F. Liu, R. Sha and N.C. Seeman "Modifying the Surface Features of Two-Dimensional DNA Crystals," *J. Am. Chem. Soc.* 121 (1999): 917-22.

68. E. Winfree, F. Liu, L.A. Wenzler, and N.C. Seeman, "Design and Self-Assembly of Two-Dimensional DNA Crystals," *Nature* 394 (1998): 539-43.

69. H. Yan, T.H. LaBean, L. Feng and J.H. Reif, "Directed Nucleation Assembly of DNA Tile Complexes for Barcode-Patterned Lattices," *Proc. Natl. Acad. Sci.* 100 (2003): 8103-08.

70. T. Antony and V. Subramaniam, "Molecular Beacons: Nucleic Acid Hybridization and Emerging Applications," *J. Biomol. Struct. Dyn.* 19 (2001):

497-504.

71. G. Bonnet, O. Krichevsky and A. Libchaber, "Kinetics of Conformational Fluctuations in DNA Hairpin -Loops," *Proc. Natl. Acad. Sci.* 95 (1998): 8602-06.

72. R.A.J. Darby, M. Sollogoub, C. McKeen, L. Brown, A. Risitano, N. Brown, C. Barton, T. Brown and K.R. Fox, "High Throughput Measurement of Duplex, Triplex and Quadruplex Melting Curves Using Molecular Beacons and a Lightcycler," *Nucleic Acids Res.* 30 (2002): e39.

73. J.L. Mergny, A.S. Boutorine, T. Garestier, F. Belloc, M. Rougee, N.V. Bulychev, A.A. Koshin, J. Bourson, A.V. Lebedev, B. Valeur, N.T. Thuong and C. Helene, "Fluorescence Energy Transfer as a Probe for Nucleic Acid Structures and Sequences.," *Nucleic Acids Res.* 22 (1994): 920-28.

74. D. Whitecombe, J. Theaker, S.P. Guy, T. Brown and S. Little, "Detection of Pcr Products Using Self-Probing Amplicons and Fluorescence," *Nature Biotechnology* 17 (1999): 804-07.

75. B. Schweitzer and S. Kingsmore, "Combining Nucleic Acid Amplification and Detection," *curr. Opin. Biotec.* 12 (2001): 21-27.

76. Z. Tang, K. Wang, W. Tan, J. Li, L. Liu, Q. Guo, X. Meng, C. Ma and S. Huang, "Real-Time Monitoring of Nucleic Acid Ligation in Homogenous Solutions Using Molecular Beacons," *Nucleic Acids Res.* 31 (2003): e148.

77. E. Braun, Y. Eichen, U. Sivan and G. Ben-Yoseph, "DNA-Templated Assembly and Electrode Attachment of a Conducting Silver Wire," *Nature* 391 (1998): 775-78.

78. H. Yan, S.H. Park, G. Finkelstein, J.H. Reif and T.H. LaBean, "DNA-Templated Self-Assembly of Protein Arrays and Highly Conductive Nanowires," *Science* 301 (2003): 1882-84.

79. S.J. Park, T.A. Taton and C.A. Mirkin "Array-Based Electrical Detection of DNA with Nanoparticle Probes," *Science* 295 (2002): 1503-06.

80. C.A. Mirkin, R.L. Letsinger, R.C. Mucic and J.J. Storhoff, "A DNA-Based Method for Rationally Assembling Nanoparticles into Macroscopic Materials," *Nature* 382 (1996): 607-09.

81. R. Elghanian, J.J. Storhoff, R.C. Mucic, R.L. Letsinger and C.A. Mirkin, "Selective Colorimetric Detection of Polynucleotides Based on the Distance-Dependent Optical Properties of Gold Nanoparticles," *Science* 277 (1997): 1078-80.

82. R. Jin, G. Wu, Z. Li, C.A. Mirkin and G.C. Schatz, "What Controls the Melting Properties of DNA-Linked Gold Nanoparticles Assembles?" *J. Am. Chem. Soc.* 125 (2002): 1643-54.

83. T.A. Taton, C.A. Mirkin and R.L. Letsinger "Scanometric DNA Array Detection with Nanoparticle Probes," *Science* 289 (2000): 1757-60.

84. A. Csaki, R. Moller, W. Straube, J.M. Kohler and W. Fritzsche, "DNA Monolayer on Gold Substrates Characterized by Nanoparticle Labelling and Scanning Force Microscopy," *Nucleic Acids Res.* 29 (2001): e81.

85. A.P. Alivisatos, K.P. Johnsson, X. Peng, T.E. Wilson, C.J. Loweth, M.P. Bruchez Jr and P.G. Schultz, "Organization of "Nanocrystal Molecules" Using DNA," *Nature* 382 (1996): 609-11.

86. B. Yurke, A. J. Turberfield, A. P. Mills, Jr., F. C. Simmel, and J. L.Neumann, "A DNA-Fuelled Molecular Machine Made of DNA," *Nature* 406 (2000): 605-08.

87. W.B. Sherman and N.C. Seeman, "A Precisely Controlled DNA Biped Walking Device," *NanoLetters* 4 (2004): 1203-07.

88. Y. Tian and C. Mao, "Molecular Gears: A Pair of DNA Circles Continuously Rolls against Each Other," *J. Am. Chem. Soc.* 126 (2004): 11410-11.

89. W.M. Shih, J.D. Quispe and G.F. Joyce, "A 1.7-Kilobase Single-Stranded DNA That Folds into a Nanoscale Octahedron," *Nature* 427 (2004): 618-21.

90. W.U. Dittmer, A. Reuter and F.C. Simmel, "A DNA-Based Machine That Can Cyclically Bind and Release Thrombin," *Angew. Chem. Int. Ed.* 43 (2004): 3549.

91. S.S. Thach and R.E. Thach, "Mechanism of Viral Replication. I. Structure of Replication Complexes of R17 Bacteriophage.," *J. Mol. Biol.* 81 (1973): 367-80.

92. H.J. Vollenweider, J.M. Sogo AND T.H. Koller, "A Routine Method for

Protein-Free Spreading of Double- and Single-Stranded Nucleic Acid Molecules," *proc. Natl. Acad. Sci.* 72 (1975): 83-87.

93. W. Stoeckenius, "Electron Microscopy of DNA Molecules "Stained" with Heavy Metal Salts," *J. Biophysic. and Biochem. Cyto.* 11 (1961): 297-310.

94. J.L. Mergny and L. Lacroix, "Analysis of thermal melting curves." *Oligonucleotides*, 13 (2003): 515-537.

95. P.L. Hülser and H.H. Klump,"Unfolding of a branched double-helical DNA three-way junction with triple-helical ends," *Archives of Biochemistry and Biophysics*, 313(1994): 29-38.

96. P.L. Hülser and H.H. Klump, "Unfolding of a Branched Double-Helical DNA Three-Way Junction with Triple-Helical Ends.," *Archives of Biochemistry and Biophysics* 313 (1994): 29-38.

97. D. Freifelder, *Physical Biochemistry: Applications to Biochemistry and Molecular Biology*W. H. Freeman and Company, 1976).

98. H.H. Klump, M.Chauhan., M. Mills and C.T. Lin. Progress in designing nucleic acid structures and fine-tuning their interactions. *Arch. Biochem. Biophys*. 2006 Feb [Epub].

99. H.R. Jacobs, *Mathematics: A Human Endeavor*. Second edition, Chapter 5, Lesson 3, 257-264 edW.H. Freeman and company.

## Figure legend

Chapter 1

**Figure 1.4.1** The size of a dsDNA and size between two types of base pairs.

**Figure 1.4.2** The kinase reaction scheme using DNA kinase (top); the ligation reaction scheme using DNA ligase (bottom).

**Figure 1.4.2.3** Structures of the A, B-, and Z-forms of the DNA double helix.

**Figure 1.4.4** The *syn* conformation of Z-form DNA.

**Figure 1.4.5** The schematic diagram of branched DNA. Left: three-way junction DNA; Right: Four-way junction DNA.

**Figure 1.4.6** The schematic diagram of G-quartet (left) and i-Motif (right).

**Figure 1.4.7** A schematic diagram of a three-way junction DNA formed by sequence design.

**Figure 1.4.8** The schematic diagram of a double-cross over DNA made by hybridizing 5 different lengths ssDNA.

**Figure 1.4.9** The schematic diagram of DNA ligation monitored in real time using molecular beacon.

**Figure 1.4.10** The schematic diagram of use of nanoparticles with DNA. a) DNA nano-wire using gold and sliver nanoparticle deposition; b) Hybridization of DNA containing gold nanoparticles.

**Figure 1.4.11** The mechanism of a molecular forceps made by DNA. ("T" defines as the "tweezer" strand, and "F" is the fuel strand)

**Figure 1.4.12** A biped walking DNA across the supporting platform.

**Figure 1.4.13** A molecular gear system made by two circular ssDNA and their interactions.

## Chapter 2

in 25000); top-middle: 10 minutes (1 in 25000); top-right: 20 minutes (1in 16000); bottom-left: 30 minutes (1 in 25000); bottom-middle and right: 60 minutes (1 in 16000)

## Chapter 3

**Figure 3.4.1** The plot represents the percentage of fluorescence intensity change at increasing $NaClO_4$ concentrations.

## Chapter 4

**Figure 4.1.1** Hairpin loop DNA structure showing the base pairing of alternating CG sequences and the interaction between triplet repeats.

**Figure 4.1.2** Formation of a partially mismatching stem-loop DNA structure from the fuel strand and the hairpin loop DNA structure, and the fuel strand is removed by addition of the complementary strand.

**Figure 4.1.3** Formation of a double helix with a 3'extension that replaces the initial hairpin loop DNA structure followed by the removal of the fuel strand by a perfectly complementary second single strand.

**Figure 4.1.4** A schematic diagram of the hairpin loop DNA structure containing 6 consecutive sections of sequences that are complementary to specific sections (a), and form a structure that contains extensions at the both 5'- and 3'- ends (b).

**Figure 4.1.5** A schematic diagram of the linked hairpin loop DNA structure using single strand extensions. The linking process is bi-directional.

**Figure 4.1.6** A schematic diagram showing the linkage of hairpin loop DNA structures can be stopped by blocking the sequences in the loop section (left) or the at the extension strands (right).

**Figure 4.3.1** UV thermal unfolding analysis (absorbance at 260nm as function of temperature) of folded single strands and their combinations as they appear in the intermediate steps of the first mechanism. (Panel **f** shows the progressive changes observed in panels **a** to **e**)

**Figure 4.3.2** UV thermal unfolding analysis (absorbance at 260nm as function of temperature) of folded single strands and their combinations as they appear in the intermediate steps of the second mechanism. (Panel **d** shows curves **a**, **b**, and **c** plotted together)

**Figure 4.3.3** on-denaturing PAGE gel photograph of oligonucleotide A and various combinations of oligonucleotides A, B and C involved in the first mechanism proposed (see text). Lane 1 (from left): the stem-loop DNA structure of oligonucleotide A; lane 2: the mismatched complex of oligonucleotides A and B; lane 3: the hairpin loop DNA structure A and the 17mer duplex B,C; lane 4: the 17mer duplex B,C.

**Figure 4.3.4** Non-denaturing PAGE gel photograph of oligonucleotide A and various combinations of oligonucleotides A, D and E involved in the second mechanism proposed (see text). Lane 1 (from left): the stem-loop DNA structure A; lane 2: the duplex with overhangs A,D; lane 3: the stem-loop DNA structure A and the 18mer duplex D,E; lane 4: the 18mer duplex D,E.

**Figure 4.3.5** The UV absorbance spectrum of the DNA hairpin loop structures with single strand extensions (LOL01) in 1M NaCl, 10mM Na-cacodylate, pH 7.0 at low and high temperatures from 220 to 320 nm. The optimal wavelength was found to be 272 nm (vertical line).

**Figure 4.3.6** The UV melting curve of LOL01 in 1M NaCl, 10mM Na-cacodylate, pH 7.0 at 272 nm.

**Figure 4.3.7** UV melting analysis of the sample containing LOL01 only (a) with addition of equal concentrations of ssDNA in the following order: LOL02 (b), LOL01 (c) and LOL02 (d).

**Figure 4.3.8** The thermal unfolding process of LOL01 with increasing concentration of LOL02. (LOL02 concentration in **a**: 0 μM; **b**: 0.2 μM; **c**: 0.4 μM; **d**: 0.6 μM; **e**: 0.8 μM; **f**: 1 μM)

**Figure 4.3.9** The thermal unfolding process of the sample containing LOL01 only (a) with addition of equal concentrations of ssDNA in the following order: LOL03 (b), LOL01 (c) and LOL03 (d).

**Figure 4.3.10** The thermal unfolding of LOL01 as a function of increasing LOL03 concentration. (LOL03 concentration in **a**: 0 μM; **b**: 0.2 μM; **c**: 0.4 μM; **d**: 0.6 μM; **e**: 0.8 μM; **f**: 1 μM)

**Figure 4.3.11** A 4% native PAGE gel showing the DNA structures formed in the presence of varying amounts of LOL01 (Lane 1 to 4, from left) and that the linking process was interrupted with the increasing amounts of LOL02 present in the LOL01 system.

**Figure 4.3.12** A 4% native PAGE gel showing the complexes formed by combining LOL01, LOL02 and LOL03. Lane 1: LOL01 only (structure was too large to be resolved); Lane 2: LOL01 and LOL02; Lane 3: LOL01 and LOL03; Lane 4: LOL01, LOL02 and LOL03 mixed at the same time; Lane 5: LOL01-LOL02 complex followed by addition of LOL03; Lane 6: LOL01-LOL03 complex followed by addition of LOL02; Lane 7: LOL02 and LOL03 duplex.

**Figure 4.3.13** Non-denaturing PAGE gel electrophoretic analysis of the products obtained from mixing LOL01 (0.5μM) with LOL02 in different ratios. Lane1: LOL01 only; lane 2: LOL01 to LOL02 in a ratio of 5:1; lane 3: in 5:2; lane 4: in 2:1; lane 5: in 5:3; lane 6: in 5:3.5; lane 7: in 5:4; lane 8: in 5:4.5; and lane 9: in 1:1 ratio.

**Figure 4.3.14** Gel electrophoresis experiment of mixing LOL01 (0.5μM) with LOL03 in different ratios. Lane 1: LOL01 to LOL03 in a ratio of in 5:2; lane 2: in 2:1; lane 3: in 5:3; lane 4: in 5:3.5; lane 5: in 5:4; lane 6: in 5:4.5; and lane 7: in 1:1 ratio.

**Figure 4.4.1** The changes in free energy level when moving along the thermodynamic cycle upon the addition of the different single strands to the initial hairpin-loop structure.

**Figure 4.4.2** The combined first and second mechanisms presented as a thermodynamic cycle driven with two additions of two different fuel strands (C and E).

**Figure 4.4.3** The free energy change in the combined mechanism.

## Chapter 5

**Figure 5.1.1** Schematic diagram of three-way junction DNA network binding with transcription factors (TF). a) three way junction DNA with sticky end sequence recognizable by transcription factor; b) sticky ends hybridization and ligation; c) addition of transcription factors after ligation; d) binding of transcription factors to

DNA network. (This drawing is not according to scale)

**Figure 5.2.1** A schematic diagram of single mismatch detection using hexagonal DNA nanoswitches at a fixed temperature. Change from the "ON" state to the "OFF" state when complementary ssDNA is added (left). The hexagonal DNA nanoswitch stays the "ON" state when a ssDNA with a single mismatch is present.

**Figure 5.2.2** The schematic diagram demonstrating the ssDNA separation using hexagonal DNA nanoswitches.

**Figure 5.2.3** The schematic diagram of a binary memory system using hexagonal DNA nanoswitches. The "ON" state represents the state of "1" (left); the "OFF" state represents the state of "0" (right).

**Figure 5.3.1** A flow chart showing the target-conveyance system based upon meta-stable state DNA nanostructures.

**Figure 5.3.2** A schematic diagram of a protein conveyance system. Top) Design of DNA hairpin loop and Fuel(+)/(-) strands; bottom left) to complex when the protein is loaded; bottom right) the duplex that is formed when the protein is released. (This drawing is not according to scale).

**Figure 5.3.3** The flow chart showing multiple targets-convey system.

**Figure 5.3.4** The schematic diagram showing modified hairpin loop structure carrying different protein when different Fuel(+) strand is added. a.) modified hairpin loop structure (cloverleaf structure); b.) Protein 1 loading; c.) Protein 2 loading; d.) Protein 3 loading.

**Figure 5.3.5** The schematic diagram of a new DNA hairpin loop with two extra sections that bind to two ssDNA with gold nanoparticles attached.

**Figure 5.3.6** A schematic diagram illustrating the modified DNA hairpin loop structures in both hairpin loop and extension sequences.

**Figure 5.3.7** The extension of DNA hairpin loop structure using different sequences in an alternating pattern.

**Figure 5.3.8** The schematic diagram of DNA nanowire using alternating DNA hairpin loop linkage (a). A two-dimensional DNA structure containing DNA nanowires in an elongated fashion (b).

## Table legends